

GLUT-1 TARGETED GENE DELIVERY TO BRAIN FOR THE TREATMENT OF
ALZHEIMER'S DISEASE

A Dissertation
Submitted to the Graduate Faculty
of the
North Dakota State University
of Agriculture and Applied Science

By

Sanjay Arora

In Partial Fulfillment of the Requirements
for the Degree of
DOCTOR OF PHILOSOPHY

Major Department:
Pharmaceutical Sciences

March 2021

Fargo, North Dakota

North Dakota State University
Graduate School

Title

GLUT-1 TARGETED GENE DELIVERY TO BRAIN FOR THE
TREATMENT OF ALZHEIMER'S DISEASE

By

Sanjay Arora

The Supervisory Committee certifies that this *disquisition* complies with
North Dakota State University's regulations and meets the accepted
standards for the degree of

DOCTOR OF PHILOSOPHY

SUPERVISORY COMMITTEE:

Jagdish Singh, Ph.D.

Chair

Chengwen Sun, Ph.D.

Rhonda Magel, Ph.D.

John Ballantyne, Ph.D.

Buddhadev Layek, Ph.D.

Approved:

3/17/2021

Date

Dr. Jagdish Singh

Department Chair

ABSTRACT

Alzheimer's disease (AD) is a neurodegenerative disorder resulting in debilitating dementia with progressive loss of motor functions. Genetic modulation of neurotrophic factors and apolipoprotein E (ApoE) have emerged as powerful strategies offering preventive and protective effect against AD pathophysiology. Brain derived neurotrophic factor (BDNF), apolipoprotein E2 (ApoE2) and vgf (non-acronymic) which play a major role in neuronal plasticity, synapse formation, amyloid-beta regulation and cognition, are found to be reduced in the brain of AD patients. However, delivery of such large polar proteins (BDNF, ApoE2 and vgf) across blood brain barrier (BBB) is one of the most challenging tasks. Therefore, in this study, we developed and optimized liposomal nanoparticles capable of delivering gene encoding for BDNF, ApoE2 and vgf to the brain in a targeted manner. These nanoparticles were surface modified with glucose transporter-1 targeting ligand (mannose) and various cell penetrating peptides to promote selective and enhanced delivery to brain. Dual-modified nanoparticles demonstrated homogenous size between 150-200 nm with positive zeta potential. These nanoparticles demonstrated ~50% higher transport across *in vitro* BBB model and showed significantly higher transfection of encapsulated pDNA in bEnd.3 cells, primary astrocytes and neuronal cells. Surface functionalized nanoparticles also demonstrated significantly higher transport (~7% of injected dose/gram of tissue) and gene transfection (1.5 - 2 times higher than baseline level) across BBB following single intravenous administration in C57BL/6 mice without any signs of toxicity. Furthermore, liposomal nanoparticles encapsulating pBDNF tested in early (6-months) and advanced stages (9-months) of transgenic APP/PS1 mouse model of AD showed good functional efficacy. The dual-modified nanoparticles enhanced BDNF expression by ~2 times and resulted in >40% ($p < 0.05$) reduction in toxic amyloid-beta in 6- and 9- months old APP/PS1 mice brains compared to their age-matched

untreated controls. Plaque load was reduced ~7 and ~3 times ($p < 0.05$), respectively, whereas synaptic proteins, synaptophysin and PSD-95, were found to be increased by >90% ($p < 0.05$) in both age groups of transgenic mice following BDNF treatment using dual-modified nanoparticles in comparison to their age-matched controls. Moreover, no untowardly adverse effects were observed throughout treatment, suggesting a safe and effective strategy for treatment of AD pathophysiology.

ACKNOWLEDGEMENTS

I would like to express my sincere gratitude to my advisor, Dr. Jagdish Singh, whose research perspective, expertise, constructive criticism, and attention to detail considerably added to my graduate experience.

I genuinely thank my graduate advisory committee members, Dr. Chengwen Sun, Dr. Rhonda Magel, Dr. John Ballantyne, and Dr. Buddhadev Layek for their expertise which significantly contributed to different stages of my research.

I convey my sincere thanks to my seniors, lab colleagues and fellow graduate students, Dr. Sushant Lakkadwala, Dr. Bruna Rodriguez, Dr. Divya Sharma, Riddhi Trivedi, Bivek Chaulagain, and Richard Nii Lante Lamptey for creating a supportive environment at work.

I acknowledge all the current and previous faculty members, staff and students of the department of Pharmaceutical Sciences for helping me directly or indirectly during my research.

My warm and sincere thanks to Janet Krom, Diana Kowalski, and Tiffany Olson, for their assistance with administrative work, Dr. Jodie Haring and Megan Ruch for help with animal work, and Dana Davis & CHP Ambassadors for contributing to my overall personal and professional development.

I gratefully acknowledge financial supports from the NIH (grant# R01 AG051574), and the Department of Pharmaceutical Sciences, NDSU, for making my research possible.

Finally, I am immensely thankful of my family members, Dr. Divya Sharma, Pinky Arora, and Ramnik Arora, for their constant support, love, and understanding.

DEDICATION

Dedicated to my mother,

Mrs. Pinky Arora

and my father,

Mr. Ramnik Arora.

TABLE OF CONTENTS

ABSTRACT	iii
ACKNOWLEDGEMENTS	v
DEDICATION	vi
LIST OF TABLES	x
LIST OF FIGURES	xi
LIST OF ABBREVIATIONS.....	xvi
1. INTRODUCTION	1
1.1. Background and Significance.....	1
1.1.1. Alzheimer’s Disease	1
1.1.2. Barriers to Gene Therapy	4
1.1.3. Viral vs. Non-viral Gene Therapy	9
1.1.4. Non-viral Gene Therapy for Alzheimer’s Disease	11
1.2. Statement of Problem and Research Objective	26
1.2.1. Specific Aim 1: To Synthesize and Characterize MAN and CPP Coupled Liposomes Encapsulating Plasmid DNA and Chitosan Complexes	32
1.2.2. Specific Aim 2: To Assess Biocompatibility, Biodistribution and Transfection Efficiency of Dual Modified Liposomes <i>In Vivo</i> in C57BL/6 Mice	33
1.2.3. Specific Aim 3: To Assess Formulation Efficacy <i>In Vivo</i> in Transgenic Mouse Model of Alzheimer’s Disease	33
2. MATERIALS AND METHODS.....	34
2.1. Materials.....	34
2.2. Animals	35
2.3. Experimental Methods	35
2.3.1. Coupling of Cell Penetrating Peptide to DSPE-PEG(2000)-NHS	35
2.3.2. Preparation and Characterization of Liposomes.....	35

2.3.3. DNase Protection Assay	36
2.3.4. Cell Culture	36
2.3.5. <i>In Vitro</i> Biocompatibility Assay.....	37
2.3.6. Cellular Uptake.....	37
2.3.7. Cellular Mechanism of Uptake and Competition Assay	37
2.3.8. <i>In Vitro</i> Transfection Efficiency.....	38
2.3.9. Synaptic Vesicles Formation.....	39
2.3.10. <i>In Vitro</i> Co-culture BBB Model	39
2.3.11. Transport Across <i>In Vitro</i> BBB Model	40
2.3.12. Transfection Across <i>In Vitro</i> BBB Model.....	40
2.3.13. Animal Experiments in Wild Type Mice	41
2.3.14. <i>In Vivo</i> Biodistribution	41
2.3.15. <i>In Vivo</i> Biocompatibility and Gene Transfection in Wild Type Mice	42
2.3.16. Alzheimer’s Disease Experimental Design.....	43
2.3.17. BDNF Protein Transfection in Alzheimer’s Disease Mice	43
2.3.18. Quantification of Amyloid Beta Peptides.....	43
2.3.19. Immunohistochemical Analysis	44
2.3.20. Synaptophysin and PSD-95 Protein Quantification	44
2.3.21. Nesting.....	45
2.3.22. Statistical Analysis	45
3. RESULTS AND DISCUSSION.....	46
3.1. Preparation and Characterization of Liposomes	46
3.2. DNase Protection Assay.....	47
3.3. <i>In Vitro</i> Biocompatibility Assay	48
3.4. Cellular Uptake	50

3.5. Cellular Mechanism of Uptake and Competition Assay	52
3.6. <i>In Vitro</i> Transfection Efficiency.....	55
3.7. Synaptic Vesicle Formation	60
3.8. <i>In Vitro</i> Co-culture Blood Brain Barrier Model.....	61
3.9. Transport Across <i>In Vitro</i> BBB Model	63
3.10. Transfection Across <i>In Vitro</i> BBB Model.....	64
3.11. <i>In Vivo</i> Biodistribution.....	68
3.12. <i>In Vivo</i> Biocompatibility and Gene Transfection in Wild Type Mice	69
3.13. BDNF Protein Transfection in AD Mice	77
3.14. Quantification of Amyloid Beta Peptides	78
3.15. Plaque Load.....	83
3.16. Cell Proliferation	88
3.17. Synaptophysin and PSD-95 Protein Quantification	89
3.18. Nesting	92
4. SUMMARY AND CONCLUSION	96
4.1. Future Directions.....	99
REFERENCES	101

LIST OF TABLES

<u>Table</u>		<u>Page</u>
1.	Non-viral gene delivery methods for the treatment of Alzheimer's disease.	22
2.	Materials used and their source.....	34
3.	Chromatographic conditions for studying biodistribution using RP-HPLC.....	42
4.	Liposome characterization. Data is expressed as mean \pm S.D, n = 4.	47

LIST OF FIGURES

<u>Figure</u>	<u>Page</u>
1. Potential route to the central nervous system following administration of a typical therapeutic.....	7
2. Active and passive translocation across the blood brain barrier. (Key: BEC: Brain endothelial cells, SCMT: Solute carrier mediated transcytosis, RMT: Receptor mediated transcytosis, AMT: Adsorption mediated transcytosis)	9
3. Various methods for non-viral gene therapy to treat Alzheimer’s Disease.....	12
4. Schematic of surface functionalized liposomal nanoparticles-based delivery system administered using tail vein injection in mouse model for transportation of genetic cargo (plasmid DNA complexed with chitosan polymer) across blood brain barrier for the treatment of Alzheimer’s disease.	32
5. Synthesis of liposomes via film hydration technique.	36
6. Protection of encapsulated pDNA previously complexed to chitosan (N/P 5) against DNaseI degradation. Column A, naked pDNA; column B, pDNA + DNase1; column C-H, Liposome, MAN-liposome, Pen-liposome, MAN-Pen-liposomes, RVG-liposomes, RVG-MAN-liposomes containing chitosan-DNA complexes, respectively + DNase I.....	48
7. <i>In vitro</i> cytocompatibility of unmodified (plain), mannose (MAN), penetratin (Pen), rabies virus glycoprotein peptide (RVG), rabies virus glycoprotein peptide-9R (RVG9R), rabies virus derived peptide (RDP), and CGN (CGNHPHLAKYNGT) liposomes at various phospholipid concentrations on (A) bEnd.3, (B) primary astrocytes, and (C) primary neurons. Data represent mean ± SD of four replicates.	49
8. Cellular uptake of unmodified (plain), mannose (MAN), penetratin (Pen), rabies virus glycoprotein peptide (RVG), rabies virus glycoprotein peptide-9R (RVG9R), rabies virus derived peptide (RDP), and CGN (CGNHPHLAKYNGT) modified liposomes in (A) bEnd.3, (B) primary astrocytes, and (C) primary neurons. Data represent mean ± SD of four replicates.	51
9. Quantitative analysis of A) cellular uptake mechanism and B) competition assay in bEnd.3 cells. Data is presented as mean ± SD (n = 4). Statistically significance (p < 0.05) is shown as (*) with plain liposomes, (#) with MAN liposomes, (+) with Pen liposomes, (&) with RVG liposomes.....	54

10.	BDNF expression levels post 48h after transfection in A) bEnd.3 cells, B) primary glial cells and C) primary neuronal cells treated with different liposomal formulations entrapping chitosan-pBDNF complexes (1µg) . Data is presented as mean ± SD (n = 4). Statistically significance (p < 0.05) is shown as (!) with naked DNA, (*) with plain liposomes, (#) with MAN liposomes, (+) with Pen liposomes, (&) with RVG liposomes, and (~) with lipofectamine.	57
11.	ApoE expression levels post 48h after transfection in A) bEnd.3 cells, B) primary glial cells and C) primary neuronal cells treated with different liposomal formulations entrapping chitosan-pBDNF complexes (1µg) . Data is presented as mean ± SD (n = 4). Statistically significance (p < 0.05) is shown as (!) with naked DNA, (*) with plain liposomes, (#) with MAN liposomes, (+) with Pen liposomes, (&) with RVG liposomes, and (~) with lipofectamine.	58
12.	Vgf expression levels post 48h after transfection in A) bEnd.3 cells, B) primary glial cells and C) primary neuronal cells treated with different liposomal formulations entrapping chitosan-pBDNF complexes (1µg) . Data is presented as mean ± SD (n = 4). Statistically significance (p < 0.05) is shown as ~, , @, #, *, --, +, and “ show statistically significant difference (p<0.05) from untreated, naked DNA, plain, Pen, MAN, CGN, RVG9R and RDP liposomes, respectively.	59
13.	A) Effect of BDNF protein transfected using PENMAN liposomes entrapping chitosan-pBDNF (1 µg) on synaptophysin protein levels at various time points in primary neuronal cells. B) Qualitative assessment of synaptophysin levels in primary neuronal cells using fluorescence microscope a5t predetermined time points. Data is presented as mean ± SD (n = 4). Statistically significance differences (p < 0.05) are shown as (*).....	61
14.	A) Transendothelial electrical resistance (TEER) and B) permeability of sodium fluorescein dye across BBB models. Statistically significant differences (p < 0.05) are shown as *.....	63
15.	Transport of various liposomal formulations through in vitro BBB model over a period of 24 h. Statistically significant differences (p < 0.05) is shown as (*) with plain liposomes, (#) with MAN liposomes, (+) with Pen liposomes, (&) with RVG liposomes, (--) with CGN liposomes (!) with RVG9R liposomes, and (“) with RDP liposomes.	64
16.	A) ApoE2, B) BDNF, C) Vgf transfection across BBB model post treatment with liposomes entrapping 1 µg pBDNF/chitosan complexes. Data shown as mean (SD) with 4 repeats. @, #, *, ~, --, +, and “ shows statistical significance (p < 0.05) from plain, Pen, MAN, RVG, CGN, RVG9R and RDP liposomes, respectively.	67

17. A) HPLC chromatogram of lissamine rhodamine dye. B) Distribution of lissamine rhodamine labelled MAN-liposomes in brain of C57BL/6 mice over a period of 24hours (n = 6). C) Biodistribution of lissamine rhodamine labelled liposomal formulations in different organs of C57BL/6 mice at 12hrs to analyze the effect of CPPs in combination with mannose (n = 6). Data is presented as mean \pm SD (n = 6). Statistically significance ($p < 0.05$) is shown as (*) with plain liposomes, (#) with MAN liposomes, (+) with Pen liposomes, (&) with RVG liposomes. 69
18. BDNF expression levels post 5 days after transfection *in-vivo* in different organs (A. Brain; B. Kidney; C. Lungs; D. Spleen; E. Liver; F. Plasma; G. Heart) of C57BL/6 mice using liposomal formulations (15.2 μ M of phospholipids/kg body weight) entrapping chitosan-pBDNF complexes (40 μ g/100g body weight). Data is presented as mean \pm SD (n = 6). Statistically significance ($p < 0.05$) is shown as (!) with naked DNA, (*) with plain liposomes, (#) with MAN liposomes, (+) with Pen liposomes, (&) with RVG liposomes, and (~) with control..... 73
19. ApoE expression levels post 5 days after transfection *in-vivo* in different organs (A. Brain; B. Heart; C. Liver; D. Spleen; E. Lungs; F. Kidney; G. Plasma) of C57BL/6 mice using liposomal formulations (15.2 μ M of phospholipids/kg body weight) entrapping chitosan-pBDNF complexes (40 μ g/100g body weight). Data is presented as mean \pm SD (n = 6). Statistically significance ($p < 0.05$) is shown as (!) with naked DNA, (*) with plain liposomes, (#) with MAN liposomes, (+) with Pen liposomes, (&) with RVG liposomes, and (~) with control..... 74
20. Vgf expression levels post 5 days after transfection *in-vivo* in different organs. A) Brain, B) Heart, C) Kidney, D) Lungs, E) Liver, F) Spleen, and G) Plasma. Data shown as mean (SD) with 6 repeats. ~, |, @, #, *, --, +, and “ shows statistical significance ($p < 0.05$) from control, naked DNA, plain, Pen, MAN, CGN, RVG9R and RDP liposomes, respectively. 75
21. Biocompatibility analysis via H&E staining of tissue sections from different organs of C57BL/6 mice 5 days post treatment with various liposomal formulations entrapping A) chitosan-pApoE complexes, B) chitosan-pVGF complexes and C) chitosan-pBDNF complexes. 76
22. BDNF expression levels in A) 6-months and B) 9-months mice brain post four weekly intravenous administration of liposomes entrapping pBDNF/chitosan complexes. Data presents mean \pm SEM of 6 animals. Statistically significant difference ($p < 0.05$) is shown as (#) with C57BL/6, (*) with APP/PS1, (†) with naked DNA, and (¶) with Plain liposomes. 78
23. Levels of various fractions of abeta in 6-months old mice brain post four weekly intravenous administration of liposomes entrapping pBDNF/chitosan complexes. A,B,C) Abeta 40 and D,E,F) Abeta 42. A,D) TBS B,E) TBSX and C,F) GDN fraction. Data presents mean \pm SEM of 6 animals. Statistically significant difference ($p < 0.05$) is shown as (#) with C57BL/6, (*) with APP/PS1, (†) with naked DNA, (¶) with Plain liposomes and (§) with RDP liposomes..... 81

24.	Levels of various fractions of abeta in 9-months old mice brain post four weekly intravenous administration of liposomes entrapping pBDNF/chitosan complexes. A,B,C) Abeta 40 and D,E,F) Abeta 42. A,D) TBS B,E) TBSX and C,F) GDN fraction. Data presents mean \pm SEM of 6 animals. Statistically significant difference ($p < 0.05$) is shown as (#) with C57BL/6, (*) with APP/PS1, (†) with naked DNA, (¶) with Plain liposomes, (“) with MAN liposomes, (!) with Pen liposomes and (§) with RDP liposomes.....	82
25.	Plaque load in mice brain post four weekly intravenous administration of liposomes entrapping pBDNF/chitosan complexes. A,B,C) 6-months and D,E,F) 9-months. A,D) cortex B,E) hippocampus and C,F) total (cortex + hippocampus). Data presents mean \pm SEM of 6 animals. Statistically significant difference ($p < 0.05$) is shown as (#) with C57BL/6, (*) with APP/PS1, (†) with naked DNA, (¶) with Plain liposomes and (§) with RDP liposomes.	85
26.	Anti-amyloid beta antibody stained brain sections of 6-months-old mice post four weekly intravenous administration of liposomes entrapping pBDNF/chitosan complexes. C57BL/6 and APP/PS1 represent untreated healthy and AD controls, respectively.	86
27.	Anti-amyloid beta antibody stained brain sections of 9-months-old mice post four weekly intravenous administration of liposomes entrapping pBDNF/chitosan complexes. C57BL/6 and APP/PS1 represent untreated healthy and AD controls, respectively.	87
28.	Cell proliferation in the brains of 6-month old mice post four weekly intravenous administration of liposomes entrapping pBDNF/chitosan complexes. A) percentage positive ki67 cells. Ki67 positive cells in the brain sections of B) C57BL/6, C) APP/PS1, and D) APP/PS1 treated with MANPen liposomes. Data presents mean \pm SEM of 6 animals. Statistically significant difference ($p < 0.05$) is shown as (#) with C57BL/6, and (*) with APP/PS1.....	89
29.	Levels of synaptic proteins in mice brain post four weekly intravenous administration of liposomes entrapping pBDNF/chitosan complexes. A,C) 6-months and B,D) 9-months. A,B) Synaptophysin C,D) PSD95. Data presents mean \pm SEM of 6 animals. Statistically significant difference ($p < 0.05$) is shown as (#) with C57BL/6, (*) with APP/PS1, (†) with naked DNA, and (¶) with Plain liposomes.	91
30.	Nesting score in A) 6-month and B) 9-month old mice post four weekly intravenous administration of liposomes entrapping pBDNF/chitosan complexes. Data presents mean \pm SEM of 6 animals.	93
31.	Nests built by 6-month-old mice post four weekly intravenous administration of liposomes entrapping pBDNF/chitosan complexes. C57BL/6 and APP/PS1 represent untreated healthy and AD controls, respectively.	94

32. Nests built by 9-month-old mice post four weekly intravenous administration of liposomes entrapping pBDNF/chitosan complexes. C57BL/6 and APP/PS1 represent untreated healthy and AD controls, respectively. 95

LIST OF ABBREVIATIONS

AFM.....	Atomic force microscope
ANOVA.....	Analysis of variance
BCA.....	Bicinchoninic acid
CMC.....	Critical micelle concentration
CNS.....	Central nervous system
CPP.....	Cell penetrating peptides
DAPI.....	4',6-diamidino-2-phenylindole
DLS.....	Dynamic light scattering
DMEM.....	Dulbecco's Modified Eagle's Medium
DMSO.....	Dimethyl sulfoxide
DNA.....	Deoxyribonucleic acid
DNase.....	Deoxyribonuclease
DOPE.....	1, 2-dioleoyl-sn-glycero-3-phosphoethanolamine
DOTAP.....	1, 2-dioleoyl-3-trimethylammonium-propane chloride
DPBS.....	Dulbecco's phosphate buffered saline
ELISA.....	Enzyme linked immunosorbent assay
EtBr.....	Ethidium bromide
FACS.....	Fluorescence activated cell sorting
FBS.....	Fetal bovine serum
GFP.....	Green fluorescent protein
GLUT-1.....	Glucose transporter-1
H&E.....	Hematoxylin & eosin

HEPES.....	Hematoxylin & eosin
HPLC.....	High performance liquid chromatography
IgG.....	Immunoglobulin G
kb.....	Kilobase
kDa.....	Kilodalton
MAN.....	α -D-mannopyranosylphenyl isothiocyanate
MTT.....	3-(4,5-dimethylthiazol-2-yl)-2,5-diphenyltetrazolium bromide
Mw.....	Molecular weight
MWCO.....	Molecular weight cut-off
N/P ratio.....	Ratio of free amino groups on the polymer to phosphate groups in DNA
Na-F.....	Sodium fluorescein
NHS.....	N-hydroxysuccinimide
PBS.....	Phosphate buffered saline
PDI.....	Polydispersity index
pDNA.....	Plasmid DNA
PEG.....	Polyethylene glycol
PEI.....	Polyethylenimine
pGFP.....	Plasmid DNA encoding green fluorescent protein
PLGA.....	Poly lactide-coglycolide
p β -gal.....	Plasmid DNA encoding β -galactosidase
RP-HPLC.....	Reversed phase high performance liquid chromatography
rpm.....	Revolutions per minute
RT.....	Room temperature

SD..... Standard deviation
SEC..... Size exclusion chromatography
TBE..... Tris-borate-ethylenediaminetetraacetic acid
TFA..... Trifluoroacetic acid
UV..... Ultraviolet

1. INTRODUCTION

1.1. Background and Significance

1.1.1. Alzheimer's Disease

One of the major progressive lifetime neurodegenerative disorders of the CNS is Alzheimer's disease (AD) accounting for 60-80% of dementia cases around the world.¹ AD is generally classified into familial AD, which is early-onset (<65 years of age), seen in 5% of AD population, and sporadic AD which is late-onset age (>65 years of age) seen in 95% of AD population. This disease currently affects more than 5 million people in the US alone and is predicted to rise by 3-fold by 2050. The cognitive, social and behavioral impairment due to AD leads to an increase in the socioeconomic burden on the lives of AD patients, their families, as well as the country. AD economic cost to the US is around \$305 billion in 2020 alone.² Rapid progression and lack of treatment options makes AD the 6th leading cause of death in the US. It is of grave concern that deaths from AD have increased by 146% from the year 2000. Mortality related to AD is mainly due to aspiration pneumonia and serious infections in the later stage of the disease. Therefore, AD treatment capable of halting the disease progression will offer a huge benefit. Currently approved treatments of AD only help in the management of its symptoms. Researchers are working to develop innovative therapies aimed towards maintenance of cognitive functions, behavior, and attenuation of disease progression.²

The pathophysiology of AD involves the accumulation of amyloid beta (abeta) plaques and neurofibrillary tangles (NFTs) in the brain.³ Abeta deposits are present as diffuse and neuritic plaques extracellularly whereas NFTs are composed of hyperphosphorylated tau (ptau) protein intracellularly.³ Additionally, imbalance of neuronal signaling molecules alongside loss of synaptic proteins are also characterized as important markers in AD.^{4,5} The extent of the damage

to the synapses prior to the overload of ptau or abeta in the brain are chief reasons associated to AD related dementia.^{6,7} Besides these markers, inflammation of the CNS was shown to be closely associated with the progression of AD.⁸ Abeta protein has been linked to neuroinflammation, neurodegeneration, and cognitive decline. However, therapies using neurotrophic factors were found to attenuate these adverse effects associated with the abeta protein.⁹⁻¹¹

Brain-derived neurotrophic factor (BDNF), a neurotrophic factor, has been considered of highest therapeutic value in the treatment of AD. This crucial protein helps in neuronal plasticity, synapse formation, and long term potentiation.¹² Activation of TrkB receptor *via* BDNF leads to differentiation, plasticity, and survival of neurons in the CNS as well as in the peripheral nervous system (PNS).¹³ Additionally, it is linked to the activation of translational machinery and protein synthesis in neurons.¹⁴ Decreased levels of BDNF protein are frequently associated with neurodegeneration in the hippocampus and cortex regions of AD patients.¹⁵⁻¹⁷ Moreover, loss of BDNF signaling has also been implicated in the increase of APP and activation of amyloidogenic pathways.¹⁸ This also results in the downregulation of neurotrophin stimulated protein, vgf (non-acronymic). Vgf plays crucial role in memory formation, learning, enhancement of synaptic activity, and neurogenesis.¹⁹⁻²⁶ Vgf expression can be stimulated by neurotrophin-3 (NT-3), BDNF or nerve growth factor.^{27,28} Rescuing the levels the BDNF or vgf protein has shown to attenuate AD related phenotypes including reduction in the abeta toxicity and neuroinflammation.²⁹⁻³³ Apolipoprotein E (ApoE) is another major factor associated with the clearance of abeta. ApoE has three isoforms, ApoE2, ApoE3, and ApoE4, which differ at two positions in their amino acid sequence.³⁴ The ApoE4 isoform has been found to accelerate disease progression in sporadic as well as familial AD patients.^{35,36} Conversely, ApoE2 isoform has been found to be protective in nature and delays the onset of AD.^{36,37} The presence of two copies of ApoE4 in the genome is one

of the most significant risk factors for developing late-onset AD.³⁸ Furthermore, the accretion of toxic reactive oxygen species (ROS) in the brains of AD patients, has also been strongly suggested as a possible mechanism for the development of AD. The brain consumes the most amount of oxygen (~20 %) compared to other organs, making it more vulnerable to ROS-mediated toxicity.³⁹ The repair process of oxidative damage leads to overexpression of APP, leading to abeta accumulation and cell death in AD patients.^{40,41}

Based on all evidence, the present understanding of underlying AD mechanisms includes genetic risk factors, imbalance of neurotrophic factors, oxidative stress, and microtubules instability.^{42,43} The search for genetic risk factors in AD has led to the identification of more than 21 distinct loci in the genome.⁴⁴ Therefore, delivery of gene-based therapeutics, such as plasmid DNA (pDNA), short interfering RNA (siRNA), messenger RNA (mRNA), to the brain has a huge potential for developing disease modifying therapies for AD. These treatment modalities can restore normal cellular functions permanently or induce characteristic cell proliferation to replace lost cells. However, in practice, delivery of genetic material is plagued with several hurdles including its encapsulation, stability, transport to target site, and efficiency of expression/suppression of the target protein. Moreover, the presence of the blood-brain barrier (BBB) impedes the delivery of therapeutics to the CNS. Therefore, here we summarize the recent advances in the treatment of AD using non-viral gene therapies. Various barriers to gene therapy are also discussed briefly. The importance and need for developing non-viral gene delivery vectors are emphasized followed by detailed intervention into various non-viral gene delivery methods for AD.

1.1.2. Barriers to Gene Therapy

The success of gene therapy heavily relies upon development of a gene delivery system that can safely deliver the therapeutic gene to its target site. However, multiple extracellular and intracellular barriers make it a challenging task for the gene delivery vectors to transfer the therapeutic gene into the target cells. Major barriers to non-viral gene therapy are discussed below.

1.1.2.1. Extracellular Barrier

Extracellular barriers are unavoidable due to the interaction between the non-viral vector and the extracellular environment. Interaction between the delivery vector and extracellular components can lead to rapid elimination or degradation of the therapeutic carriers resulting in ineffective therapy. The therapeutic half-life of the gene delivery system depends on the physicochemical stability of the therapeutic gene and the carrier system. Intravenous administration is typically the chosen route of administration for gene therapy. However, nucleases present in the physiological fluids can degrade an unprotected therapeutic gene within minutes following its systemic availability.⁴⁵ This can be overcome by encapsulation of gene inside nanoparticles or complexing it with a cationic polymer that is able to prevent its interaction with extracellular enzymatic environment.⁴⁶⁻⁵⁰ Post complexation of the gene of interest, colloidal stability of these complexes or nanoparticles is another serious concern in the physiological fluids. The high amount of salts present in the blood can result in the aggregation of these complexes.⁵¹ Incorporation of polyethylene glycols (PEG) or helper lipids such as 1,2-dioleoylphosphatidylethanolamine (DOPE) and cholesterol have shown to be effective in improving the colloidal stability of such complexes.⁵²⁻⁵⁵ Lastly, the size, shape, and physicochemical properties of the nanoparticles can result in their leakage into organs such as the liver and spleen due to the presence of fenestrated and discontinuous endothelium with pore size

greater than 100 nm.⁵⁶ Depending on the desired site of action, these properties must be accordingly altered for maximizing therapeutic efficacy while minimizing off-target adverse effects.

1.1.2.2. Intracellular Barrier

Inside a cell, intracellular barriers function to compartmentalize the biological functions within each organelle. However, intracellular barriers act as hurdles in the path of gene delivery vectors, leading to ineffective transport to the nucleus or degradation of the foreign genetic material. The endocytosis pathway is the chief pathway for internalization of non-viral vectors. Following endocytosis, the delivery system is engulfed in vesicles with low pH called endosomes which culminate into enzymatic degradation of the genetic cargo. Therefore, non-viral gene delivery systems heavily rely on the escape properties of the vector from the endosome to the cytoplasm. There are four major barriers, specifically endosomal escape, cytoplasmic trafficking, nuclear localization, and vector unpacking, which a gene delivery vector needs to overcome to obtain efficient transfection efficiency. Following endocytosis, the incapability of gene delivery vector to escape endosome leads to its trafficking into the lysosome which contains acidic pH of ~4.5 along with various enzymes such as lipases, nucleases, and proteases capable of digesting most nucleic acids.⁵⁷ Therefore, various mechanisms have been developed to escape this vesicle such as destabilization of endosome membrane, proton sponge effect, and use of fusogenic or pore-forming peptides.^{58,59} Post successful release of therapeutic material into the cytoplasm, pDNA must travel to the nucleus to express the gene of interest, whereas mRNA, miRNA, and siRNA show their action outside the nucleus. Since the half-life of the foreign genetic material is around 60 minutes in the cytoplasm, owing to the presence of cytosolic nucleases, this presents a major obstacle for pDNA for nuclear entry.^{60,61} Several studies have shown the involvement of

microtubules and dynein motor proteins in the translocation of pDNA to the nucleus, which can be increased by incorporating different transcription factor binding positions, such as cyclic AMP response-element binding protein (CREB) within the plasmid.⁶²⁻⁶⁵ Subsequent entry of pDNA into the nucleus can occur in at least three different ways, such as during the breakdown of the nuclear membrane during the process of mitosis, *via* nuclear pores, and transportation across the nuclear membrane using kariophilic proteins.^{66,67} Finally, unpacking of the vector inside the nucleus is assumed to be an essential step in gene expression, although the influence of vector/gene dissociation on gene expression is difficult to understand and remains unclear.

1.1.2.3. Blood Brain Barrier

The most complex hurdle for gene delivery to the brain is the presence of the BBB. BBB is a network of tight cellular junctions and cerebral blood vessels that prevents the entry of toxins into the brain parenchyma. It acts as a barricade separating the circulatory blood from the brain tissue. BBB strictly regulates the transport of metabolically essential compounds to the brain by forming an enzymatic and physical blockade that restricts the infiltration of foreign molecules inside the brain.⁶⁸ Endothelial cells of the vasculature in the brain majorly comprise the BBB, connected *via* tight junctions and adherens, with pericytes forming a scant layer on the abluminal side. These tight junctions are less than 1 nm in diameter, severely restricting the entry of almost all macromolecules such as proteins and nucleic acids, and ~98% of small molecules.⁶⁹ Conversely, the distribution of various transmembrane proteins (adherens, claudins, and zona occludens) along the BBB helps in maintaining its integrity and facilitates the diffusion of low molecular weight hydrophobic molecules. The brain endothelium is further surrounded by end-foot processes of the astrocytes and a basement membrane. Under normal physiological conditions, microglia and neurons are also vital for the conventional integrity of the BBB.⁷⁰ Thus,

BBB by its explicit design poses a major hurdle for the transportation of therapeutic molecules to the brain parenchyma for the treatment of CNS disorders. Since, conventional methods for delivering therapeutics to the brain included BBB disruption or direct intracerebral injections, discovering and developing less invasive brain targeting routes has gained lots of attention over the past decade. This has also resulted in an increase interest in generating *in vitro* BBB models to assess new modalities for therapeutic delivery to brain.

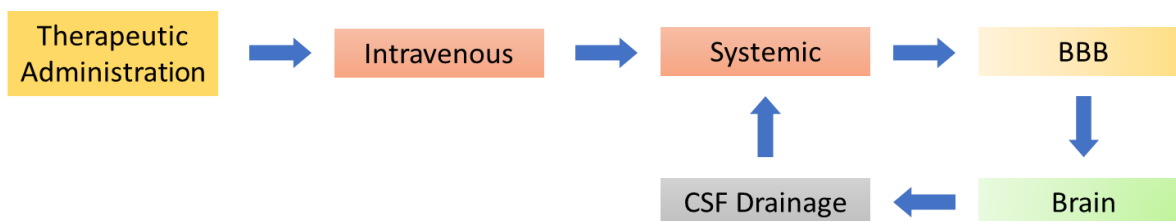


Figure 1. Potential route to the central nervous system following administration of a typical therapeutic.

The development of *in vitro* BBB models is of high significance for not only brain targeted therapeutics but also for translational research. Although, BBB model should ideally encompass all physiological and molecular characteristics of an *in vivo* system, current models are far from ideal. Over the last decade, improvement of existing methods with introduction of new technologies has resulted in significant modeling development of *in vitro* BBB. Numerous approaches had been explored to mimic BBB such as utilization of static and dynamic platforms incorporating immortalized, primary or stem cells with varying structural complexity. Even though primary cells offer various advantages by being analogous to the *in vivo* system, they are plagued with issues such as availability, yield, and purity.⁷¹ On the other hand, immortalized cells may help overcome limitations of primary cells, but they may exhibit altered expression of tight junction proteins, transporters and insensitivity to glial cells.⁷² Keeping this in mind, appropriate scientific risks must be taken in understanding the limitations while doing justice to the research conducted.

Immortalized endothelial cells for developing BBB model can be derived from different sources including murine (RBE4, bEnd.5, and bEnd.3), humans (HBB19, TY10, and HCMEC/D3) and porcine brain endothelial cells.⁷² HCMEC/D3, RBE4 and bEnd.3 are majorly utilized to develop BBB either alone or in combination with other cells.⁷³ Under static conditions, BBB models consisting endothelial cells monolayer, seeded on a semipermeable membrane, are the most simple and feasible to develop. However, these monolayer models lack modulating stimuli provided by neighboring glial cells for barrier development.⁷⁴ Therefore, BBB models consisting endothelial cells in combination with astrocytes or pericytes or both are generally employed for conducting permeability studies of the investigated therapeutic.⁷⁵ Incorporation of multiple neurovascular cell types results in improved model paracellular tightness *via* stimulation of junctional proteins expression.^{74,75} Additionally, glucocorticoids are also involved in the regulation of BBB properties along with signaling from adjacent cells.⁷⁶ Previous studies have demonstrated enhanced expression of junctional proteins (occludins and claudins) in endothelial cells of murine, porcine and human origin post glucocorticoid addition.⁷⁷⁻⁸¹ Inclusion of such factors overall results in the improvement of transendothelial electrical resistance (TEER) and prevention of BBB disruption. Hydrocortisone and dexamethasone are commonly employed glucocorticoids for modulating tightness of *in vitro* BBB models.

Various strategies have been explored to circumvent BBB to facilitate the transport of carrier vector to the brain parenchyma (**Figure 2**). These strategies include paracellular transport post disruption of tight junctions, carrier mediated transcytosis and adsorption mediated transcytosis. Paracellular transport across BBB *via* opening of tight junctions can be associated with brain disorder such as AD or can be achieved using stimuli such as ultrasounds or magnetic fields.⁸²⁻⁸⁴ Another successful strategy used over the past several decades is solute carrier mediated

and receptor mediated transcytosis to shuttle therapeutics inside the brain. This generally achieved using specific ligands to target various solute carriers (glucose transporters, amino acid transporters and organic anion transporting polypeptide) or receptors (insulin receptors, transferrin receptors, low-density lipoprotein receptors and neurotropic virulence factor receptors) present on BBB.⁸⁵ Similar to carrier mediated transcytosis, adsorption mediated transcytosis is initiated *via* electrostatic interactions between cell membrane and the carrier vector.

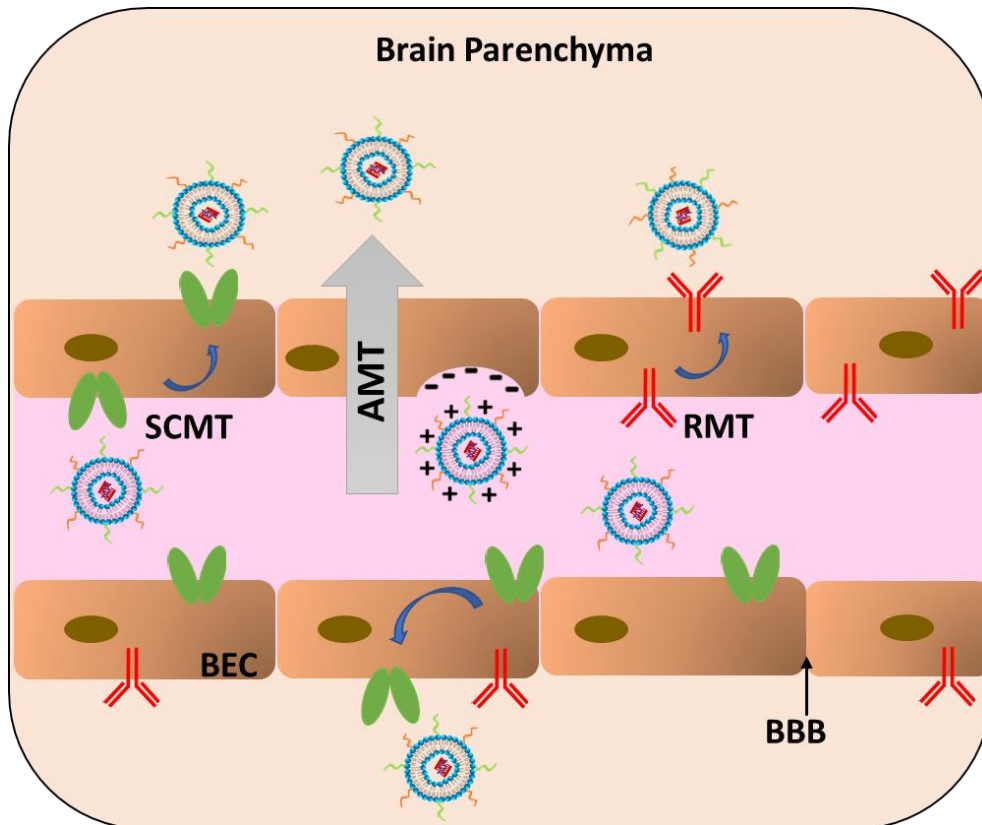


Figure 2. Active and passive translocation across the blood brain barrier. (Key: BEC: Brain endothelial cells, SCMT: Solute carrier mediated transcytosis, RMT: Receptor mediated transcytosis, AMT: Adsorption mediated transcytosis)

1.1.3. Viral vs. Non-viral Gene Therapy

Since discovering the inherent ability of viruses to transfer genetic material to the cell nucleus, it is not surprising that viruses were utilized for initial advancements in gene therapy. DNA and RNA-based therapeutics were successfully delivered in mammalian cells using

lentivirus vectors resulting in permanent modification in dividing cells *via* integration of foreign nucleic acid in the genome of the target cells. Genetic modification of cells achieved in this manner can typically lead to a permanent cure for various genetic disorders. Regarding disorders related to the CNS, most clinical trials on gene therapy adopted the method to directly introduce the virus particles in brain parenchyma *via* neurosurgical infusion in order to avoid the need to cross the BBB.⁸⁶ However, this technique is associated with serious downsides such as spatial restrictions and surgery-related side effects.⁸⁷ Less invasive routes such as intracerebroventricular (ICV) or intrathecal (IT) injections have also been explored for viral vector based gene therapy.^{88,89} Moreover, systemic administration of viral particles has also been explored for ubiquitous and non-invasive gene therapy in the brain.^{90,91} Still, these methods result in high off-target effects due to peripheral biodistribution, significant loss of virus particles, along with significant immunogenicity and toxicity concerns.^{92,93} Since virus particles have the potential to provoke strong immune responses with high levels of cytokines, safety is the foremost consideration in the development of viral gene therapies.⁹⁴ Co-administration of immunosuppressants with virus-based gene therapies is adopted in numerous clinical approaches to address immunogenicity issues. Reasonably, such therapies requiring dosage for prolonged period can severely compromise a patient's immune response, elevating risks of contracting other opportunistic disorders.⁹⁵ Furthermore, small packaging capacity, low titers, integration, modification of genome in the germ cells, and activation or potential to combine with endogenous viruses resulting in a new virus agent are some additional concerns associated with viral vectors, which has urged researchers to find safe and effective non-viral-vectors for gene therapy.⁸⁶

Non-viral gene therapy provides various advantages with respect to biocompatibility, localized gene transfection, and cost-effectiveness. Non-viral vectors are chiefly composed of

natural or synthetic compounds with low cytotoxicity and immunogenicity. These vectors usually contain high packaging capacity for genetic cargo along with ease of surface modification compared to their viral counterparts.⁸⁶ Moreover, non-viral particles are easier to manufacture and can be injected multiple times without inducing any strong immune responses.⁸⁶ Although non-viral vectors are not as efficient as viral vectors in terms of transfection efficiency and duration of gene expression, exciting advancements over the past decade have made non-viral gene therapy clinically relevant. Overall, non-viral vectors offer great flexibility in terms of their design, physicochemical characteristics, size, surface modification with different targeting moieties and other small molecules providing a major advantage over viral gene delivery systems.

1.1.4. Non-viral Gene Therapy for Alzheimer's Disease

Over the past decade, non-viral gene therapy has attracted increasing interest due to its various advantages over its viral counterparts. Moreover, advancements in non-viral gene delivery technology has led to their increasing contributions in clinical trials.⁹⁶ Non-viral gene therapy can be broadly categorized into physical or chemical methods. The physical methods of gene transfer use physical force to allow entry of therapeutic genes inside the cells, eliminating the need for a specific gene carrier for transportation purposes. Most common physical methods for gene therapy include microinjection, electroporation, gene gun, hydrodynamic injection, magnetofection, and sonoporation (**Figure 3**). These methods offer certain advantages such as simplicity and safety over other methods. However, understandably gene delivery through these methods to internal organs requires surgical interventions in order to access the target site.⁹⁷ Chemical methods utilize compounds of synthetic or natural origin to deliver an exogenous therapeutic gene inside the cells. Several advantages associated with such methods include simplicity biocompatibility, and

proficiency for sizable production. Various physical and chemical methods for non-viral gene delivery to the brain are discussed in the following sections (**Table 1**).

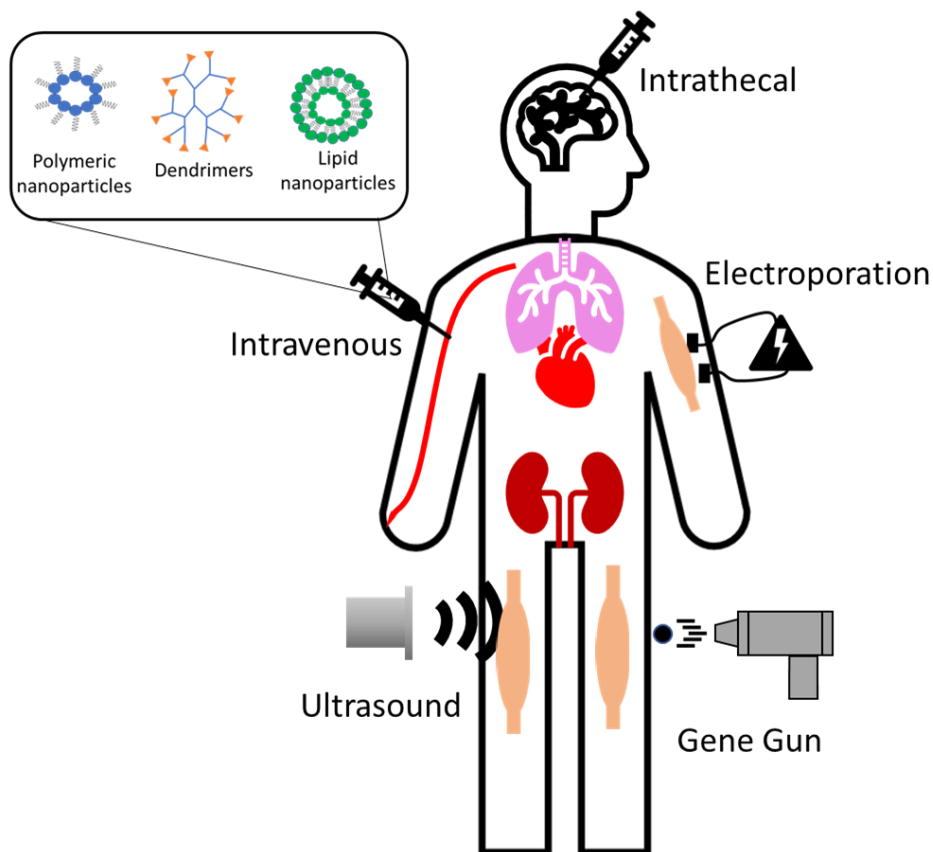


Figure 3. Various methods for non-viral gene therapy to treat Alzheimer's Disease.

1.1.4.1. Electroporation

Electroporation is a technique used to deliver DNA inside the cells with the help of electrical pulses that permeabilize the cell membrane to deliver negatively charged DNA along with the electric field. This technique is widely used *in vitro* for transfection in cells, which otherwise show poor transfection efficiency using other common methods such as lipofection or calcium–phosphate.^{98,99} The effectiveness of electroporation *in vivo* was first demonstrated in 1991 in the skin of newborn mice.¹⁰⁰ More than 50 clinical trials have been documented since then using electroporation-based DNA transfer method in patients for various disorders including cancer and

HIV.¹⁰¹⁻¹⁰³ Various attempts have also been made to develop DNA vaccines for the treatment of AD using this technique. DNA electroporation immunization *via* intramuscular administration has been explored in mice models of AD in an attempt to reduce abeta. Moreover, gene vaccine administration *via* intramuscular route has shown to increase transfection efficiency and vaccine immunogenicity by several folds.¹⁰⁴ Sha et al. had developed a novel vaccine (p(abeta₃₋₁₀)10-MT) that results in the expression of melatonin with ten repeats of abeta₃₋₁₀.¹⁰⁵ This vaccine was tested in 3 months age Tg-APP^{swE}/PSEN1^{dE9} (Tg) mice administered *via* electroporation intramuscularly in the hind leg. Post 10 immunizations 3 weeks apart, the vaccine was able to induce a high titer of antibodies against abeta. This enhanced antibody level resulted in the reduction of plaques in mice brains with improved cognition assessed by the Morris Water Maze Test.¹⁰⁵ A similar vaccine, p(abeta₃₋₁₀)10-mIL-4, resulted in the expression of interleukin-4 (IL-4) with ten repeats of abeta₃₋₁₀, was tested in 8-month age APP/PS1 transgenic mice.¹⁰⁶ The group administered the vaccine intramuscularly in the left hind leg at every 2-weeks interval and at 4-weeks intervals post third vaccination for a total of 9 injections. This resulted in the clearance of abeta with improved cognition and inflammation reduction in the brains of transgenic mice.¹⁰⁶ Electroporation has also been assessed in the macaques. AV-1955 vaccine was developed and administered in rhesus macaques inducing a strong IgG antibody response against abeta in animals receiving both low and high doses of vaccine.¹⁰⁷ Similar results were found when the same vaccine was administered in rabbits.¹⁰⁸

1.1.4.2. Gene Gun

Biolytic particle delivery system, also known as a gene gun, was first designed for genetic transformation in plant cells.¹⁰⁹ Later, this technique was successfully employed for gene delivery in mammals.^{110,111} Gene gun as a technique is relatively simple, fast, and highly effective. It

delivers gene of interest to the target tissue without any toxic chemicals. Also, this technique is independent of the type of cell and size of the plasmid. Another major advantage of this technique is that delivered gene directly enters the nucleus of the cell, evading the endo-lysosomal enzymes, preserving the dose of the therapeutic gene. Since this technique efficiently delivers a small dose of a gene to induce responses, it is an effective method for genetic immunization. Several studies have been performed to assess DNA based abeta immunization therapy in mice.¹¹²⁻¹²⁰ In 2006, Qu et al. group showed the effectiveness of DNA abeta₄₂ immunization in transgenic mouse models of AD.^{112,121} Immunization against abeta₄₂ reduced its concentration by 41% and plaques by 50% in the brains of APP^{swe}/PS1^{DeltaE9} transgenic mice.^{112,121} These results were later confirmed by other groups, which results in a strongly polarized Th2 immune response, increasing confidence in immunization against abeta.¹²² Thereafter, vaccines were developed against full-length abeta, unlike previous studies, which used parts of the abeta peptide to avoid damaging Th1 T cell response.^{119,123} A recently developed DNA vaccine against abeta₄₂ tested in rabbits and non-human primates (rhesus monkeys) *via* intradermal immunization using gene gun demonstrated a high antibody response with no signs of inflammation.^{124,125} Mounting evidence has shown that DNA abeta₄₂ immunization is safe and effective for possible clinical trial in AD patients.

1.1.4.3. Dendrimers

Since their discovery in the early 1980s, dendrimers have laid the foundation for a whole new range of novel strategies for non-viral therapeutic gene delivery applications.¹²⁶ Dendrimers are composed of synthetic macromolecules exhibiting branched, monodispersed, and distinct tree-like structures. It consists of a central core acting as an origin from which various highly branched tree-like structures originate in an organized and symmetrical manner. Their distinct molecular structure benefits them in attaining well-defined size with relatively low PDI (polydispersity

index).¹²⁷ Moreover, the high density of dendrimer terminal groups provides numerous conjugation sites for therapeutics or targeting molecules, enabling their use for targeted drug as well as gene delivery. The presence of amine groups on the surface helps in condensing DNA or RNA units into dendriplexes *via* electrostatic interactions.^{128–131} Moreover, the presence of tertiary amines can enable the endosomal escape of these nanoparticles through proton-sponge effect.¹³¹ Alkaline modified dendrimers have commonly been used as efficient gene delivery vectors for RNA and DNA based therapeutics.¹²⁷

The evaluation of gene therapy using dendrimers for the treatment of AD has not been explored much. Over the past decade, we were only able to find 3 studies that explored dendrimer-based gene delivery system for the treatment of AD. In 2016, Lie et al. developed amine-rich dendritic structures comprised of L-lysine monomers.¹³² These poly-L-lysine dendrigraft were used for the delivery of BACE1-AS shRNA to the brain post systemic administration. The cleavage of APP to form abeta peptide is through β -site APP cleaving enzyme 1 (BACE1). The BACE1 enzyme activity was found to be elevated in patients with AD, predominantly in neuronal cells surrounding abeta plaques.^{133,134} The poly-L-lysine dendrigrafts were targeted to the brain using a 29-amino acid peptide called rabies virus glycoprotein (RVG), which targets nicotinic acetylcholine receptors extensively present on brain cells and BBB.¹³⁵ Hence, gene targeting to the brain for silencing the expression of BACE1 mRNA using poly-L-lysine dendrigrafts is a promising approach to decrease the abeta burden.¹³⁶ This study demonstrated the reduction in the level of BACE1 mRNA in AD mice post-treatment with nanoparticles complexed with shRNA against BACE1, further leading to the reduction of abeta formation in mice brain. These nanoparticles were also able to attenuate the advancing of AD behavioral indicators.¹³² Interestingly, BACE1 gene silencing efficacy using dendrimers was also studied recently using

siRNA *in vitro* as well as *in vivo*. These dendrimers were surface modified to target brain neurons utilizing Apo A-I and NL4 peptide. Apo A-I protein was used for targeting scavenger receptor B1 (SRB1) on BBB, whereas NL4 peptide was used to target tyrosine kinase A receptors present on neurons. These dendrimers resulted in 87.5% BACE1 gene knockdown capacity *in vitro* in bEnd.3 and PC12 cells.¹³⁷ The *in vivo* efficacy of this treatment was evaluated using mean escape latency in APP/PS1 transgenic mice, which improved the spatial learning and memory of these AD mice with no signs of toxicity to the animals.¹³⁸

1.1.4.4. Polymers

Polymers are one of the most used materials for gene therapy due to their numerous distinct characteristics, such as ease of synthesis, flexibility in structural conformations, biocompatibility, and biodegradability. These advantages provide a wide range in the designing of polymeric gene delivery vectors with desired characteristics. The differences in the shape (branched/linear), molecular weight, as well as number and type of monomer units altogether affect the physicochemical properties of the resulting polymeric vectors. There are various natural and synthetic polymers that exhibit desired characteristics to be used as gene delivery vectors. The major complexing mechanism for polymers to associate with the gene of interest is electrostatic interactions between gene and polymer chains, which also protects the therapeutic gene from enzymatic degradation. These polyplexes can be surface modified with different ligands to target or improve internalization into cells.¹³⁹ Various cationic polymers have been explored, however, poly-L-lysine (PLL) and poly(ethylenimine) (PEI) are the most widely used synthetic polymers by researchers around the globe. Alternatively, chitosan is one of the most widely used natural polymer used as a gene delivery vector. Chitosan is a naturally derived cationic carbohydrate polymer which is an attractive candidate as a gene delivery vector due to its biodegradability and

wide safety profile.¹⁴⁰ Given the various strengths of these polymeric vectors, they provide a promising approach as a non-viral gene delivery technology for the treatment of AD.

Over the past decade, polymeric vectors have been used extensively to deliver various types of siRNAs and plasmid DNAs across the BBB to treat AD. siRNA gene therapy had been used to influence the neural stem cells (NSCs) for the recovery of CNS.¹⁴¹ PEG-PEI was used to deliver siRNA to NSCs. The size of these nanocomplexes was around 200 nm and demonstrated effective transfection efficiency with low toxicity in NSCs compared to commercially available reagent lipofectamine. These nanoparticles successfully silenced the Nogo receptor (NgR) gene expression, which may act as a potential CNS regeneration strategy.¹⁴¹ In another study, PEG-PEI nanoparticles were used for the delivery of siRNA against ROCKII. ROCKII is a transcription factor, which inhibits growth in an injured environment in the AD brain. The intrathecal injection of this PEG-PEI/siRNA led to enhance spatial learning in senescence-accelerated mice model of age related cognitive decline.¹⁴² PEG-PEI based nanoparticles were also used to deliver siRNA against BACE1 and APP, which are the major targets of AD. Different micellar nanoparticles were developed in worm, rod, and spherical shapes, tested to be stable in physiological conditions. However, *in vivo* rod-shaped micelles demonstrated the most effective and selective knockdown of BACE1 gene post intraventricular infusion in mice.¹⁴³ Recently, PEGylated poly(2-(N,N-dimethylamino) ethyl methacrylate) (PEG-PDMAEMA) based nanoparticles were developed and assessed for their efficiency to deliver siRNA against BACE1 in double transgenic APP/PS1 mouse model of AD.¹⁴⁴ These nanoparticles were modified with CGN (d-CGNHPhLAkYNGT) peptide for BBB targeting and QSH (QSHYRHISPAQVC) peptide which helped in its binding to the $\text{A}\beta_{1-42}$ having a dissociation constant in the lower micromolar range.¹⁴⁵ These nanoparticles post complexation with siRNA demonstrated the size of approximately 70 nm with no signs of

aggregation in blood or brain tissues. Evaluation of pharmacokinetic parameters was also performed post intravenous administration of these nanoparticles, indicating major distribution in the liver, kidneys and spleen.¹⁴⁴ Quantification of injected dose in the hippocampus showed 3.18% ID/g tissue indicating that QSH surface modification helped in directing these nanocomplexes to amyloid plaques. The treatment also resulted in effective inhibition of BACE1 expression and its downstream pathway. Intravenous administration of these nanoparticles also resulted in improved cognitive performance in transgenic mice evaluated using the Morris water maze test.¹⁴⁴

1.1.4.5. Lipid-based Nanoparticles

Lipid-based nanoparticles are one of the most common and well-explored non-viral vectors for targeted delivery of therapeutics. These nanocarriers have shown potential for improving the stability and pharmacokinetics of therapeutic compounds, alongside allowing efficient internalization in target tissues *in vivo*. Lipid nanoparticles majorly comprise solid lipid nanoparticles (SLN) and liposomes. Liposomes and SLN are generally spherical in shape composed of biodegradable lipids. SLN contains a solid lipid core, which is stabilized by the presence of surfactants, whereas, liposomes are phospholipid vesicles that are hollow at the center, enclosing discrete aqueous spaces. Liposomes can be small unilamellar or multilamellar based on the lipid composition and the method of preparation of these nanoparticles. Liposomes have the unique property to encapsulate both hydrophobic and hydrophilic molecules, enabling them to entrap a diverse range of therapeutic moieties. Lipophilic compounds get entrapped into the lipid bilayer, whereas hydrophilic compounds get inserted in the aqueous core of these nanoparticles. As a non-viral vector, lipid-based nanoparticles offer numerous advantages such as biocompatibility, high encapsulation efficiency, and ease of modification to alter physicochemical and biophysical properties to achieve desired characteristics.

In the recent decade, various types of lipid nanoparticles have been explored for brain-targeted delivery of siRNAs and pDNAs to treat AD. One of the most used lipid nanoparticles for gene therapy are cationic liposomes, which spontaneously self-assemble by electrostatic complexation with the therapeutic gene for efficient transfection *in vitro* and *in vivo*. Cationic liposomes have been extensively explored for the delivery of various therapeutic genes such as NGF (nerve growth factor), ApoE2, and siRNA against BACE1 enzyme. Anionic liposomes, conjugated to a cationic peptide, have also been explored for the delivery of genetic material. Anionic PEGylated liposomes composed of DOPG: DOPE (1:1) and short cationic peptides have been utilized to deliver siRNA for BACE1 enzyme for treating AD.¹⁴⁶ Although, packaging of siRNA in the anionic liposomes was found to be less efficient than their cationic counterparts, anionic liposomes demonstrated superior stability in the presence of serum. These anionic nanoparticles showed comparable gene silencing with that of Lipofectamine 2000 *in vitro* in Neuro-2A cells.¹⁴⁶ *In vivo* evaluation of these liposomes was performed in adult Wistar rats (male) *via* direct infusion to the striatum in the brain, resulting in silencing of BACE1 mRNA expression (60%) compared to the control.¹⁴⁶ This study demonstrates the potential of anionic nanoparticles in gene silencing for treating AD. SLNs have also been explored for the delivery of siRNA against the BACE1 as a nose-to-brain delivery system.¹⁴⁷ These SLNs were coated with chitosan to enhance their paracellular transport across BBB and to increase the mucoadhesive properties of the system. RVG-R9 peptide was used for complexing siRNA and enhancing neuronal uptake of the therapeutic gene. Although the authors did not analyze the efficacy of the delivery system, these nanoparticles were able to efficiently encapsulate and deliver siRNA across the cell membrane in Caco-2 cells.¹⁴⁷

Recently, our group has explored the potential of liposomes to deliver NGF pDNA to the brain for the treatment of AD. NGF protein is one of the vital neurotrophic factors required for proper functioning and maintenance of the central as well as peripheral nervous system.¹⁴⁸ These factors prevent degenerative processes by promoting functioning and development of brain cells. In AD, regulation of NGF appears to be disturbed leading to neuronal degeneration. Hence, these essential proteins have been explored extensively to treat AD.¹⁴⁸ In these studies, cationic lipid DOTAP, DOPE (helper lipid), and PEGylated lipid DSPE were utilized to manufacture liposomal nanoparticles with various targeting ligands for directing the genetic cargo to the brain.¹⁴⁹ In these studies, pDNA was complexed with chitosan prior to encapsulation inside liposomes, which further helped in the condensation of the therapeutic gene, protection from nuclease present in biological fluids, and facilitation of escape from endosomal compartment post endocytosis.^{150–152} These nanoparticles were targeted to the brain *via* modification with transferrin (Tf), a substrate for transferrin receptor that is present in high density at BBB. Additionally, in order to enhance the cell penetration and attenuate the competition with physiological substrates, these liposomes were further modified with cell-penetrating peptides (CPP), penetratin (Pen). TfPen modified cationic liposomes were 150-200 nm in size and did not demonstrate any toxic effects *in vitro* and *in vivo*. These liposomes were also capable of preventing the degradation of the encapsulated therapeutic gene in the presence of nucleases.^{153,154} Additionally, transfection of NGF protein in primary neuronal cells led to an increase in synaptophysin protein, a presynaptic marker, which shows the potential of these nanoparticles to salvage brain cells from synapse dysfunction in AD. Notably, Tf receptor targeting also helped transport liposomes inside the brain to allow transfection in brain cells to produce NGF protein *in vivo*.^{155,156} Interestingly, these nanoparticles were able to rescue APP/PS1 mice by reducing toxic abeta peptides levels (insoluble and soluble fractions)

increasing levels of both pre- and post-synaptic markers. Additionally, NGF protein expression also resulted in neurogenesis in AD mice model evaluated using ki-67 mitosis marker.¹⁵⁶ Thus, gene delivery for selective neurotrophic factors has the potential to treat AD pathology *via* reduction in abeta protein, increase of synaptic activity, and neurogenesis.

Table 1. Non-viral gene delivery methods for the treatment of Alzheimer's disease.

Delivery technique/system	Therapeutic cargo	Targeting moiety	CPP	Animal model	Route of administration	Major effects	Ref
Physical methods							
Injection	DNA vaccine encoding A β gene	-	-	TgCRND8 mice	Intramuscular injection in the tibialis anterior muscle	<ul style="list-style-type: none"> Reduced plaque load by $36 \pm 8\%$ and insoluble Aβ42 levels by $56 \pm 3\%$ Decreased cerebral amyloid angiopathy by $69 \pm 12\%$ 	¹²²
Electroporation (50 V/cm, 6 pulses, 20ms per pulse)	Plasmid encoding human neprilysin (phNEP)	-	-	KunMing mice	Intramuscular injection on the hindlimb skeletal muscle followed by electroporation	<ul style="list-style-type: none"> Efficient long-term expression of the encoded polypeptide 	¹⁵⁷
Electroporation	DNA vaccine encoding ten tandem repeats of A β ₃₋₁₀ fused with mouse IL-4 (p(A β ₃₋₁₀)10-mIL-4)	-	-	APP/PS1 transgenic mice	Intramuscular injection in the quadriceps femoris muscles of left hind legs followed by electroporation	<ul style="list-style-type: none"> Induced a Th2-type immune response with high-titer anti-Aβ antibodies Reduced Aβ deposition and decreased inflammation in the mice brain, leading to improved cognitive functions 	¹⁰⁶
Electroporation with variable pulse parameters	DNA vaccine encoding A β 42 trimer	-	-	BALB/C-Foxp3 EGFP/J transgenic mice	Intradermal immunization <i>via</i> electroporation	<ul style="list-style-type: none"> Induced high anti-Aβ42 antibody titers and low levels of inflammatory cytokines Low voltage and short pulse duration led to higher IgG1 antibody level 	¹²⁰
Gene gun	DNA vaccine encoding A β 42 gene (pSP72-E3L-A β 42)	-	-	APPswe/PS1 Δ E9 transgenic mice	Immunizations on ear skin using gene gun	<ul style="list-style-type: none"> Induced a Th2-type immune response with high titers of anti-Aβ42 antibody Aβ42 levels in the treated mice brain decreased by 60–77.5% 	¹²⁰
Gene gun	DNA vaccine encoding A β 42 trimer	-	-	New Zealand White rabbits	Intradermal immunizations into skin of the outer ear using gene gun	<ul style="list-style-type: none"> Induced good anti-Aβ antibody response with no signs of inflammation Low numbers of IFNγ and IL-17 producing cells were detected in spleen 	¹²⁴

Table 1. Non-viral gene delivery methods for the treatment of Alzheimer's disease (continued).

Delivery technique/system	Therapeutic cargo	Targeting moiety	CPP	Animal model	Route of administration	Major effects	Ref
Gene gun	DNA vaccine encoding A β 42 trimer	-	-	Rhesus monkeys	Intradermal immunization into the skin of the upper inner arm using gene gun	<ul style="list-style-type: none"> Induced high antibody response with no signs of inflammation T-cell responses revealed no IFN-γ- and IL-17-producing cells from PBMCs 	¹²⁵
Chemical methods							
RVG-modified poly (mannitol-co-PEI (R-PEG-PMT) polymer	siBACE1	-	RVG	BALB/C mice	Intravenous injection	<ul style="list-style-type: none"> R-PEG-PMT/siBACE1 complexes exhibited 2.32-fold and 3.03-fold reduction of BACE1 expression in cortex and hippocampus parts of the mice brain BACE1 down-regulation was strongly related with the reduction of Aβ42 level 	¹⁵⁸
PEGylated poly(2-(N,N-dimethyl amino) ethyl methacrylate) (PEG-PDMAEMA) polymer surface-modified with both CGN and QSH peptides.	BACE1-siRNA	CGN peptide (BBB targeting ligand), QSH peptide (A β -targeting ligand)	-	APP/PS1 transgenic mice	Intravenous injection	<ul style="list-style-type: none"> Effective inhibition of BACE1 expression Improvement in synaptophysin level and restored cognitive performance in APP/PS1 transgenic mice 	¹⁴⁴
RVG29 and D-peptide modified PEGylated dendrigraft poly-L-lysine (DGLs-PEG-RVG29)	Plasmid encoding BACE1-AS shRNA	-	RVG29	Transgenic AD mice	Intravenous injection	<ul style="list-style-type: none"> Reduction of Aβ level by BACE1-AS knockdown Simultaneous delivery of the D-protein into brain results in reduction of neurofibrillary tangles 	¹³²

Table 1. Non-viral gene delivery methods for the treatment of Alzheimer's disease (continued).

Delivery technique/system	Therapeutic cargo	Targeting moiety	CPP	Animal model	Route of administration	Major effects	Ref
NL4 peptide and apolipoprotein A-I (Apo A-I) modified dendrigraft poly-L-lysine	BACE1 siRNA	NL4 peptide (target tyrosine kinase A receptors present on neurons), Apo A-I (target scavenger receptor B1 on BBB)	-	APP/PS1 transgenic mice	Intravenous injection	<ul style="list-style-type: none"> Significantly reduced BACE1 RNA level Improvement in the spatial learning and memory of APP/PS1 transgenic mice 	¹³⁸
PEGylated poly (2- (N, N-dimethylamino) ethyl methacrylate) (PEG-PDMAEMA) surface-modified with both CGN and QSH peptides.	BACE1-siRNA	CGN peptide (BBB targeting ligand), QSH peptide (A β -targeting ligand)		APP/PS1 transgenic mice	Intravenous injection	<ul style="list-style-type: none"> Effective inhibition of BACE1 expression Improvement in synaptophysin level and restore cognitive performance in APP/PS1 transgenic mice 	¹⁴⁴
Transferrin and penetratin dual functionalized liposomes	Plasmid expressing nerve growth factor (pNGF)	Transferrin (target transferrin receptor on BBB)	Penetratin	APP/PS1 transgenic mice	Intravenous injection	<ul style="list-style-type: none"> Reduction of the levels of toxic soluble and insoluble Aβ peptides Improvement in synaptophysin level 	¹⁵⁶
Transferrin and penetratin dual functionalized liposomes	Plasmid encoding ApoE2 (pApoE2)	Transferrin (target transferrin receptor on BBB)	Penetratin	C57BL/6 mice	Intravenous injection	<ul style="list-style-type: none"> Dual functionalized liposomes efficiently delivered pApoE2 gene into the mouse brain and enhanced ApoE2 expression Formulations were biocompatible and safe 	¹⁴⁹

1.1.4.6. Peptides

Non-viral gene delivery vectors, majorly nanoparticles, have relied heavily on various brain targeting peptides for their efficient and effective transport across the BBB. Therefore, in this section we have briefly discussed various peptides commonly used for brain targeting. These peptides are generally defined as short chain amino acid residues (≤ 50 amino acids) with extensive structural properties that enable them to express various functionalities for gene delivery applications. The popularity of peptide vectors has increased over the past decade due to their relative stability and ease of modification to achieve high biocompatibility and low immunogenicity profile of non-viral gene delivery vectors.^{159,160} Large proteins and antibodies have also been explored with good success, however, activation of immune response and expensive manufacturing pose as major hurdles in their development. Since peptides are small and do not possess any rigid structure, they are easier to synthesize and characterize by allowing modification using various functional groups. Peptides that enable brain targeting in a non-specific manner are categorized as cell-penetrating peptides (CPPs). These peptides majorly contain small cationic or amphiphilic amino acid chains which can transport across cellular membranes without the aid of any transporter or receptor. However, endocytosis remains the major mechanism of internalization for these CPPs.¹⁶¹ At first, various CPPs were produced as derivatives of proteins e.g. penetratin. However, synthetically designed chimeric peptides with desired features of CPPs have also been successfully produced e.g. RVG-9R. These peptide sequences have been successfully utilized either alone or conjugated to the surface of various nanoparticles for delivering therapeutic molecules to the brain.¹⁶² A recent study utilized R7L10 peptide for downregulation of the BACE1 gene *via* CRISPR–Cas9 technology.¹⁶³ Nanocomplexes were prepared using R7L10 peptide and Cas9–sgRNA, and were injected directly inside the brain of 6-

month old AD mice. These injections resulted in successful targeting of the BACE1 gene with minimal off-target effects in mice.¹⁶³ In another study, CPP transportan (GWTLSAGYLLGKINLKALAALAKKIL), was modified with myristic acid and transferrin receptor-targeting peptide for Neuro-siRNA therapy.¹⁶⁴ The human placental alkaline phosphatase (hPAP) reporter assay and luciferase assay were performed *in vitro* to demonstrate gene silencing *via* this peptide/gene complex. However, further *in vivo* studies are required for validating the gene silencing ability of this chimeric peptide inside the brain.¹⁶⁴

1.2. Statement of Problem and Research Objective

AD is a serious health issue and the most common form of dementia around the world causing a huge burden on the public health system. The cause of AD is believed to be due to complex interactions among genetic, environmental, and lifestyle factors.¹⁶⁵ AD is a chronic disorder that leads to a progressive decline in various brain functions, including memory, intellectual, direction, comprehension, logical, linguistic, and judgment ability.¹⁶⁶ High incidence and huge socioeconomic cost associated with AD makes it a priority for medical research today. Although rigorous attempts have been made in favor of AD research over past few decades, current treatments only provide symptomatic relief.¹⁶⁶ Currently, only four drugs have been approved by the FDA for the treatment of AD, which primarily work to improve the quality of life of affected patients by managing the symptoms. Unfortunately, none of these drugs can halt the rapid and lethal advancement of AD progression.¹⁶⁷ Moreover, as the disease advances, the efficacy of these therapeutics reduces despite their increasing dosage. However, recent advancements in medical technology have helped in understanding AD pathophysiology. It has been found that neurotrophic factors and apolipoprotein E (ApoE) are the major factors associated with this disorder.^{148,168}

Neuroinflammation, neurodegeneration, and cognitive decline due to abeta protein can be potentially rescued by therapies using neurotrophic factors.⁹⁻¹¹ Brain-derived neurotrophic factor (BDNF) is a member of the neurotrophic factor family that has been considered of highest therapeutic value in the treatment of AD. BDNF plays a major role in neuronal plasticity, synapse formation, and long term potentiation.¹² BDNF protein activates its receptor, TrkB, which leads to differentiation, plasticity, and survival of neuronal cells in the CNS as well as in the peripheral nervous system (PNS).¹³ Additionally, BDNF is linked to the activation of translational machinery and protein synthesis in neurons.¹⁴ Decreased levels of BDNF protein are frequently associated with neurodegeneration in the hippocampus and cortex regions of AD patients.¹⁵⁻¹⁷ Moreover, loss of BDNF signaling has also been implicated in the increase of APP and activation of amyloidogenic pathways.¹⁸ Whereas, rescuing BDNF signaling has shown to attenuate abeta formation with enhanced synaptic proteins level.^{30,31,169} Therefore, BDNF delivery to the brain can potentially ameliorate AD-related pathophysiology. However, due to short *in vivo* half-life and poor pharmacokinetic properties, safe and efficient delivery of BDNF to the brain remains a significant hurdle in the development of disease-modifying therapy for AD.¹⁷⁰

Another protein which is involved in the processing of abeta is ApoE. ApoE is the primary apolipoprotein present in the brain, and is involved in synaptogenesis and cholesterol transportation and distribution.¹⁷¹ ApoE has three isoforms, namely E2, E3, and E4, each of them predominantly expressed in the brain and liver.¹⁷² These isoforms differ from one another at 112 and 158 positions in their protein structure.¹⁷³ Inheritance of ApoE4 is found to be the major risk factor for AD.¹⁶⁸ Moreover, ApoE4 homozygotes have an approximately 14.5-fold higher risk of developing AD in comparison to ApoE3 homozygotes.^{174,175} On the other hand, the E2 allele is found to be protective. ApoE2 allele reduces AD risk by 50%, and even in the presence of the E4

allele has been found to delay the age of onset.^{176,177} Experimental evidence shows that ApoE isoforms are chief elements influencing concentration and quality of abeta peptide as well as abeta burden in the brain that accumulate during aging.¹⁷⁸ ApoE regulates abeta clearance in an isoform dependent manner.¹⁷⁹ The isoform E4 was found to be least effective in clearing abeta from the brain in mouse model of AD, whereas isoform E2 was found to be most effective.¹⁷⁹ This can be attributed to the poor binding affinity of ApoE4 towards abeta compared to other isoforms, resulting in isoform dependent clearance (E2 > E3 > E4) through neurons and microglia.^{180–182} ApoE4 isoform is also shown to be linked with shorter dendrites, lower spine densities in basal shaft dendrites, and declining cognitive performance compared to E2 isoform.¹⁸³ Moreover, during aging, ApoE levels were found to be reduced in the hypothalamus and cortex which may further attenuate the clearance of toxic abeta proteins.¹⁸⁴

Additionally, vgf, a neurotrophin stimulated protein, which plays crucial role in memory formation, learning, enhancement of synaptic activity, and neurogenesis, has been found to be downregulated in the AD.^{19–26} Vgf is a neurotrophic factor inducible protein, which can be stimulated by neurotrophin-3 (NT-3), BDNF and NGF.^{27,28} Post synthesis, vgf protein is processed intracellularly with tissue and cell specificity leading to the formation of various bioactive peptides, which are then released from the cells. These secreted peptides are involved in various functions such as memory formation, depression, learning and neurodegenerative disorders including AD.^{33,185,186} Increase in the expression of the vgf protein has shown to attenuate AD related phenotypes including reduction in the abeta toxicity and neuroinflammation.^{32,33} Therefore, transport of vgf inside the brain can result in promising beneficial effects for attenuating AD pathophysiology.

However, BBB, the very impediment that protects the brain from harmful toxins and pathogens, is a major limitation of current therapies in treating various brain disorders. BDNF, ApoE2, and vgf being large polar proteins, ranging from 35 – 65 kDa, are unable to transport across the BBB and cellular membranes. Highly invasive intracerebroventricular delivery of these proteins has shown promising results in attenuating AD related pathophysiology.^{32,169,187} However, in order to deliver high levels of these therapeutic proteins to the brain while eliminating highly invasive and complicated procedures, a safe and efficient gene delivery vector is critical.

Recent advancements in the medical field have paved the way for the development of gene therapies for the treatment of AD. Gene therapy has the potential to modify the expression of specific proteins, which can help in improved neuroprotection, synaptic plasticity, neuronal plasticity, etc. However, the success of gene therapy majorly depends on the development of safe and efficient gene delivery vectors to improve cellular delivery and half-life of therapeutic genes.¹⁸⁸ Another major obstacle in the path of gene delivery is the presence of the BBB. The BBB is a transport barrier that prevents the entry of any foreign molecules inside the brain. Viral vectors such as adeno associated virus (AAV) and lentiviral particles have been used for gene delivery to the brain.^{189,190} However, the biodistribution profiles of these vectors and deactivation by serum proteins make their utilization *in vivo* a challenging task.¹⁹¹ Moreover, insertional mutagenesis, inflammatory responses, cellular or humoral immunological responses are some of the critical drawbacks associated with popular viral vectors.¹⁹² Fatal consequences have been reported owing to serious adverse reaction of viral vectors promoting increased interest in the development of safe and effective non-viral gene delivery systems.^{94,191}

Over the past few decades various non-viral gene delivery systems have been developed. Among them, cationic liposomes have been extensively explored for the delivery of various

therapeutic genes. Liposomes are versatile and can be efficiently surface modified along with favorable physicochemical properties by using selective composition of phospholipids. These lipid nanoparticles were shown to be safe and effective in delivering their genetic cargo.¹⁹³ Furthermore, complexation of pDNA with chitosan prior to encapsulation inside liposomes helps in the condensation of the therapeutic gene, protection from nuclease present in biological fluids, and facilitation of escape from endosomal compartment post endocytosis.^{140,194} An important characteristic of liposomal nanoparticles is their ability to be surface modified easily. Chemical conjugation of specific ligands to the lipids can be efficiently used to target selective receptors and transporters. GLUT-1 (SLC2A1), a sodium independent facilitative transporter, is the most abundant transporter present at the BBB.^{195,196} This transporter also recognizes and transports mannose, glucosamine, and galactose.¹⁹⁷ Inside the brain, GLUT-1 and GLUT-3 are the major transporters present on astrocytes, glial cells, and neurons.¹⁹⁷ Consequently, these transporters are increasingly recognized as targets to deliver therapeutics inside the brain. Liposomal nanoparticles can be surface modified with mannose to target GLUT-1 transporters present on the BBB. A study on human tissues reported that GLUT-1 is either absent or below the limit of detection in many normal tissues, including breast, ovary, pancreas, uterus, thyroid, stomach, and skeletal muscles.¹⁹⁸ Therefore, targeting GLUT-1 will also lead to minimal off-target effects. To enhance the cell penetration and overcome competition with physiological sugars, these liposomes can further be modified with cell-penetrating peptides (CPP).

CPPs such as penetratin (Pen), rabies virus glycoprotein peptide (RVG), rabies virus glycoprotein peptide-9R (RVG9R), rabies virus derived peptide (RDP), or CGN (CGNHPHLAKYNGT) peptide can be used to decorate the surface of liposomes. The surface modification with these CPPs has shown enhanced transportation across BBB *via* direct

penetration or by acetylcholine receptor-mediated transcytosis.¹⁹⁹⁻²⁰² RVG9R and RDP both are derived from rabies virus glycoprotein, whereas CGN peptide is obtained from *in vivo* phage display screening.²⁰³⁻²⁰⁵ Monumental evidence suggests that nanoparticles modified using brain targeted ligands in combination with RVG and its derivatives (RVG9R and RDP) have resulted in very promising brain targeting for treatment of glioblastoma, AD, Parkinson's disease, etc.^{155,206,207} Pen is a CPP that has been previously evaluated in multiple *in vivo* studies from our group as well as other researchers with very promising results for the delivery of nanoparticles, nucleic acids, and antibodies to brain for the treatment of brain cancer, Alzheimer's disease and various other brain disorders.²⁰⁸⁻²¹⁰ Moreover, a comprehensive study evaluating the pharmacokinetics of various CPPs have shown Pen as the most favorable for selective delivery to the brain.²¹¹

Based on these observations, **we hypothesize that surface modification of liposomal nanoparticles with brain targeting ligands (MAN) in combination with CPP will improve their translocation across BBB via GLUT-1 transporter targeting and enhanced cellular penetration, to deliver genetic material (pDNA encoding for BDNF, vgf or ApoE2) capable of transfecting brain cells and producing the respective protein (Figure 4).**

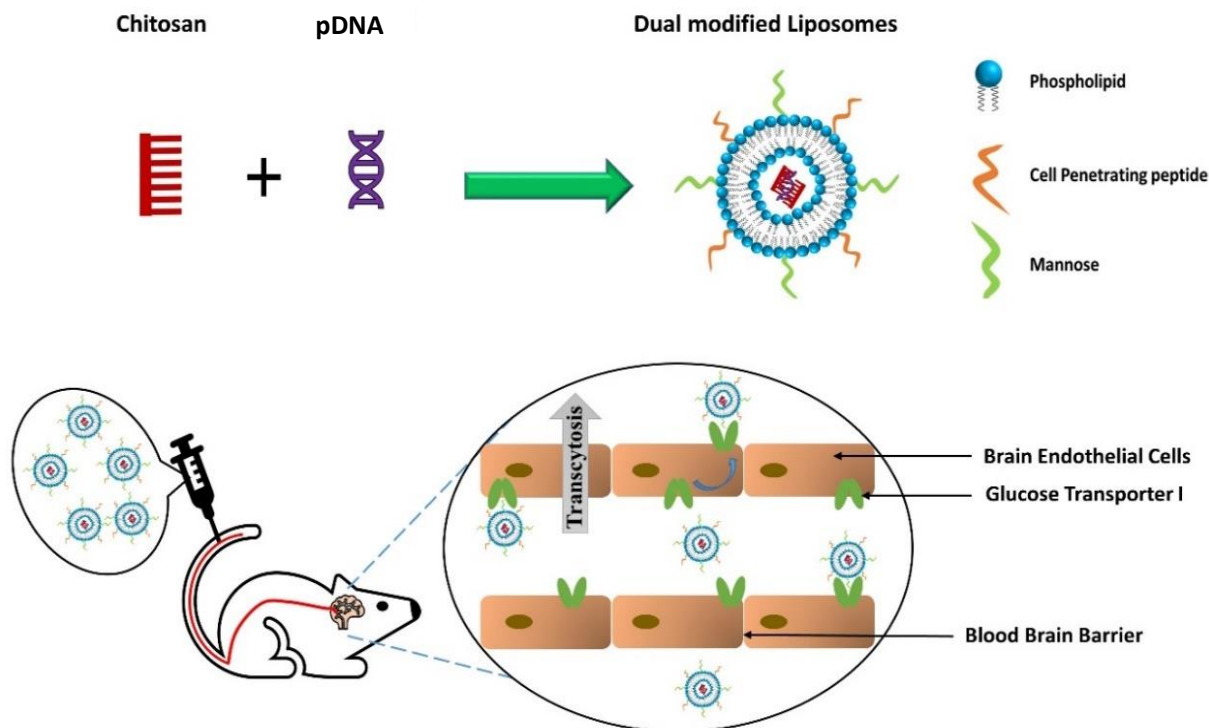


Figure 4. Schematic of surface functionalized liposomal nanoparticles-based delivery system administered using tail vein injection in mouse model for transportation of genetic cargo (plasmid DNA complexed with chitosan polymer) across blood brain barrier for the treatment of Alzheimer’s disease.

We tested our hypotheses through the following specific aims:

1.2.1. Specific Aim 1: To Synthesize and Characterize MAN and CPP Coupled Liposomes

Encapsulating Plasmid DNA and Chitosan Complexes

- To synthesize and characterize DSPE-PEG-NHS conjugated to cell penetrating peptides.
- To prepare brain targeted liposomes using modified DSPE-PEG *via* film hydration technique and characterize them for their size, charge, polydispersity index, and encapsulation efficiency of the therapeutic gene.
- To study ability of liposomes to protect therapeutic gene from DNase enzyme.
- To study cellular toxicity, uptake, internalization mechanism, and transfection using liposomes encapsulating pDNA.

- To assess transport and transfection efficiency of liposomal nanoparticles across *in vitro* BBB model.

1.2.2. Specific Aim 2: To Assess Biocompatibility, Biodistribution and Transfection

Efficiency of Dual Modified Liposomes *In Vivo* in C57BL/6 Mice

- To evaluate *in vivo* biodistribution of surface modified liposomes entrapping lissamine rhodamine dye utilizing HPLC.
- To evaluate *in vivo* transfection efficiency of liposomes entrapping therapeutic plasmid DNA using ELISA.
- To evaluate *in vivo* biocompatibility of liposomes entrapping therapeutic plasmid DNA *via* histological analysis of tissue sections from various organs.

1.2.3. Specific Aim 3: To Assess Formulation Efficacy *In Vivo* in Transgenic Mouse Model of Alzheimer's Disease

- To evaluate *in vivo* transfection of liposomes in the brain of 6- and 9-month old APP/PS1 transgenic AD mouse model.
- To assess various fractions of amyloid beta 40 and 42 in brain of 6- and 9-month old APP/PS1 transgenic AD mouse model post BDNF transfection.
- To assess levels of pre and post synaptic markers using ELISA in brain of 6- and 9-month old APP/PS1 transgenic AD mouse model.
- To assess plaque load and cell proliferation in the cortex and hippocampus regions of the brain utilizing immunohistochemical analysis.
- To assess nesting behavior in APP/PS1 transgenic AD mice before and after liposomal transfection.

2. MATERIALS AND METHODS

2.1. Materials

The list of materials used in this study is presented in **Table 2**.

Table 2. Materials used and their source.

Materials	Source and location
10% Neutral buffered formalin	Richard-Allan Scientific (Kalamazoo, MI, USA)
2,4,6-Trinitrobenzenesulfonic acid solution (TNBSA)	Sigma–Aldrich (MO, USA)
3-(4,5-Dimethylthiazol-2-yl)-2,5-diphenyl-tetrazolium bromide (MTT)	Sigma–Aldrich (MO, USA)
bEnd.3 cells	American Type Culture Collection (ATCC, Rockville, MD, USA)
Acetonitrile	Sigma Aldrich Co. (St. Louis, MO, USA)
Beta-galactosidase enzyme assay kit	Promega (Madison, WI, USA)
Cell penetrating peptides (CPP)	Zhejiang Ontores Biotechnologies Co., Ltd. (Zhejiang, China)
Chitosan (average molecular weight 30, ~85-90% degree of deacetylation)	Glentham Life Sciences (Corsham, WT, UK)
Cholesterol	Sigma-Aldrich (St. Louis, MO, USA)
Dimethyl sufoxide	Calbiochem USA
Dioleoyl-sn-glycero-3-phosphoethanolamine (DOPE)	Avanti Polar Lipids (Birmingham, AL, USA)
Dioleoyl-3-trimethylammonium propane chloride (DOTAP)	Avanti Polar Lipids (Birmingham, AL, USA)
DSPE-PEG2000-Mannose	Biochempeg Scientific Inc. (Watertown, MA, USA).
DSPE-PEG2000-NHS	Biochempeg Scientific Inc. (Watertown, MA, USA).
Dulbecco’s modified eagle’s medium (DMEM)	American Type Culture Collection (ATCC, Rockville, MD, USA)
Fetal bovine serum (FBS)	Omega Scientific (Tarzana, CA, USA)
Hoechst 33342	Sigma-Aldrich (St. Louis, MO, USA)
Lissamine rhodamine B	Avanti Polar Lipids (Birmingham, AL, USA)
Micro BCA protein assay kit	Pierce Biotechnology Inc. (Rockford, IL, USA)
Phosphate buffered saline (PBS)	American Type Culture Collection (ATCC, Rockville, MD, USA)
Plasmid DNA encoding beta-galactosidase (Gwiz-βgal)	Aldevron LLC (Fargo, ND, USA)
Plasmid DNA encoding green fluorescent protein (Gwiz-GFP)	Aldevron LLC (Fargo, ND, USA)
Plasmid DNA encoding BDNF	Sino Biological (PA, USA)
Plasmid DNA encoding ApoE2	Addgene (USA)
Plasmid DNA encoding VGF	Sino Biological (PA, USA)
α-D-Mannopyranosylphenyl isothiocyanate	Toronto Research Chemicals (Toronto, ON, Canada)

2.2. Animals

Animal study protocol and experiments were reviewed and approved by the North Dakota State University Animal Care Use Committee (IACUC, Protocol #A20063 and #A17078). 4 weeks old C57BL/6 and APP/PS1 mice were purchased from The Jackson laboratory USA.

2.3. Experimental Methods

2.3.1. Coupling of Cell Penetrating Peptide to DSPE-PEG(2000)-NHS

Cell penetrating peptides were coupled to lipid DSPE-PEG(2000)-NHS by nucleophilic substitution reaction. The PEGylated lipid and CPP (1:3 molar ratio) were dissolved in dimethylformamide (DMF). The pH of the mixture was adjusted to 8.5 using triethylamine and stirred for 3 days at room temperature (~25 °C). The final product was dialyzed and freeze dried. Percentage conjugation of CPPs to lipid was calculated using micro bicinchoninic acid (BCA) assay. CPP conjugated lipids were stored at -20 °C until used.¹⁴⁹

2.3.2. Preparation and Characterization of Liposomes

Liposomes were prepared using a mixture of lipids using film hydration technique (**Figure 5**). DOTAP (45 mole %), DOPE (45 mole %), cholesterol (2 mole %), DSPE-PEG-CPP (4 mole %), and DSPE-PEG-MAN (4 mole %) were dissolved in chloroform: methanol (2:1 v/v). The lipid mixture was dried in a rotary evaporator and the resulting lipid film was hydrated using HEPES buffer (pH 7.4). pDNA was complexed with chitosan (N:P 5:1) by dropwise addition of chitosan solution to pDNA solution. pDNA – chitosan complex was added to the hydration buffer and the mixture was sonicated for 30 min. The resulting liposomes were characterized for their hydrodynamic size and zeta potential via dynamic light scattering (DLS) technique using Zetasizer Nano ZS 90 (Malvern Instruments, Malvern, UK) at room temperature. Entrapment efficiency pBDNF was calculated using Hoechst 33342 dye.^{149,212}

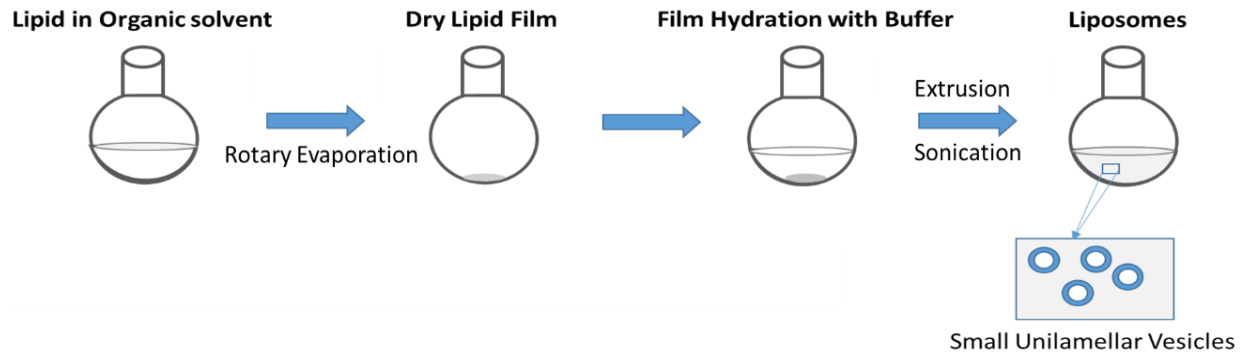


Figure 5. Synthesis of liposomes via film hydration technique.

2.3.3. DNase Protection Assay

Shielding of encapsulated plasmid from DNase I digestion was assessed by gel electrophoresis.¹⁴⁹ In brief, 1 μg of liposome entrapped chitosan/pDNA complex was incubated with DNase I enzyme (1 unit) for an hour at 37 °C. Naked plasmid was also incubated with the enzyme as positive control. Five microliters of EDTA solution (100 mM) was utilized post incubation to inactivate the DNase enzyme. Subsequently, the inactivated mixture was incubated with heparin (30 μL , 5 mg/mL) solution for 2 hrs for releasing pDNA. Agarose gel electrophoresis was performed on the resulting mixture to assess the stability of released plasmid DNA at 80 V for 1.5 hrs.¹⁴⁹

2.3.4. Cell Culture

In vitro studies were performed in brain endothelial cells (bEnd.3 cells), primary rat glial and primary rat neuronal cells. bEnd.3 cells were acquired from ATCC and maintained in DMEM with 10% (v/v) fetal bovine serum (FBS). One day old Sprague–Dawley rat pups were used for culturing primary glial cells and primary neuronal cells.^{154,213} Briefly, brain was isolated from pup head and meninges were removed. Brain tissue was minced into small fragments and digested using 0.25% trypsin containing DNase I (100 $\mu\text{g}/\text{ml}$) at 37 °C. The cells obtained were cultured with DMEM containing 10% (v/v) fetal bovine serum (FBS). Similar procedure was used to

culture primary neuronal cells with DMEM containing 10% (v/v) horse serum. Furthermore, for culture of primary neuronal cells, 10 μ M cytosine arabinoside was added to the culture media on day 3 which was replaced with fresh media on day 5. Purity of primary glial and neuronal cells was examined by fluorescence microscopy using glial fibrillary acidic protein (GFAP) and anti-MAP2 antibody, respectively.

2.3.5. *In Vitro* Biocompatibility Assay

In vitro biocompatibility assay was performed on bEnd.3, primary glial and primary neuronal cells.²¹⁴⁻²¹⁷ The cells were plated at a density of 5×10^3 cells/well in a 96-well plate. After 24 h, the cells were treated for 4 h with different concentration of liposomal nanoparticles ranging from 50 to 600 nM in serum free DMEM media. Post incubation the media was replaced with 10% (v/v) FBS containing DMEM and cell viability was analyzed after 48 h using MTT assay. Cells without any treatment were used as negative control.

2.3.6. Cellular Uptake

Ability of prepared liposomal nanoparticles to internalize inside cells was measured quantitatively as well as qualitatively. Liposomes containing lissamine rhodamine dye were incubated with bEnd.3, primary glial and neuronal cells (1×10^5 cells/well) for 0.5, 1, 2 and 4 h. For quantitative analysis, after each time point the cells were washed three times with PBS and lysed using triton X-100 (0.5% v/v). Fluorescent dye was extracted in methanol and fluorescent intensity was read using spectrophotometer (λ_{ex} 553 nm, λ_{em} 570 nm).

2.3.7. Cellular Mechanism of Uptake and Competition Assay

The detailed mechanism of nanoparticle uptake was elucidated in bEnd.3 cells. After 24 h of plating (5×10^4 cells per well), endocytosis inhibitors were added to the cell culture individually 30 min prior to liposomal treatment. Treatment at cold temperature (4 °C) or with 10 mM sodium

azide impedes all ATP-dependent internalization pathways. Clathrin-mediated endocytosis and caveolae formation by polymerization of microtubules was blocked using 10 $\mu\text{g/mL}$ chlorpromazine and 100 $\mu\text{g/mL}$ colchicine, respectively. Amiloride (50 $\mu\text{g/mL}$) was added to prevent internalization *via* micropinocytosis. Post treatment with the various inhibitors, lissamine rhodamine labeled liposomes were added to culture media containing each inhibitor and incubated for 1 hr. Thereafter, PBS was used to wash cells and lysed using triton X-100. The lissamine rhodamine intensity was measured (λ_{ex} 553 nm, λ_{em} 570 nm) after extraction with methanol from cell lysates.⁵³

Competitive inhibition experiment was carried out in bEnd.3 cells using different liposomal nanoparticles. Cells were pretreated for 0.5 hrs with different strengths of D-glucose and D-mannose in PBS prior to the competition assay. Subsequently, lissamine rhodamine labeled liposomes were introduced to the cells and incubated for 1 hr.²¹⁸ Post incubation, the liposomes internalization was evaluated as described earlier by measuring lissamine rhodamine concentration.

2.3.8. *In Vitro* Transfection Efficiency

Transfection efficiency of prepared liposomal nanoparticles was assessed in all the cell lines used. Approximately, 1×10^5 cells/well were seeded in 24-well plate prior to liposomal treatment. Liposomal nanoparticles entrapping 1 μg pDNA (pBDNF or pVGF or pApoE2) were incubated with cells in serum free medium for 4 h. Post incubation, the media was replaced with 10% (v/v) FBS containing DMEM and cells were further incubated for 48 h. BDNF expression was analyzed using ELISA (Boster Biological Technology, Pleasanton, CA, USA) in cell culture supernatants as well as in cell lysates. Expression levels were normalized with regards to total protein content using BCA protein assay. Transfection efficiency was compared to marketed

transfection reagent, Lipofectamine 3000 (positive control), used according to manufacturer's protocol.

2.3.9. Synaptic Vesicles Formation

Changes in synaptophysin levels were analyzed post BDNF gene transfection in primary neuronal cells. Neuronal cells were seeded in 24-well plate at density of 1×10^5 / well. Dual modified liposomes (PenMAN) incorporating $1 \mu\text{g}$ of pBDNF – chitosan complex was incubated with the cells for 4 h. Post incubation the media was replaced with fresh media and the synaptophysin levels were analyzed at 12 h, 24 h, 48 h, 3 days, 7 days and 14 days post treatment. After each time point the cells were fixed and permeabilized. Cells were further incubated with primary antibodies, synaptophysin mouse IgG1 and NeuN rabbit IgG, followed by Alexa Fluor 647 goat anti-rabbit IgG and Alexa Fluor 488 goat anti mouse IgG secondary antibodies at room temperature ($\sim 25^\circ\text{C}$). Qualitative estimation was done using Leica DMI8 fluorescence microscope (Leica Microsystems Inc., Buffalo Grove, IL). Synaptophysin protein level was analyzed using synaptophysin ELISA kit (Boster Biological Technology, Pleasanton, CA, USA) normalized to total protein content using BCA protein assay.

2.3.10. *In Vitro* Co-culture BBB Model

The formation of the BBB model was performed in accordance with the protocol described in the literature.¹⁵⁵ bEnd3 cells and primary astrocytes were used for preparing the BBB model at a density of 15×10^4 / cm^2 and 15×10^3 / cm^2 , respectively. Barrier insert (0.4 μm membrane) was used to seed the astrocytes and bEnd3 cells on its lower and upper side, respectively. Similarly, another barrier was made using human brain microvascular endothelial cell line (hCMEC/D3), human astrocytes (HA) and SHSY5Y cells (HN). HA and SHSY5Y cells (1.5×10^4 / cm^2) were seeded on the bottom side and hCMEC/D3 (1.5×10^5 / cm^2) were seeded on top side of the culture

inserts. Integrity of the resulting barrier was assessed using Epithelial Volt/Ohm Meter 2 (EVOM) by measuring the transendothelial electrical resistance (TEER). TEER of the control barrier, made utilizing either bEnd.3 or hCMEC/D3 cells only, was also determined for reference.²¹⁹

Flux of sodium–fluorescein (Na–F) was used to estimate paracellular transport across murine *in vitro* BBB model as previously described.^{220,221} Co-culture murine BBB model or monolayer model (bEnd.3 cells alone) was transferred to 24-well with 0.5 mL of PBS. In the culture insert 10µg/mL Na–F in PBS was incubated for different time points (5, 15, 30, and 60 min). The amount of fluorescent dye in culture insert and 24-well plate was determined using SpectraMax®M5 multimode microplate reader (Molecular devices, Sunnyvale, CA. λ_{ex} 485 nm, λ_{em} 535 nm). Flux was also measured for blank culture insert and transendothelial permeability coefficients (Pe) was measured for co-culture as well as monolayer model.^{221,222}

2.3.11. Transport Across *In Vitro* BBB Model

Ability of surface modified liposomes to get transcytosed across BBB was assessed using *in vitro* BBB model.²¹⁹ Liposomes containing lissamine rhodamine dye were incubated in the upper compartment of the culture insert containing 0.5 mL PBS with 10% v/v FBS. The inserts were then placed in 24-well plate containing 0.5 ml of PBS. Concentration of liposomes in the lower compartment was determined after 1, 2, 4, 8, 16 and 24 h using Spectra Max®M5 multimode microplate reader (λ_{ex} : 553 nm, λ_{em} :570 nm).

2.3.12. Transfection Across *In Vitro* BBB Model

Ability of prepared liposomes to transfect cells following transport across *in vitro* BBB model was assessed using primary neuronal cells cultured at the bottom of 24-well plate. The BBB model insert was placed over cultured neuronal cells.²¹⁹ Liposomes encapsulating pDNA (pBDNF or pVGF or pApoE2) were added to the upper chamber of the culture insert and incubated for 16

h. Post incubation the insert was removed and transfection was analyzed in primary neuronal cells (seeded at bottom) after 48 h. Gene expression was analyzed using ELISA (Boster Biological Technology, Pleasanton, CA, USA) in cell culture supernatants and cell lysates. Total protein content of cells was used to normalize transfected protein concentration using BCA protein assay.

2.3.13. Animal Experiments in Wild Type Mice

All animal experiments were performed in accordance with Institutional Animal Care and Use Committee (IACUC) approved protocol. Each group was comprised of 6 animals. Equal number of male and female C57BL/6 mice (Jackson Laboratory, Bar Harbor, ME, USA) were used in all experiments. Animals were kept under proper housing conditions with free access to food and water.

2.3.14. *In Vivo* Biodistribution

Post acclimatization, the mice were injected intravenously with MAN modified liposomes containing lissamine rhodamine dye at a dose of 15.2 μmol s of phospholipids/kg body weight. Animals injected with PBS were taken as negative control. At different time points (2, 4, 8, 12 and 24 h) mice brain was extracted and distribution of dye was determined by homogenizing the tissue sample in PBS. Dye was extracted from homogenate in chloroform: methanol (3:1 v/v).²²³ Extract was centrifuged at 20,000 rcf and the supernatant was analyzed using HPLC-FLD (λ_{ex} : 553 nm, λ_{em} :570 nm).²²⁴ The analysis was performed using gradient method (**Table 2**) utilizing C-18 column (Thermoscientific Hypersil BDS, 5 μm , 250 x 4.6 mm) at a flow rate of 0.9 ml/min. Eluent A was composed of water and methanol (1:1 v/v), eluent B was methanol and ethanol (3:2 v/v) supplemented with 0.01 % v/v TFA. All data were normalized as percentage of injected dose (ID) per gram of the tissue. At optimized time point plain, single modified (MAN, Pen, or RVG) and dual modified (PenMAN and RVGMAN) liposomal nanoparticles were injected to see the effect

of cell penetrating peptides in combination with GLUT-1 targeting ligand MAN. Six animals were used per group and liposomes containing lissamine rhodamine dye were dosed at 15.2 μ mol/kg body weight of mice. Post incubation time, mice organs were harvested and analyzed for distributed of dye as described earlier.

Table 3. Chromatographic conditions for studying biodistribution using RP-HPLC.

Column	Thermo Scientific™ Hypersil GOLD™ C18 column (250 x 4.6 mm, 5 μ m)
Mobile phase A	0.1% v/v TFA in water and methanol (1:1 v/v)
Mobile phase B	0.1% v/v TFA in methanol and ethanol (3:2 v/v)
Elution	Gradient
Flow rate	0.9 ml/min
Injection volume	25 μ l
Run time	20 min
Detector, Detection wavelength	FLD, λ_{ex} : 553 nm, λ_{em} :570 nm)

2.3.15. *In Vivo* Biocompatibility and Gene Transfection in Wild Type Mice

Biocompatibility of liposomes was analyzed *in vivo* using histological evaluation of tissue sections obtained from various organs 5 days following liposomal treatment. C57BL/6 mice were injected intravenously with liposomal nanoparticles (~15.2 μ moles phospholipids/kg body weight) encapsulating pDNA (40 μ g pBDNF or pVGF/100 g body weight and 1 μ g pApoE2/ g body weight).²¹⁹ Blood and different tissues (brain, liver, kidneys, heart, lungs, and spleen) were extracted from mice 5 days post nanoparticles administration. Extracted tissues were weighed and homogenized in RIPA buffer comprising proteinase and phosphatase inhibitor cocktail. Homogenate obtained was centrifuged at 4,000 rpm, at 4 °C for 15 min and BDNF levels were estimated in the supernatant as described previously.

Tissue sections obtained from each organ were fixed in 10% (v/v) neutral buffered formalin and embedded in paraffin. Tissue sections (5 μ m thick) were fixed on poly lysine coated slides and

stained using hematoxylin eosin (H&E) stain for visualization of cell morphology, inflammatory cells, necrosis, and any other signs of toxicity.²²⁵

2.3.16. Alzheimer's Disease Experimental Design

6-months and 9-months old APP/PS1 mice (3 males and 3 females in each age group) were administered intravenously with four doses of BDNF gene (400 µg/ Kg body weight) incorporated liposomes (~15.2 nmol phospholipids/g body weight), once per week. The animals were analyzed on the 6th day after the last dose.¹⁵⁴ Age matched C57BL/6 and APP/PS1 mice treated with phosphate buffered saline (PBS) were used as controls. Brains of mice were harvested and stored in -80 °C until further analysis.

2.3.17. BDNF Protein Transfection in Alzheimer's Disease Mice

Transfection efficiency of the liposomal nanoparticles were assessed in 6-months and 9-months old APP/PS1 mice. Extracted brain tissues were weighed and homogenized in RIPA buffer with proteinase/phosphatase inhibitor. The resulting tissue homogenate was centrifuged (4 °C, 4000 rpm, for 0.25 hrs) and BDNF protein was quantified in the supernatant utilizing ELISA (Boster Biological Technology, Pleasanton, CA, USA). BDNF protein content was normalized to the total protein content.

2.3.18. Quantification of Amyloid Beta Peptides

Abeta peptide (1-40 and 1-42) levels, post liposomal treatment, were quantified in the brain tissues. Different peptide fractions were extracted in sequence from brain homogenates in tris buffered saline (TBS), tris buffered saline supplemented with 1% Triton X-100 (TBSX), and finally guanidine HCl (5 M) in 50 mM Tris (GDN), pH 8.0. Initially, brain homogenate in TBS containing proteinase/phosphatase inhibitor were centrifuged at 1,00,000 g for 1 hr at 4 °C. The resulting supernatant was marked as TBS fraction and resulting pellet was resuspended in TBSX

and incubated at 4 °C for 0.5 hrs on gentle shaking. Afterwards, the mixture was centrifuged at 1,00,000 g for 1 hr at 4 °C, with supernatant marked as TBSX fraction. The final resulting pellet was mixed with 5 M guanidine for 12 to 16 hrs at 25 °C, and centrifuged at 16000 g for 0.5 hrs with supernatant marked as GDN fraction. Abeta peptides were quantified utilizing their respective ELISA kits (AnaSpec Fremont, CA, USA) and respective protein content was normalized using the total protein content.

2.3.19. Immunohistochemical Analysis

Brain tissue was fixed in 10% neutralized buffer formalin and embedded in paraffin. Tissue sections were stained with anti-Abeta antibody (Invitrogen, Thermo Fisher Scientific) and further stained using bond polymer refine detection system (Leica). The slides were scanned using Motic Easy Scan and areas covered by plaques were analyzed using ImageJ software. The area covered by plaques was quantified in the hippocampus as well as in the cortex region of the brain.

Cell proliferation and growth in the brain was also assessed using Ki-67 cell proliferation marker. Brain tissue slices were stained with anti-Ki-67 antibody (Biocare Medical, CA, USA) and processed using bond polymer refine detection system (Leica). The slides were scanned using Motic Easy Scan and number of the Ki-67 positive cells were counted and normalized to the area of the brain section utilizing ImageJ software.

2.3.20. Synaptophysin and PSD-95 Protein Quantification

Alteration in the synaptophysin and PSD-95 protein was assessed post BDNF gene transfection in the extracted brain tissues. The tissue samples were weighed and homogenized in RIPA buffer with proteinase/phosphatase inhibitor. The resulting tissue homogenates were centrifuged (4000 rpm) at 4 °C for 0.25 hrs and the supernatant was collected. Synaptophysin and

PSD-95 protein were quantified in the supernatant utilizing their respective ELISA kits (LSBio, Seattle, USA) and the respective protein content was normalized to the total protein content.

2.3.21. Nesting

C57BL/6 and APP/PS1 mice were placed in independent cages (1 mouse per cage) containing portion controlled and easy to dispense bedding material (Bed-r'Nest®, Andersons Lab Bedding). On the testing day, the nest was introduced in cages to permit nesting and the nests were assessed the following day on a 5-point scale.^{226,227} Nests which were evidently untouched were scored 1 (>90% intact), partly shredded nests were scored 2 (50–90% untouched), mainly torn but without distinguishable nesting area were scored 3 (50–90% nest is within 25% of the cage area), distinguishable but flat nests with boundaries elevated above mice height on <50% of its perimeter were scored 4, and an almost perfect nest with boundaries elevated above mice height on >50% of its perimeter were scored 5.

2.3.22. Statistical Analysis

Statistical analysis on data was performed using either two tailed t-test or one-way analysis of variance (ANOVA) with Tukey multiple comparison post-hoc test. All data is represented as mean ± standard deviation (SD) with statistical significance set at $p < 0.05$.

3. RESULTS AND DISCUSSION¹

3.1. Preparation and Characterization of Liposomes

PEGylated DSPE-PEG was used for the synthesis of CPP conjugated lipid. PEG conjugation on liposomal surface prevents them from accretion, opsonization, and phagocytosis ensuing prolong circulation time in the body.^{228–230} Moreover, hydration cloud formation due to the presence of hydrophilic PEG chains around nanoparticles sterically hinders the contact between blood components and liposomes.²³¹ Thus, this restricts foreign material penetration into PEG layer making it an efficient approach to prevent its clearance by macrophages.²³² CPP conjugated lipid was prepared by reacting N-hydroxysuccinimide ester of PEGylated lipid with primary amines of CPPs (RVG, Pen, RDP, RVG9R, and CGN) under alkaline condition. Micro BCA protein assay was utilized for evaluating the extent of CPP conjugation to DSPE-PEG. Conjugation efficiency for all CPPs was found to be in excess of 75%.

The CPP and MAN functionalized PEGylated liposomes were fabricated by lipid film hydration approach. Characterization data showed that all the liposomal nanoparticles prepared were less than 200 nm in size (**Table 4**). Addition of the ligands on the surface of the nanoparticles resulted in slight increase in their hydrodynamic diameters. The zeta potential of nanoparticles was slightly positive. The positive surface charge of these nanoparticles is primarily attributed to the presence of cationic lipid DOTAP. Polydispersity index (PDI) for all nanoparticle formulations were found to be less than 0.3, which indicates high particle homogeneity with no signs of

¹ Reprinted with permission from Arora, S.; Sharma, D.; Singh, J. GLUT-1: An Effective Target to Deliver Brain-Derived Neurotrophic Factor Gene Across the Blood Brain Barrier. *ACS Chem. Neurosci.* 2020, 11 (11), 1620–1633 and Arora, S.; Layek, B.; Singh, J. Design and Validation of Liposomal ApoE2 Gene Delivery System to Evade Blood–Brain Barrier for Effective Treatment of Alzheimer’s Disease *Molecular Pharmaceutics* 2021 18 (2), 714-725 Copyright (2020) American Chemical Society. Sanjay Arora carried out all research experiments, data collection, and data analysis. Divya Sharma and Buddhadev Layek served as a proofreader. Jagdish Singh provided research guidance and served as a proofreader.

aggregation.²³³ Lastly, more than 80% of pDNA encoding BDNF, ApoE2 and vgf was found to be associated with the liposomal nanoparticles without any influence on size or PDI.

Table 4. Liposome characterization. Data is expressed as mean \pm S.D, n = 4.

Liposomal nanoparticles	Size (nm)	Zeta Potential (mV)	PDI
Plain	138.9 \pm 11.53	14.6 \pm 1.1	0.239 \pm 0.00
Man	144.9 \pm 8.12	13.1 \pm 2.3	0.234 \pm 0.01
Pen	175.6 \pm 2.19	17.0 \pm 1.5	0.273 \pm 0.06
PenMAN	180.0 \pm 33.52	16.1 \pm 1.4	0.275 \pm 0.04
RVG	160 \pm 4.52	15 \pm 0.77	0.125 \pm 0.089
RVGMAN	172 \pm 3.74	13.5 \pm .70	0.140 \pm 0.071
CGN	141.3 \pm 17.25	15.4 \pm 1.0	0.155 \pm 0.10
CGNMAN	174.5 \pm 7.63	14.9 \pm 0.4	0.264 \pm 0.06
RVGR9	183.7 \pm 41.58	22.6 \pm 0.3	0.255 \pm 0.18
RVGR9MAN	178.1 \pm 38.82	22.8 \pm 2.8	0.159 \pm 0.12
RDP	175.1 \pm 20.44	20.5 \pm 3.0	0.219 \pm 0.20
RDPMAN	190.8 \pm 42.21	19.0 \pm 3.1	0.063 \pm 0.03

3.2. DNase Protection Assay

Gene therapy mandates protection of genetic cargo against nucleases and lysosomal enzyme digestion by the gene delivery vector. Therefore, liposomes were assessed for their ability to protect the encapsulated pDNA against DNase I enzyme. As depicted in **Figure 6 lane B**, DNase I enzyme was capable of degrading pDNA completely due to the absence of complex formation with chitosan or encapsulation into liposomes. Whereas, liposomal nanoparticles (**Figure 6 lane C-F**) were efficient in preventing the genetic payload from DNase I digestion. This evidently shows that our liposomal nanoparticles have the potential to protect therapeutic gene in biological system against nucleases.

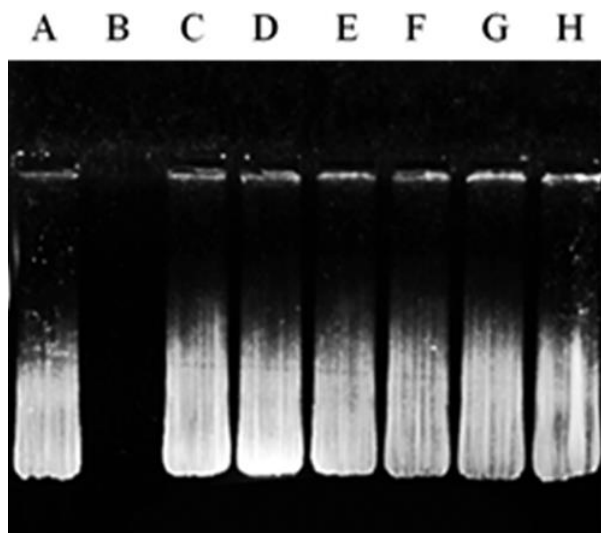


Figure 6. Protection of encapsulated pDNA previously complexed to chitosan (N/P 5) against DNaseI degradation. Column A, naked pDNA; column B, pDNA + DNaseI; column C-H, Liposome, MAN-liposome, Pen-liposome, MAN-Pen-liposomes, RVG-liposomes, RVG-MAN-liposomes containing chitosan-DNA complexes, respectively + DNase I.

3.3. *In Vitro* Biocompatibility Assay

Interaction of nanoparticles, particularly cationic nanoparticles, with cellular and extra cellular environment can trigger various biological processes which can be detrimental to biocompatibility and efficacy of the formulation.²³⁴ Therefore, prepared liposomal nanoparticles were assessed for their biocompatibility in bEnd.3, primary neurons and primary astrocytes. Cells were treated with increasing concentration of phospholipids and its effect on viability was analyzed *via* MTT assay. The relative cell viability in all the cell lines decreased with increasing concentration of the phospholipid (**Figure 7**), which is in accordance with data published by other researchers.^{235,236} Treatment with 100 nM of phospholipids demonstrated more than 80% relative cell viability irrespective of the cell lines. The toxic effect of these nanoparticles at higher concentrations can be attributed to their positive charge as highly cationic nanoparticles induce disturbance in cellular membranes leading to cell death.²³⁷ Therefore, liposomes at a dose of 100 nM of phospholipid was used in further experiments.

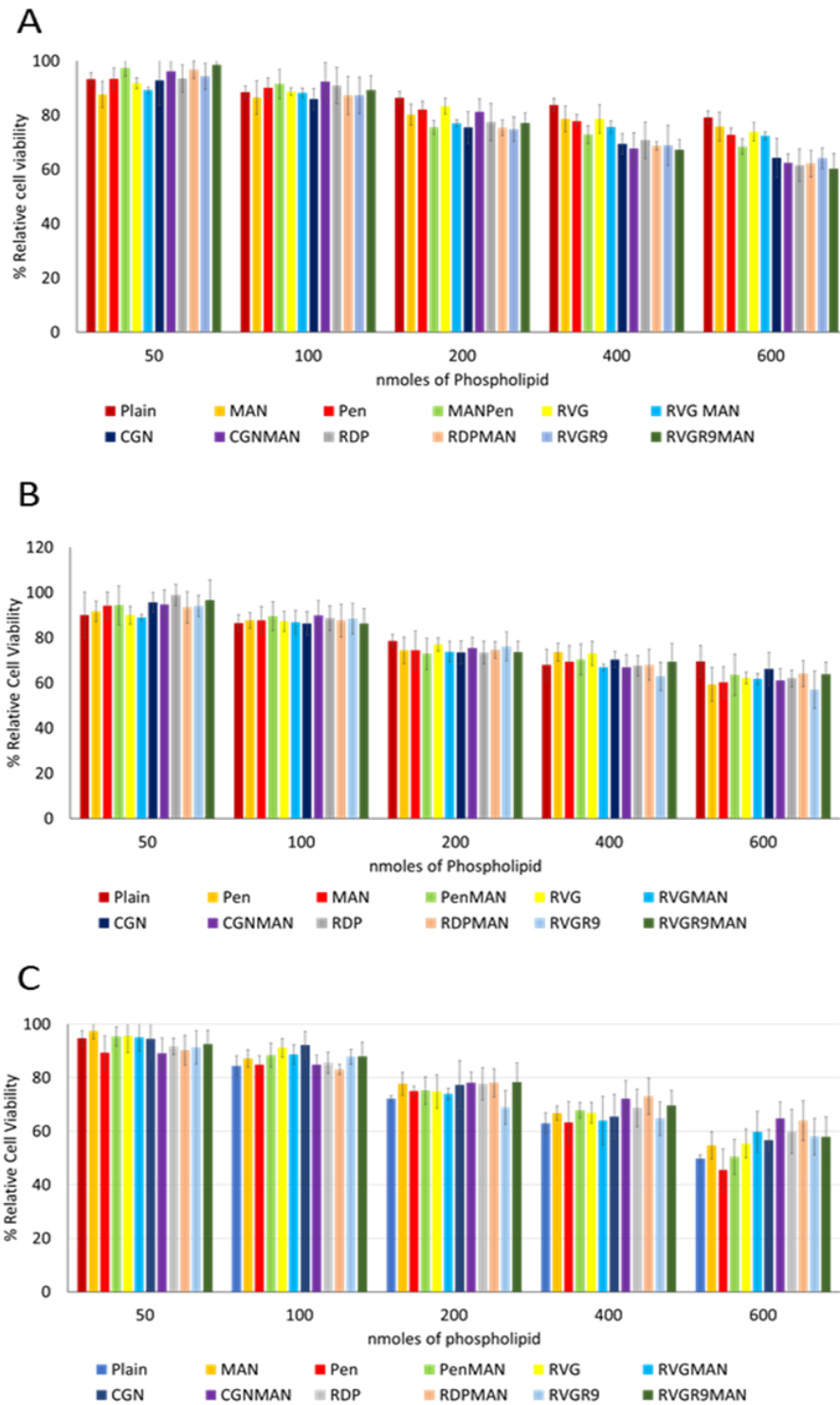


Figure 7. *In vitro* cytocompatibility of unmodified (plain), mannose (MAN), penetratin (Pen), rabies virus glycoprotein peptide (RVG), rabies virus glycoprotein peptide-9R (RVG9R), rabies virus derived peptide (RDP), and CGN (CGNHPHLAKYNGT) liposomes at various phospholipid concentrations on (A) bEnd.3, (B) primary astrocytes, and (C) primary neurons. Data represent mean \pm SD of four replicates.

3.4. Cellular Uptake

Therapeutic effects of cargo gene are highly reliant on the efficient internalization of gene delivery vectors inside cells. Internalization of nanoparticles inside the cells is majorly modulated by their physicochemical characteristics. Hence, cellular internalization of different liposomal nanoparticles prepared in this study was determined at different time points in bEnd.3, primary glial cells and primary neuronal cells quantitatively as shown in **Figure 8**. The internalization of liposomal nanoparticles steadily increased from 30 min and reached saturation by 4 h. Liposomes with dual modification were observed to be internalized ~80% post 4 h incubation in all cell lines. The differences in the uptake ability at different time points between the cell types can be due to their distinct cellular characteristics.²³⁸ Modification using MAN ligand helped target GLUT-1 transporter mediated endocytosis. Moreover, co-functionalizing with brain-specific CPPs aided in enhanced cellular penetration and overall higher uptake of these nanoparticles as compared to plain liposomes.^{208,239} Additionally, specific gene expression by primary cells and cell lines leads to differences in their phenotypes and functions, which may dictate their distinct internalization properties.²⁴⁰⁻²⁴²

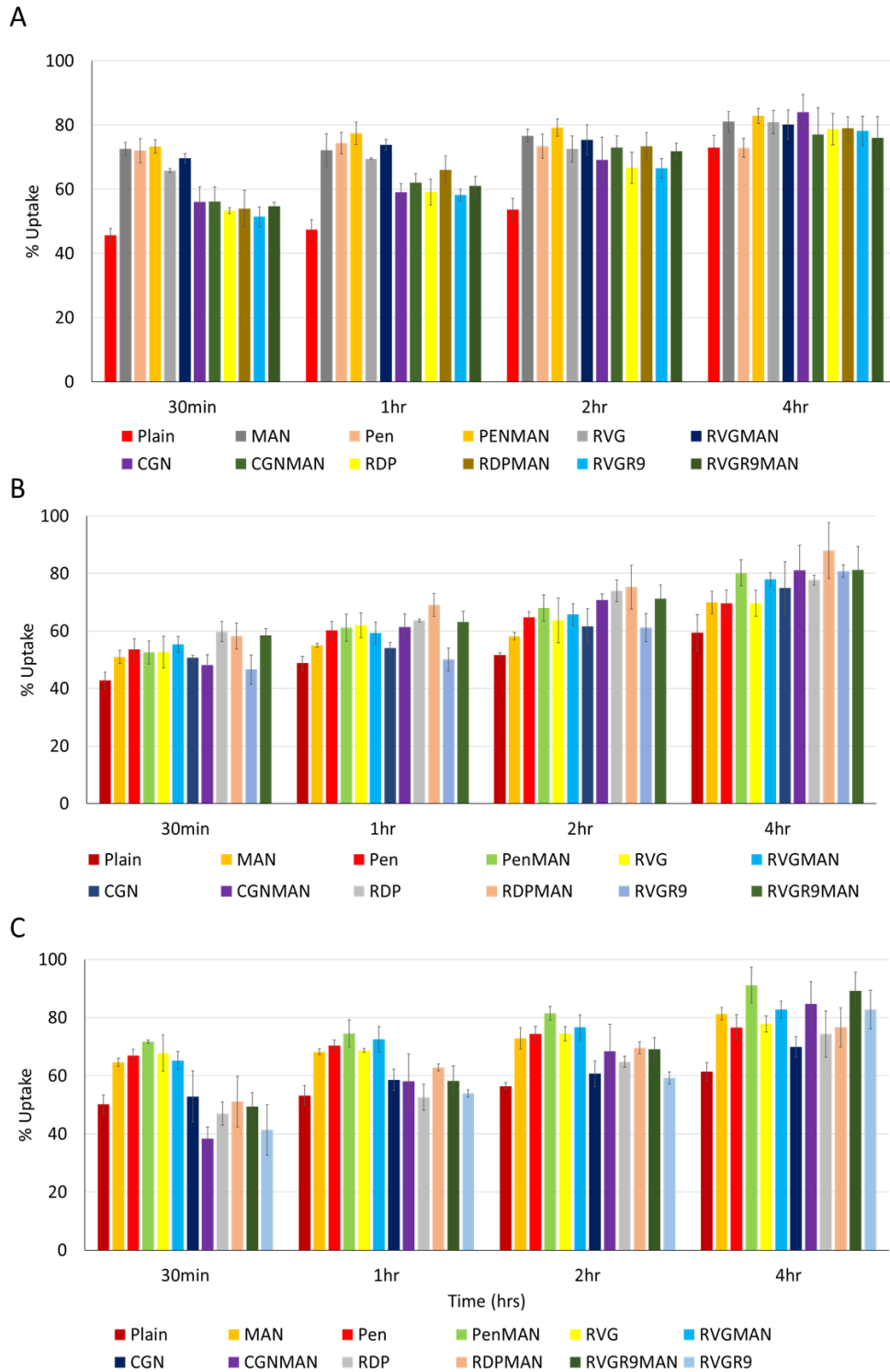


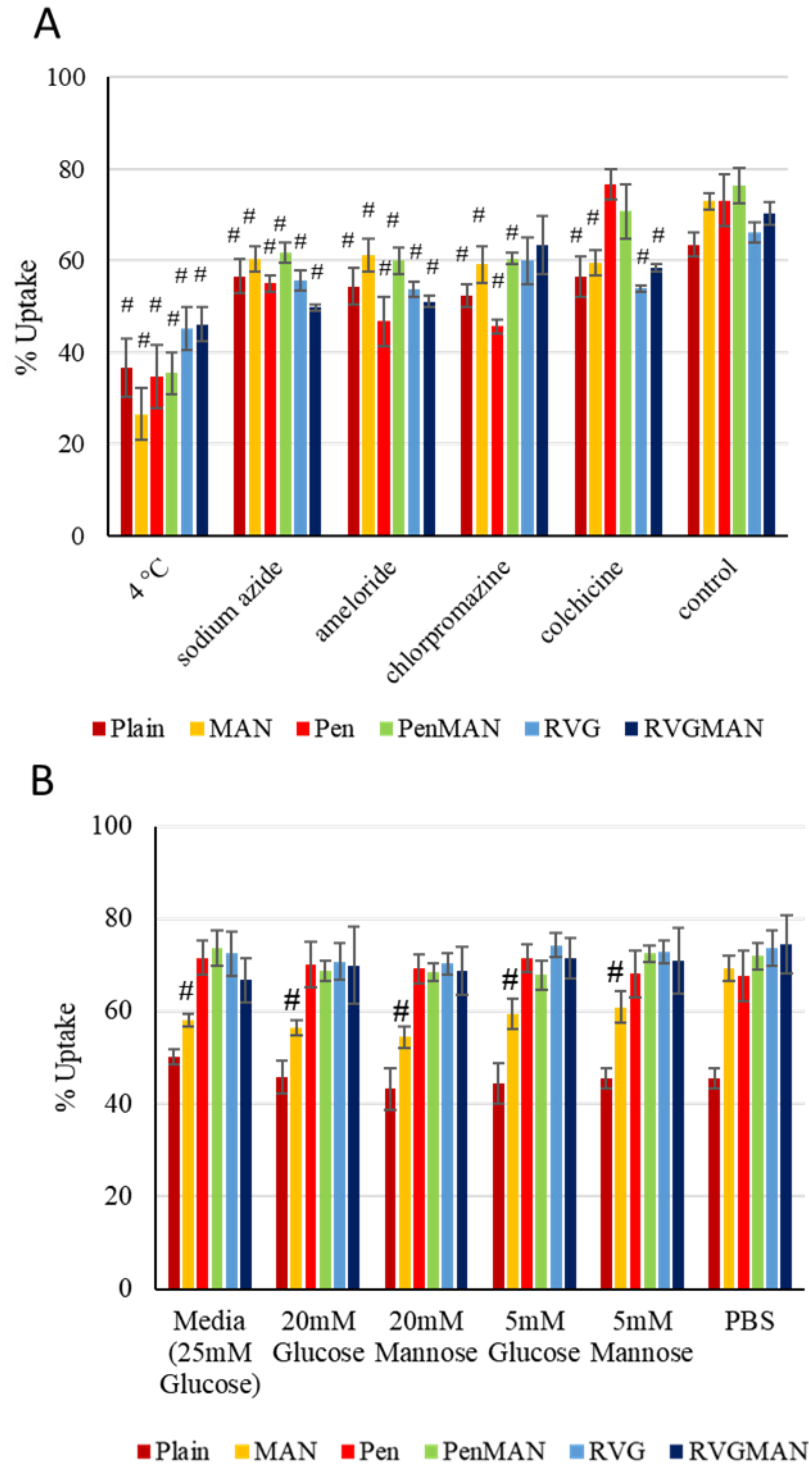
Figure 8. Cellular uptake of unmodified (plain), mannose (MAN), penetratin (Pen), rabies virus glycoprotein peptide (RVG), rabies virus glycoprotein peptide-9R (RVG9R), rabies virus derived peptide (RDP), and CGN (CGNHPHLAKYNGT) modified liposomes in (A) bEnd.3, (B) primary astrocytes, and (C) primary neurons. Data represent mean \pm SD of four replicates.

3.5. Cellular Mechanism of Uptake and Competition Assay

The ability of nanoparticles to enter cells is crucial for effective delivery of therapeutic gene to the nucleus. Depending on their physiochemical characteristics, nanoparticles are internalized through various endocytosis pathways.¹⁵⁵ Therefore, in order to elucidate the exact mechanism for internalization of liposomes different chemical moieties were used as inhibitors for different endocytosis pathways. Incubation at cold temperature (4 °C) or with sodium azide was used to prevent all ATP-dependent internalization pathways. Amiloride was used to inhibit micropinocytosis, while colchicine was used to prevent caveolae mediated endocytosis by disruption of microtubules. Chlorpromazine was used to prevent formation of clathrin vesicles. Incubation at cold temperature (4 °C) or with sodium azide demonstrated significant decrease in the internalization of all the liposomal nanoparticles (**Figure 9 A**). This suggests that more than 50% of internalization is contributed through some energy-dependent pathway. Inhibition of macropinocytosis using amiloride also resulted in more than 15% reduction in liposomal uptake. Colchicine pretreatment did not show any effect on liposomes modified using Pen and PenMAN, indicating no role of caveolae-mediated endocytosis in these two formulations. Chlorpromazine pretreatment did not show any substantial effect on cellular internalization of RVG and RVGMAN modified liposomes indicating no role of clathrin-mediated endocytosis in their internalization process. Internalization of plain liposomes and MAN-liposomes was significantly reduced by $\geq 20\%$ in the presence of various inhibitors, indicating that more than one pathway was involved in internalization process of these formulations.

Similarly, presence of physiological sugars can also affect the internalization of these liposomes by competing for GLUT-1 transporters present on astrocytes and luminal side of BBB. Therefore, cells were pretreated with physiological levels of glucose and mannose before

liposomal treatment. Also, majority of AD patients (>80%) suffer from type 2 diabetes or glucose imbalance, therefore internalization of liposomes was also assessed in the presence of diabetic concentrations of glucose and mannose.²⁴³ As demonstrated in **Figure 9 B**, various liposomal nanoparticles did not exhibit significant differences in cellular uptake by bEnd.3 cells, except MAN-functionalized liposomes. Internalization of MAN-liposomes was reduced by ~10% in the presence of physiological concentrations (5 mM), and by ~15% in the presence of diabetic sugar concentrations (20 mM). This indicates competition for glucose transporter between sugar molecules present in culture medium and the MAN ligand on liposomal surface. This competition was overcome using dual-functionalization of liposomal surface due to the presence of additional GLUT-1 independent pathway (i.e. CPP-mediated) of internalization, justifying the use of two ligands to target brain cells.



3.6. *In Vitro* Transfection Efficiency

Transfection efficiency is a vital parameter for developing a gene delivery vector. Since non-viral vectors are weighed down due to their poor transfection efficiency, we assessed the effect of liposomal surface modifications on transfection ability. The transfection efficiency was studied in bEnd.3, primary glial and primary neuronal cells using plasmid encoding BDNF, ApoE2 and vgf protein. Cells were treated with either naked pDNA or pDNA encapsulated inside the liposomal nanoparticles. Untreated cells were used as a control to estimate background levels. The transfection efficiency of pVGF was evaluated using liposomes modified with RVG9R, RDP, CGN or Pen, in combination with MAN. Whereas, the transfection efficiency pBDNF and pAPoE2 was evaluated using liposomes modified with RVG or Pen, in combination with MAN.

As shown in **Figure 10**, the pBDNF entrapping dual modified (PenMAN and RVGMAN) liposomes demonstrated significantly higher ($p < 0.05$) gene transfection compared to naked pBDNF, plain and single modified (MAN, Pen, or RVG) liposomes in all cell lines. PenMAN liposomes showed transfection efficiency in excess of 2-fold as compared to Lipofectamine 3000 in all cell lines. However, there was no significant difference between PenMAN and RVGMAN liposomes. Similar results were found for liposomal transfection ability utilizing plasmid encoding ApoE protein. RVGMAN and PenMAN liposomes demonstrated significantly ($p < 0.05$) greater ApoE protein expression than naked pDNA, plain and single modified (MAN, Pen, or RVG) liposomes in all cell lines (**Figure 11**). These dual modified nanoparticles also showed 1.5-fold greater ($p < 0.05$) protein expression than plain or monofunctionalized liposomes as well as lipofectamine.

Transfection ability of pVGF/chitosan associated liposomes was also evaluated in bEnd.3, primary glial and primary neuronal cells. It was seen that dual-modified liposomes (RVG9RMAN,

RDPMAN, PenMAN and CGNMAN) showed significantly higher ($p < 0.05$) vgf transfection efficiency than naked pDNA, plain, and single modified (MAN, RVG9R, RDP, Pen and CGN) liposomes (**Figure 12**). RDPMAN functionalized liposomes demonstrated highest transfection efficiency in all the cell lines, which was ~2 fold greater than the singly modified liposomes. Similar increase in transfection potential was observed with bifunctionalized PenMAN, RVG9RMAN and CGNMAN liposomes as compared to their single ligand (MAN or CPP only) modified counterparts. However, no significant difference was found between the different bifunctionalized liposomes.

Enhanced protein expression in the dual-functionalized liposomal nanoparticles treated cells can be attributed to their higher cellular uptake, efficient endosomal rupturing ability, and enhanced transfer of therapeutic gene to the nucleus of the cells.²¹⁴ Complexation of pDNA with chitosan in combination with these factors may have collectively shown beneficial effect in enhancing protein expression *via* dual-functionalized liposomes in comparison to naked pDNA.

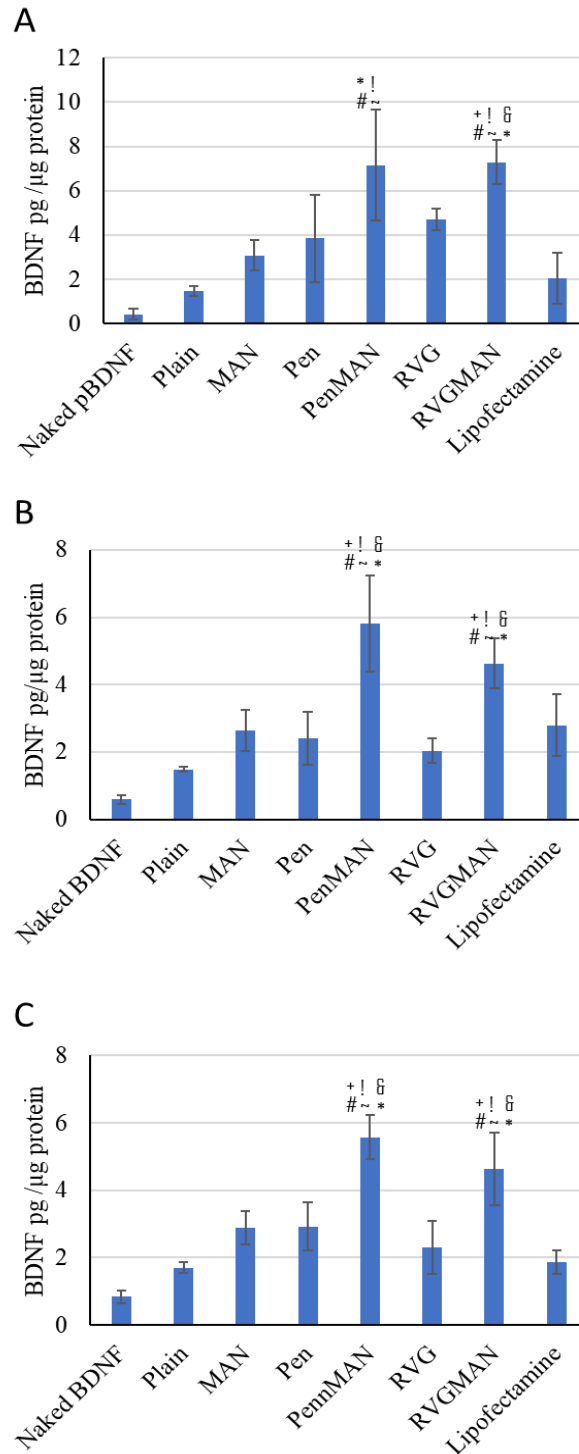


Figure 10. BDNF expression levels post 48h after transfection in A) bEnd.3 cells, B) primary glial cells and C) primary neuronal cells treated with different liposomal formulations entrapping chitosan-pBDNF complexes (1μg) . Data is presented as mean ± SD (n = 4). Statistically significance (p < 0.05) is shown as (!) with naked DNA, (*) with plain liposomes, (#) with MAN liposomes, (+) with Pen liposomes, (&) with RVG liposomes, and (~) with lipofectamine.

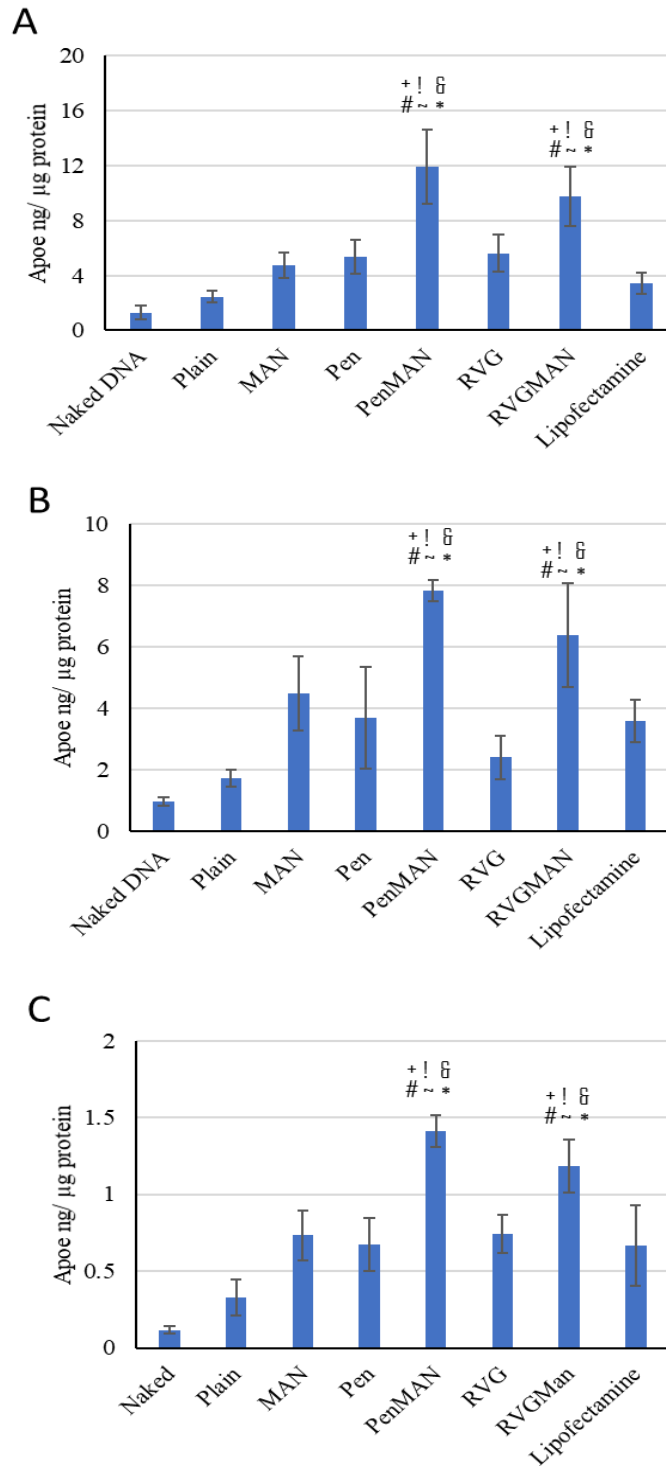


Figure 11. ApoE expression levels post 48h after transfection in A) bEnd.3 cells, B) primary glial cells and C) primary neuronal cells treated with different liposomal formulations entrapping chitosan-pBDNF complexes (1μg). Data is presented as mean ± SD (n = 4). Statistically significance (p < 0.05) is shown as (!) with naked DNA, (*) with plain liposomes, (#) with MAN liposomes, (+) with Pen liposomes, (&) with RVG liposomes, and (~) with lipofectamine.

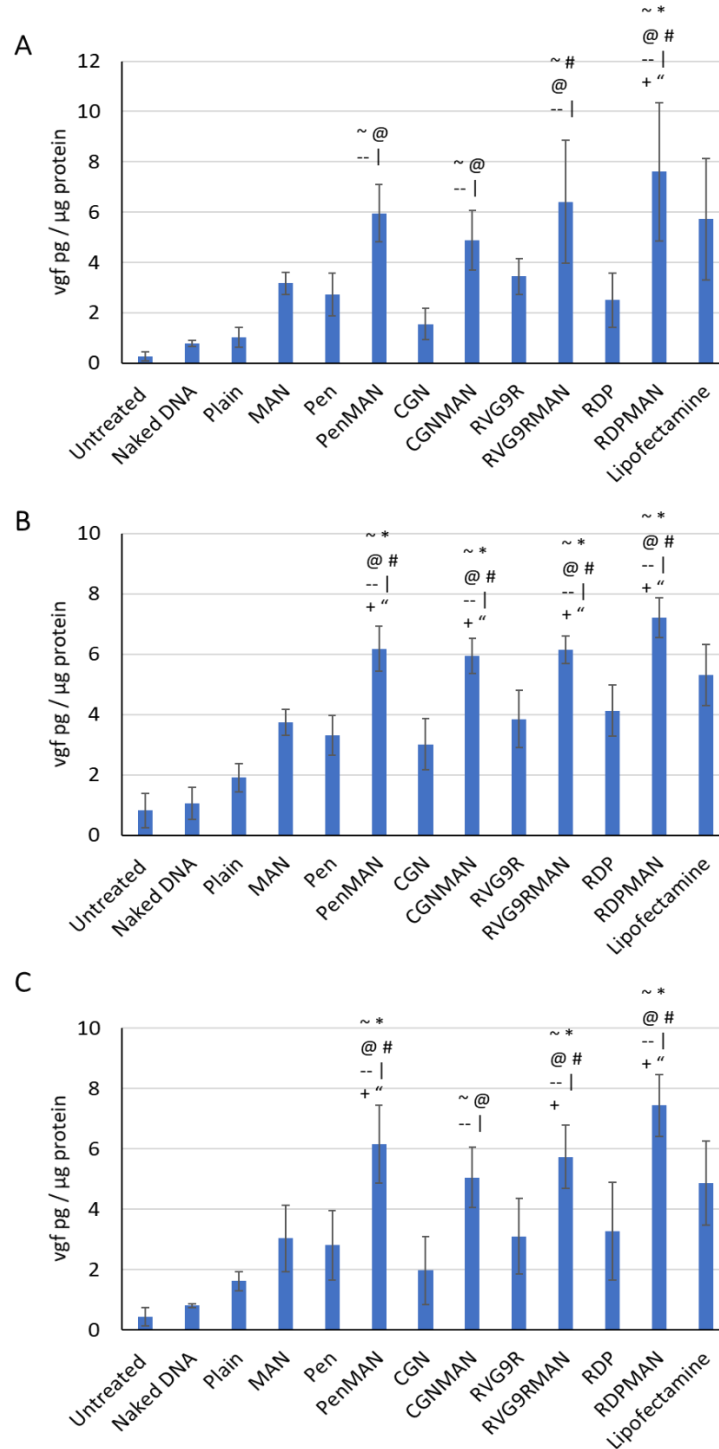


Figure 12. Vgf expression levels post 48h after transfection in A) bEnd.3 cells, B) primary glial cells and C) primary neuronal cells treated with different liposomal formulations entrapping chitosan-pBDNF complexes (1μg) . Data is presented as mean ± SD (n = 4). Statistically significance (p < 0.05) is shown as ~, |, @, #, *, --, +, and “ show statistically significant difference (p<0.05) from untreated, naked DNA, plain, Pen, MAN, CGN, RVG9R and RDP liposomes, respectively.

3.7. Synaptic Vesicle Formation

Increasing evidence has validated the role of synaptic dysfunction in various neurological disorders including AD resulting in a decline in cognitive abilities and loss of synaptic markers.^{244,245} Prevention of synapse dysfunction has been acknowledged as one of the potential tactics for attenuating cognitive decline.^{246,247} BDNF is a key neurotrophin that modulates synaptic protein levels and is majorly found to be reduced in patients with neurological disorders.^{248–250} Therefore, we investigated the effect of BDNF gene transfection on synaptophysin levels *in vitro* using PenMAN modified liposomal nanoparticle as a gene delivery vector. We evaluated synaptophysin levels quantitatively as well as qualitatively at different time points post treatment of primary neuronal cells with PenMAN liposomes entrapping chitosan – pBDNF. An increase in synaptophysin protein levels was observed post transfection with pBDNF. Protein levels increased up to 1.6 times baseline levels by 3 days and reduced to baseline levels by day 14 (**Figure 13 A**). This was confirmed with immunofluorescence imaging, where NeuN antibody was used to express neuronal cell nucleus, and synaptophysin antibody was used to express synaptophysin protein in the cytoplasm of the cell (**Figure 13 B**). These results indicate that dual modified liposomal gene delivery formulation has the potential to rescue synaptic properties in neuronal cells.

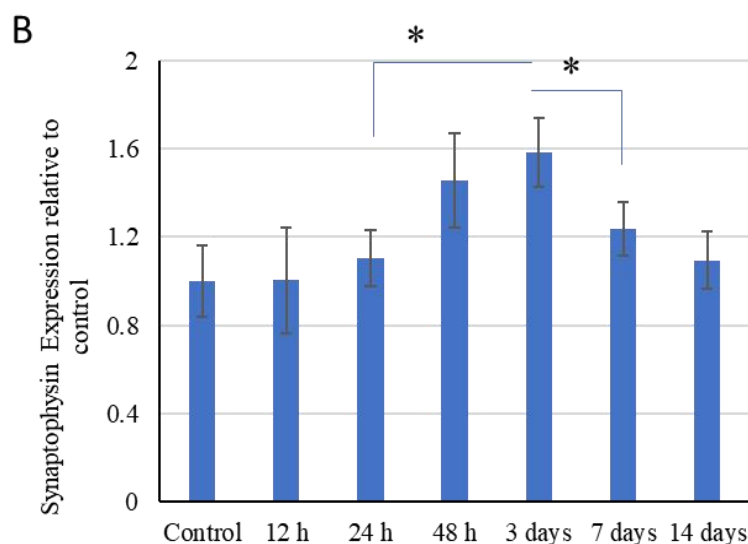
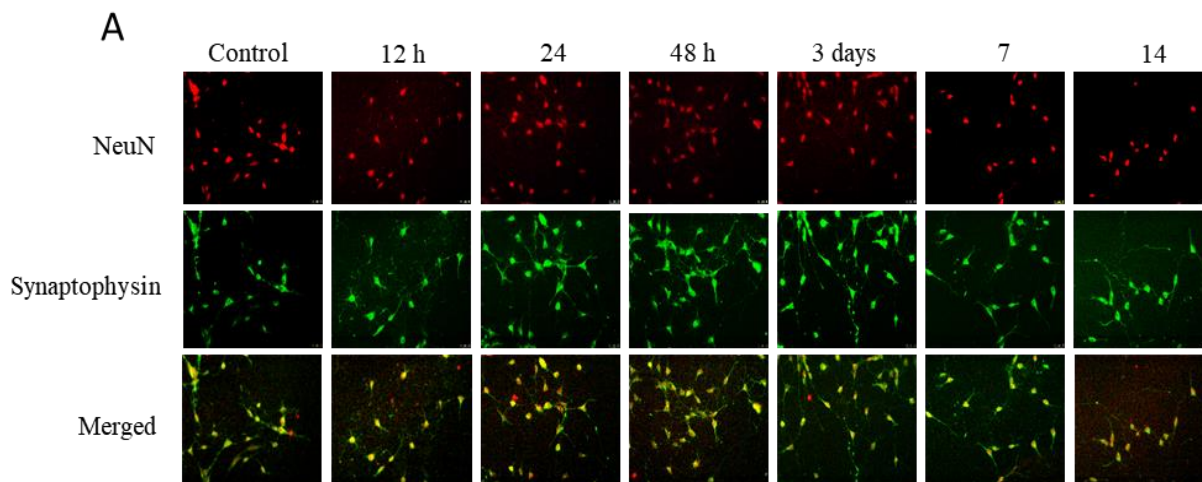


Figure 13. A) Effect of BDNF protein transfected using PENMAN liposomes entrapping chitosan-pBDNF (1 μ g) on synaptophysin protein levels at various time points in primary neuronal cells. B) Qualitative assessment of synaptophysin levels in primary neuronal cells using fluorescence microscope at predetermined time points. Data is presented as mean \pm SD (n = 4). Statistically significant differences ($p < 0.05$) are shown as (*).

3.8. *In Vitro* Co-culture Blood Brain Barrier Model

In vitro BBB model has emerged as a powerful tool for the assessment of brain targeted formulations.²⁵¹ *In vitro* BBB model was prepared using murine bEnd.3 cells and primary astrocytes, or hCMEC/D3, human astrocytes (HA) and SHSY5Y (HN) cells in a culture insert to further select liposomal nanoparticles capable of achieving high transport and transfection

efficiency across the BBB model. TEER value across the barrier layer were measured to monitor integrity of the model. As shown in **Figure 14**, the TEER of BBB model using dual cell lines was found to be significantly higher than monolayer model. Co-cultured BBB model developed using murine cell lines demonstrated TEER values of $206 \pm 37 \Omega \text{ cm}^2$, which was found to be significantly higher (~1.6 times) than the barrier developed using only bEnd.3 cells (**Figure 14**). However, the barrier cultured using hCMEC/D3, HA and SHSY5Y cells demonstrated TEER of only $79 \pm 6 \Omega \text{ cm}^2$, which was significantly lower ($p < 0.05$) than the barriers developed using the murine cell lines. Low TEER of BBB model developed using human endothelial cells have also been reported by other researchers resulting in poor integrity of the barrier.^{72,252,253} The TEER values across the barrier developed using murine cells was $\sim 200 \Omega \text{ cm}^2$, was also in accordance with data observed by other researchers.^{254,255}

Permeability coefficient of Na-F across murine mono layer model ($P_e = \sim 13.02 \times 10^{-6} \text{ cm/s}$) was found to be more than 6 times compared to murine dual layer model ($P_e = \sim 2.08 \times 10^{-6} \text{ cm/s}$), indicating the influence of glial cells on integrity of the barrier model.²⁵⁶⁻²⁵⁸ The advantage of using bEnd.3 cells in the BBB model system is that they grow rapidly and are able to retain their phenotype after several passaging making it convenient for developing efficient BBB model.²⁵⁹ Moreover, several tight junction proteins are found to be present in bEnd.3 cells for example claudin-1, -3, and -5, occludin, zonula occludens-1, and -2, etc. which are absent in human based endothelial cells.⁷³ Therefore, the barrier developed using the murine cells was selected for further evaluation of different liposomal nanoparticles.

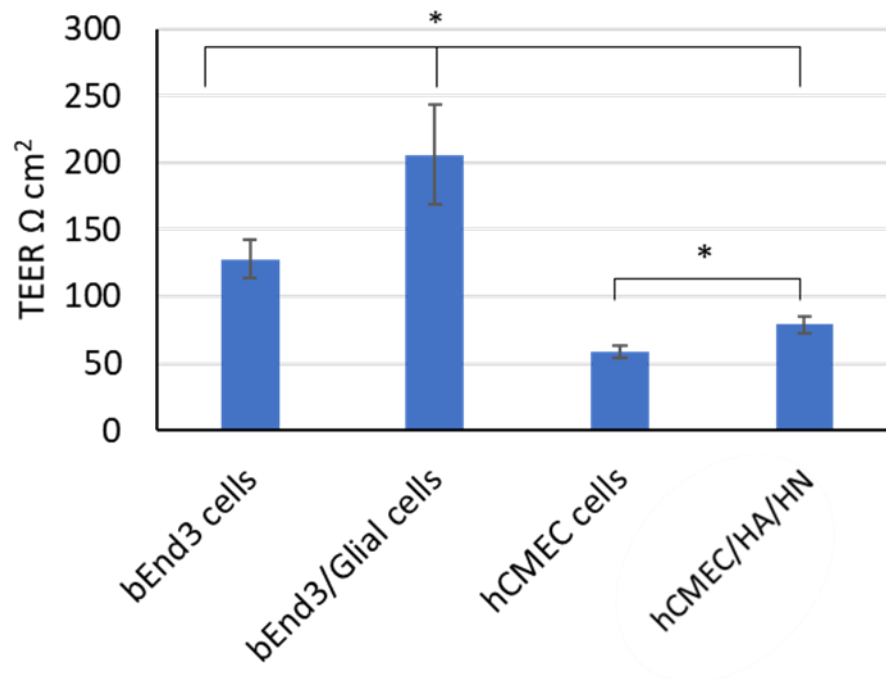


Figure 14. A) Transendothelial electrical resistance (TEER) and B) permeability of sodium fluorescein dye across BBB models. Statistically significant differences ($p < 0.05$) are shown as *.

3.9. Transport Across *In Vitro* BBB Model

A number of therapeutics intended for brain delivery have been unsuccessful due to their inability to pass the BBB. Evaluating translocation of therapeutics across the BBB can progressively affect the development of the final product. Therefore, it is of great interest to assess the transport of our liposomal nanoparticles across the *in vitro* BBB model. Liposomal nanoparticles were added to the culture insert and incubated for different time points (1, 2, 4, 8, 16, 24 h) and it was observed that with time the transport of liposomes across the BBB model increased (**Figure 15**). PenMAN and RVGMAN liposomes were able to get transported ~16% across the barrier which was significantly higher compared to other formulation controls (**Figure 15**). Liposomes that were surface modified with RVG9RMAN and RDPMAN, were also found to be transported ~15% by 16 h, which was significantly greater than plain, and singly modified

(MAN, Pen, RVG9R, RDP and CGN) liposomes. However, following 16 h incubation no significant increase in transport was observed for dual modified liposomes. Transport of single modified (MAN, Pen, RVG, RVG9R, RDP and CGN) liposomes was also observed to be saturated at ~12% following 16 h of incubation.

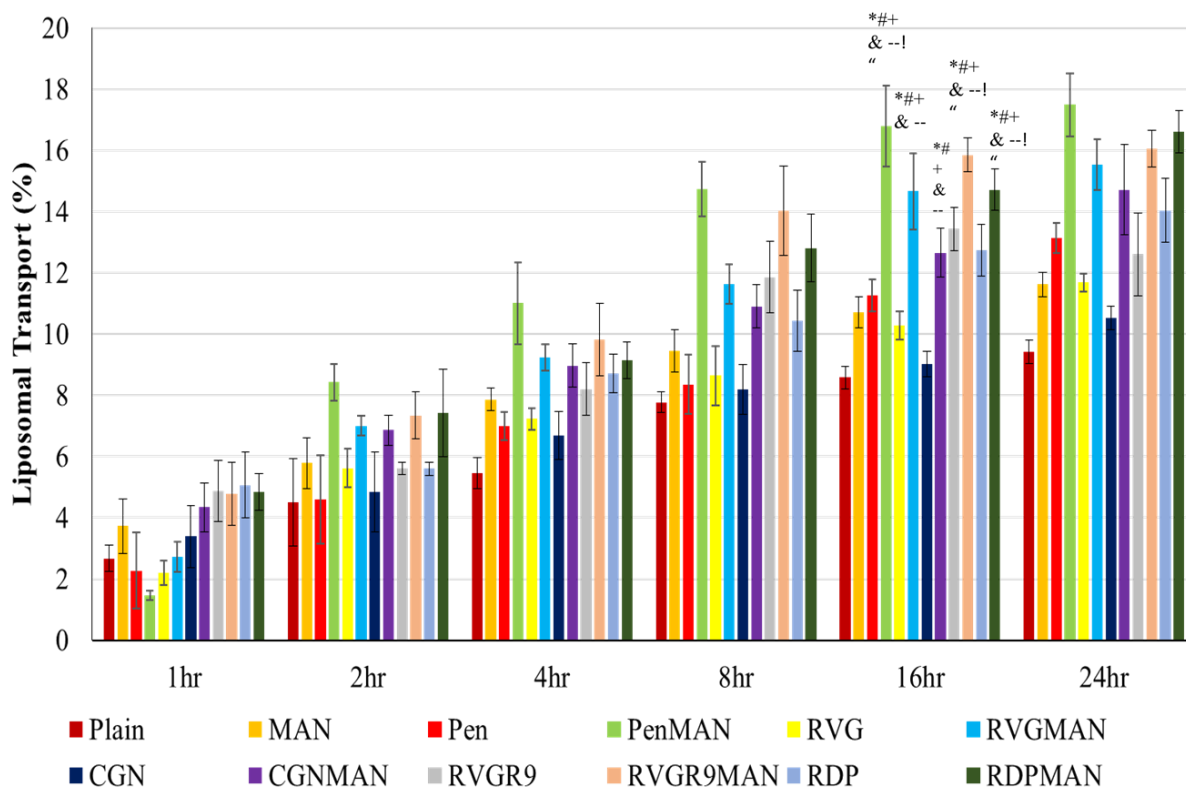


Figure 15. Transport of various liposomal formulations through *in vitro* BBB model over a period of 24 h. Statistically significant differences ($p < 0.05$) is shown as (*) with plain liposomes, (#) with MAN liposomes, (+) with Pen liposomes, (&) with RVG liposomes, (--) with CGN liposomes (!) with RVG9R liposomes, and (") with RDP liposomes.

3.10. Transfection Across *In Vitro* BBB Model

The efficacy of targeted nanoparticles is essential following their transport into the brain parenchyma. Nanoparticles should be able to deliver the desired gene of interest and transfect target cells to produce therapeutic protein. In order to assess therapeutic potential of our formulation, the transfection efficiency of liposomes entrapping pBDNF, pApoE2 or pVGF was evaluated in primary neuronal cells seeded across the *in vitro* BBB model. The transfection

efficiency pVGF was evaluated using liposomes modified with RVG9R, RDP, CGN or Pen, in combination with MAN. The transfection efficiency pBDNF and pApoE2 was evaluated using liposomes modified with RVG or Pen, in combination with MAN.

As depicted in **Figure 16 A**, RVGMAN and PenMAN liposomes encapsulating pApoE2/chitosan complexes showed 2-fold greater transfection efficiency than plain and monofunctionalized liposomes. PenMAN liposomes demonstrated ~1.1 ng ApoE protein/ μ g total protein whereas RVGMAN liposomes showed ~0.9 ng ApoE protein/ μ g total protein. Although PenMAN-liposomes resulted in slightly higher transfection than RVGMAN-liposomes, no statistically significant difference between their transfection efficiencies ($p > 0.05$) was observed.

Transfection efficiency of PenMAN modified liposomes entrapping pBDNF/chitosan complexes was found to be ~ 4 pg protein/ μ g total protein, which was significantly higher than other formulation controls (**Figure 16 B**). On the other hand, the transfection efficacy of RVGMAN modified liposomes was found to be ~ 3 pg BDNF protein/ μ g total protein, which was significantly higher than plain and RVG modified liposomes. Similarly, no statistical significance ($p > 0.05$) was observed between these two dual modified liposomes.

As depicted in **Figure 16 C**, RVG9RMAN, PenMAN and RDPMAN liposomal nanoparticles demonstrated ~2 times higher vgf expression compared to plain liposomes. Transfection efficacy was notably improved with ligand conjugation as evident with significantly higher ($p < 0.05$) transfection of vgf protein using dual modified liposomes RVG9RMAN, PenMAN and RDPMAN when compared to monofunctionalized liposomes (MAN, RVG9R, RDP, Pen and CGN). Although CGNMAN functionalized liposomes demonstrated higher transfection, no significant difference ($p > 0.05$) was observed as compared to the liposomes surface modified

with single targeting ligand. Therefore, RVG9RMAN, PenMAN and RDPMAN liposomes were selected for *in vivo* evaluation in our further studies utilizing pVGF.

Higher transfection efficiency of dual modified liposomes across BBB model can be rationalized *via* their dual transport mechanisms leading to enhanced transport of the therapeutic gene to the nucleus of cells. These observations advocate the effect of targeting ligands (MAN and CPPs) on developing liposomal nanoparticles as suitable candidates for brain-targeted gene therapy for treating AD.

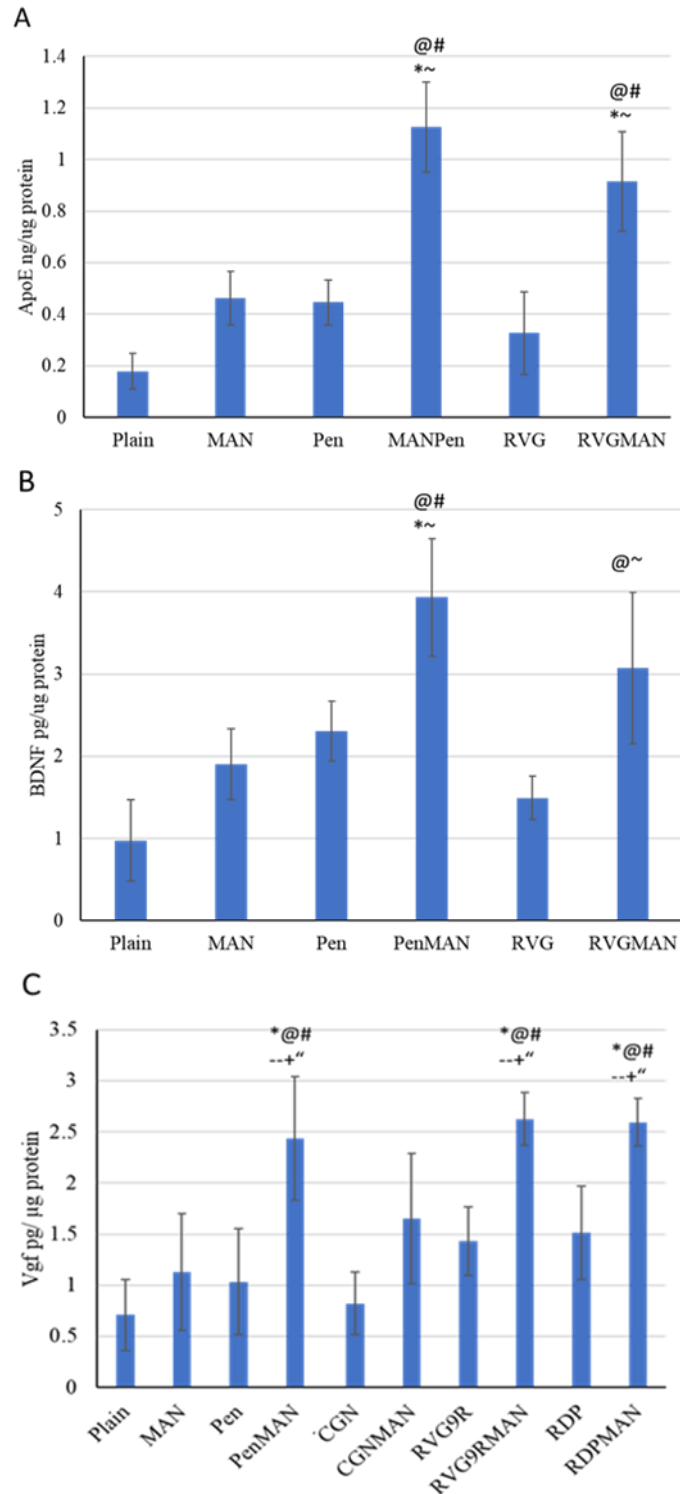


Figure 16. A) ApoE2, B) BDNF, C) Vgf transfection across BBB model post treatment with liposomes entrapping 1 μ g pBDNF/chitosan complexes. Data shown as mean (SD) with 4 repeats. @, #, *, ~, --, +, and “ shows statistical significance ($p < 0.05$) from plain, Pen, MAN, RVG, CGN, RVG9R and RDP liposomes, respectively.

3.11. *In Vivo* Biodistribution

The ability of liposomes to target brain tissue was evaluated *in vivo* in C57BL/6 mice. MAN modified liposomal nanoparticles containing lissamine rhodamine dye were injected intravenously, and brain tissues were analyzed post euthanization at predetermined time points, using HPLC-FLD analysis as described earlier. As indicated in **Figure 17 A**, the amount of MAN liposomes increased steadily up to 4.6% when assessed at 12 h and no significant change was found at 24 h. Therefore, the effect of CPPs in combination with MAN on targeting GLUT-1 transporters on BBB was seen at 12 h in further experimentation.

Biodistribution of dual modified liposomes was evaluated in the brain as well as in other organs using HPLC-FLD as explained previously. Plain and single modified (MAN, Pen, or RVG) liposomes were used as formulation controls in this experiment. It was observed that dual modified (PenMAN and RVGMAN) liposomes were able to penetrate brain tissue more efficiently than single modified or plain liposomes which was in accordance with our *in vitro* results (**Figure 17 B**). PenMAN liposomes were able to transport across BBB up to ~7.30% ID/ gram tissue whereas RVGMAN liposomes were found to be accumulated ~5.33% ID/ gram tissue in brain with no significant difference between these dual modified nanoparticles. Although, RVGMAN liposomes were found to be present in more amount than single modified or plain liposomes, we did not find any significant difference between RVGMAN, RVG and MAN modified liposomes (**Figure 17 B**). This demonstrates combinational effect of CPPs with MAN in effective translocation of these nanoparticles across the BBB as compared to other formulation controls. As expected, nanoparticles were found to be accumulated in higher amounts in the liver, and spleen, owing to internalization by macrophages in the reticuloendothelial system (RES).²⁶⁰ Fenestrations in

endothelial cells leads to trapping of foreign particles explaining non-specific accumulation in these organs.²⁶¹

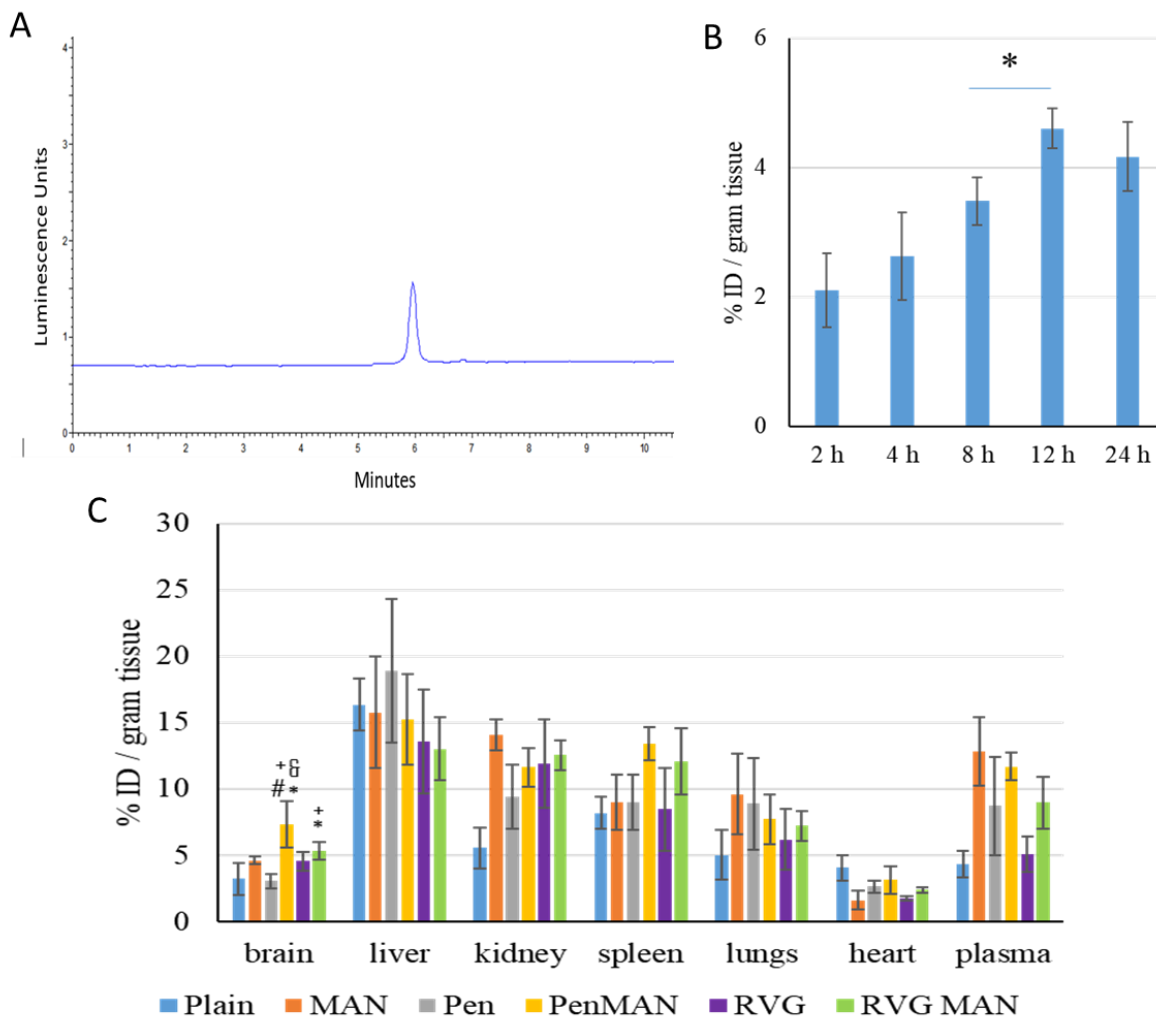


Figure 17. A) HPLC chromatogram of lissamine rhodamine dye. B) Distribution of lissamine rhodamine labelled MAN-liposomes in brain of C57BL/6 mice over a period of 24hours (n = 6). C) Biodistribution of lissamine rhodamine labelled liposomal formulations in different organs of C57BL/6 mice at 12hrs to analyze the effect of CPPs in combination with mannose (n = 6). Data is presented as mean \pm SD (n = 6). Statistically significance ($p < 0.05$) is shown as (*) with plain liposomes, (#) with MAN liposomes, (+) with Pen liposomes, (&) with RVG liposomes.

3.12. *In Vivo* Biocompatibility and Gene Transfection in Wild Type Mice

Following the transportation of nanoparticles inside the brain, the therapeutic gene must be released inside brain cells effectively as well as safely in order to produce the desired therapeutic

effect. In this study, we evaluated the transfection ability of dual modified liposomes following a single administration. Liposomes entrapping pDNA–chitosan complex were administered intravenously and mice were further housed for 5-days before harvesting organs. The transfection efficiency of pVGF was evaluated using liposomes modified with RVG9R, RDP, CGN or Pen, in combination with MAN. The transfection efficiency pBDNF and pAPoE2 was evaluated using liposomes modified with RVG or Pen, in combination with MAN.

In mice treated with BDNF plasmid, it was observed that BDNF protein was significantly increased in mice brain treated with dual modified liposomes (PenMAN and RVGMAN) as compared to other formulation controls and free plasmid (pBDNF in saline) administration (**Figure 18A**). Increased BDNF levels in the brain of dual modified liposomes treated mice compared to other control groups can be attributed to their higher transport across the BBB and internalization inside the brain cells. Dual modified (PenMAN and RVGMAN) treated mice exhibited 1.7 times higher BDNF levels compared to baseline levels. Slightly higher levels of BDNF (129.5 pg BDNF protein/ μ g total protein) were found in the brain of RVGMAN treated mice compared to PenMAN treated mice (126.8 pg BDNF protein/ μ g total protein) but no significant difference was found between these formulations. This increase in BDNF protein level in brain can activate its receptor, TrkB, leading to differentiation, plasticity, and survival of neuronal cells in CNS as well as in the peripheral nervous system (PNS). This may help in rescuing brain cells against AD associated neurodegeneration and synaptic dysfunction. BDNF protein levels were also seen to be elevated in other organs (kidney, lungs, spleen, liver, plasma, and heart) when compared to their baseline levels (**Figure 18 B – G**), which can be explained by accumulation of liposomes in these organs. Peripheral BDNF levels are found to be reduced in patients with mild cognitive impairment (MCI), and dementia including AD.^{262,263} Increase in

peripheral BDNF levels is also suggested to help improve cognitive functions in AD patients and lower the risk of damages associated with AD.^{264,265}

In mice treated with ApoE2 plasmid, as demonstrated in **Figure 19A**, dual-modified liposomes were able to successfully transfect brain cells with ~2 times higher ApoE protein expression than the endogenous ApoE level. Furthermore, RVGMAN and PenMAN liposomes demonstrated higher protein expression ($p < 0.05$) in mice brain in contrast to naked pApoE2, plain and monofunctionalized liposomes. Both RVGMAN and PenMAN showed transfection in the range of 36.47 ± 4.38 and 37.69 ± 3.89 ng ApoE/ mg protein, respectively. Naked pApoE2 did not show any significant difference from endogenous level, whereas transfection efficiency of plain or monofunctionalized liposomes was found to be ~1.25 times than endogenous levels. RVGMAN and PenMAN liposomes mediated increased ApoE protein expression can be attributed to the efficient transcytosis and gene transport inside nucleus of the cells owing to dual surface functionalization with brain-specific ligands. Dual modification might have also helped the liposomes to overcome the competition from the physiological sugars present in the body. Tissues from other organs also displayed elevated ApoE expression *in vivo* (**Figure 19 B-G**), which can be attributed to the transport of liposomes to these organs. Overall, dual-functionalized liposomes can serve as a promising candidate for brain-targeted delivery of pApoE2 to treat AD.

Mice treated with liposomal nanoparticles (RVG9RMAN, PenMAN, and RDPMAN) entrapping pVGF/chitosan complex demonstrated significantly higher ($p < 0.05$) vgf protein transfection in the brain of wild type mice compared to mice treated with saline and naked DNA (**Figure 20 A**). RVG9RMAN, PenMAN and RDPMAN functionalized liposomes demonstrated ~70 pg vgf protein per mg total protein, which was ~1.5 times the expression demonstrated by monofunctionalized liposomes. However, no statistically significant difference ($p > 0.05$) was

observed between the different bifunctionalized liposomal nanoparticles. Also, no statistically significant difference ($p > 0.05$) was observed between the plain and single modified liposomes (MAN, RVG9R, Pen and RDP). Vgf protein was also found to be increased in plasma and other organs (liver, spleen, kidney, heart, and lungs) when compared to their baseline levels.

H&E staining was performed to assess biocompatibility of the administered liposomal nanoparticles entrapping pBDNF, pApoE2 or pVGF in major tissues. Saline treated group was used as a control. Tissue sections were assessed for signs of aberrations, nucleus enlargement, inflammation, or abnormalities in cellular morphology. The results indicated that the liposomal nanoparticles did not demonstrate any form of toxicity in the brain, liver, spleen, kidney, heart, and lungs (**Figure 21**). Disruption of muscle fibers were not observed in cardiac tissue. Lung and liver tissues did not show any sign of fibrosis and ballooning, respectively. Also, abnormal alveoli thickening was not observed in the lungs. Examination of spleen and kidney tissue sections depicted no signs of nucleic enlargement, necrosis, or defects in cell morphology. Moreover, mice treated with liposomal nanoparticles did not demonstrate any changes in water/food intake, behavioral alterations, or loss of physical activity, indicating good safety profile of this delivery system.

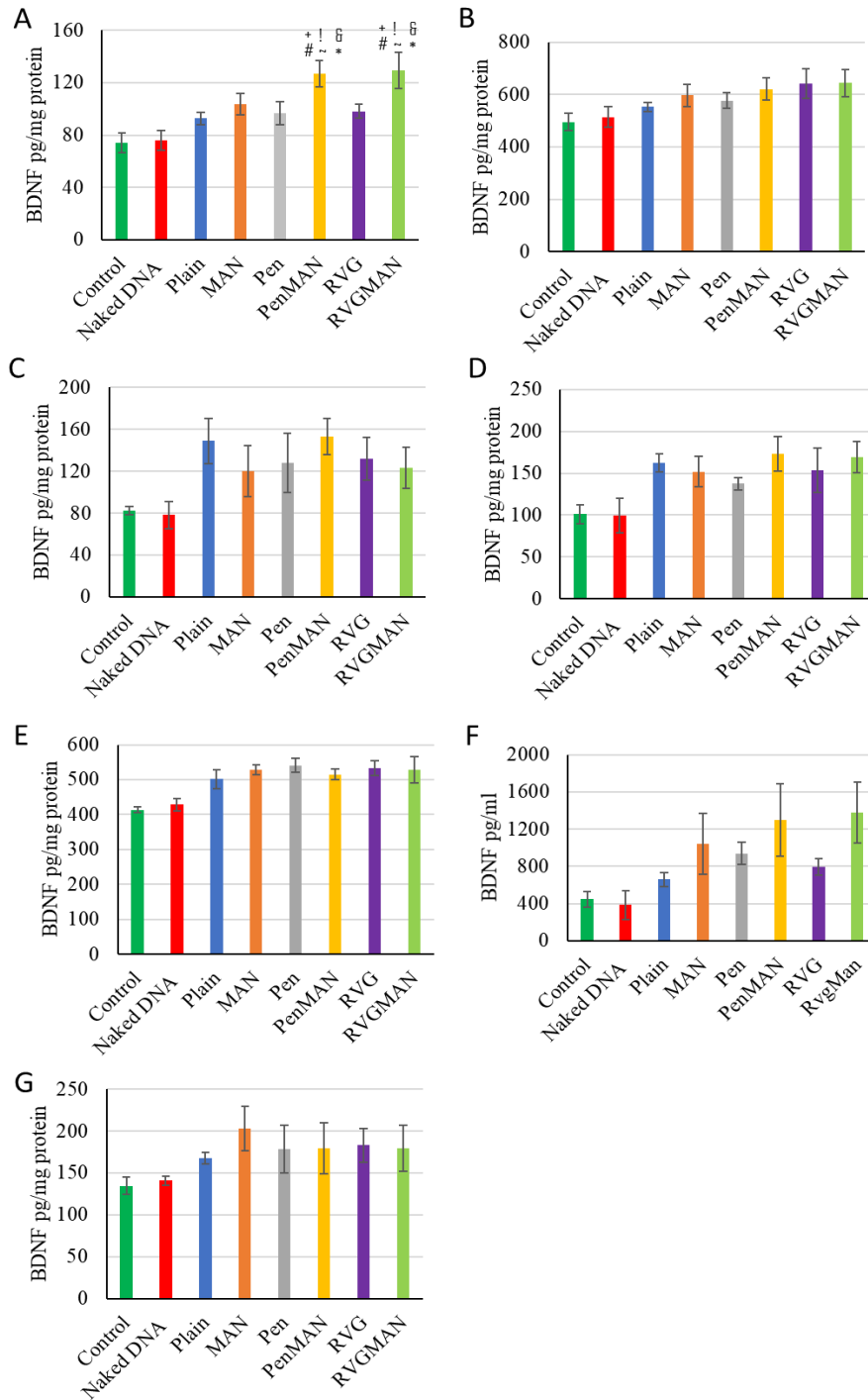


Figure 18. BDNF expression levels post 5 days after transfection *in-vivo* in different organs (A. Brain; B. Kidney; C. Lungs; D. Spleen; E. Liver; F. Plasma; G. Heart) of C57BL/6 mice using liposomal formulations (15.2 μ M of phospholipids/kg body weight) entrapping chitosan-pBDNF complexes (40 μ g/100g body weight). Data is presented as mean \pm SD (n = 6). Statistically significance (p < 0.05) is shown as (!) with naked DNA, (*) with plain liposomes, (#) with MAN liposomes, (+) with Pen liposomes, (&) with RVG liposomes, and (~) with control.

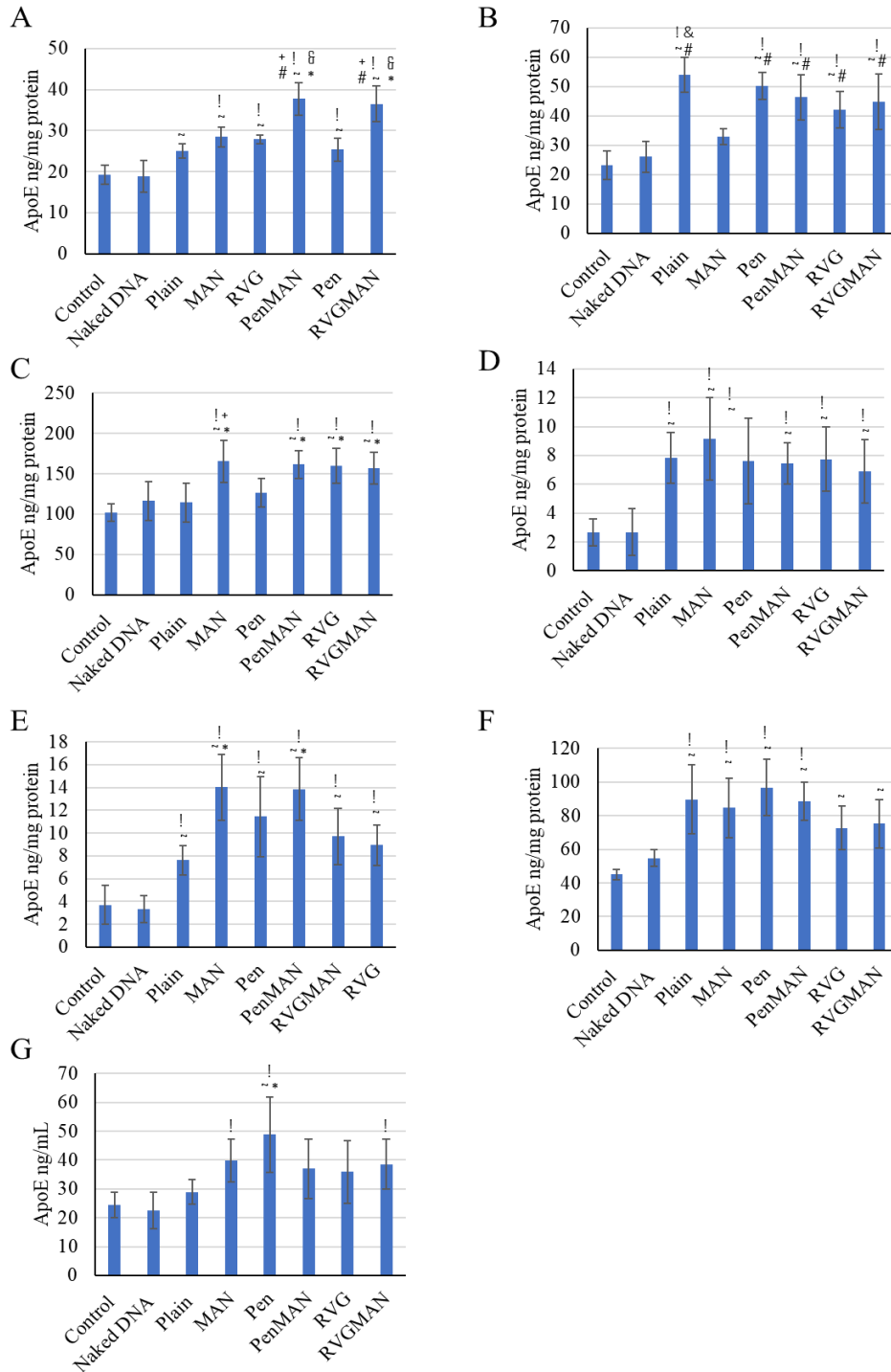


Figure 19. ApoE expression levels post 5 days after transfection *in-vivo* in different organs (A. Brain; B. Heart; C. Liver; D. Spleen; E. Lungs; F. Kidney; G. Plasma) of C57BL/6 mice using liposomal formulations (15.2 μ M of phospholipids/kg body weight) entrapping chitosan-pBDNF complexes (40 μ g/100g body weight). Data is presented as mean \pm SD (n = 6). Statistically significance (p < 0.05) is shown as (!) with naked DNA, (*) with plain liposomes, (#) with MAN liposomes, (+) with Pen liposomes, (&) with RVG liposomes, and (~) with control.

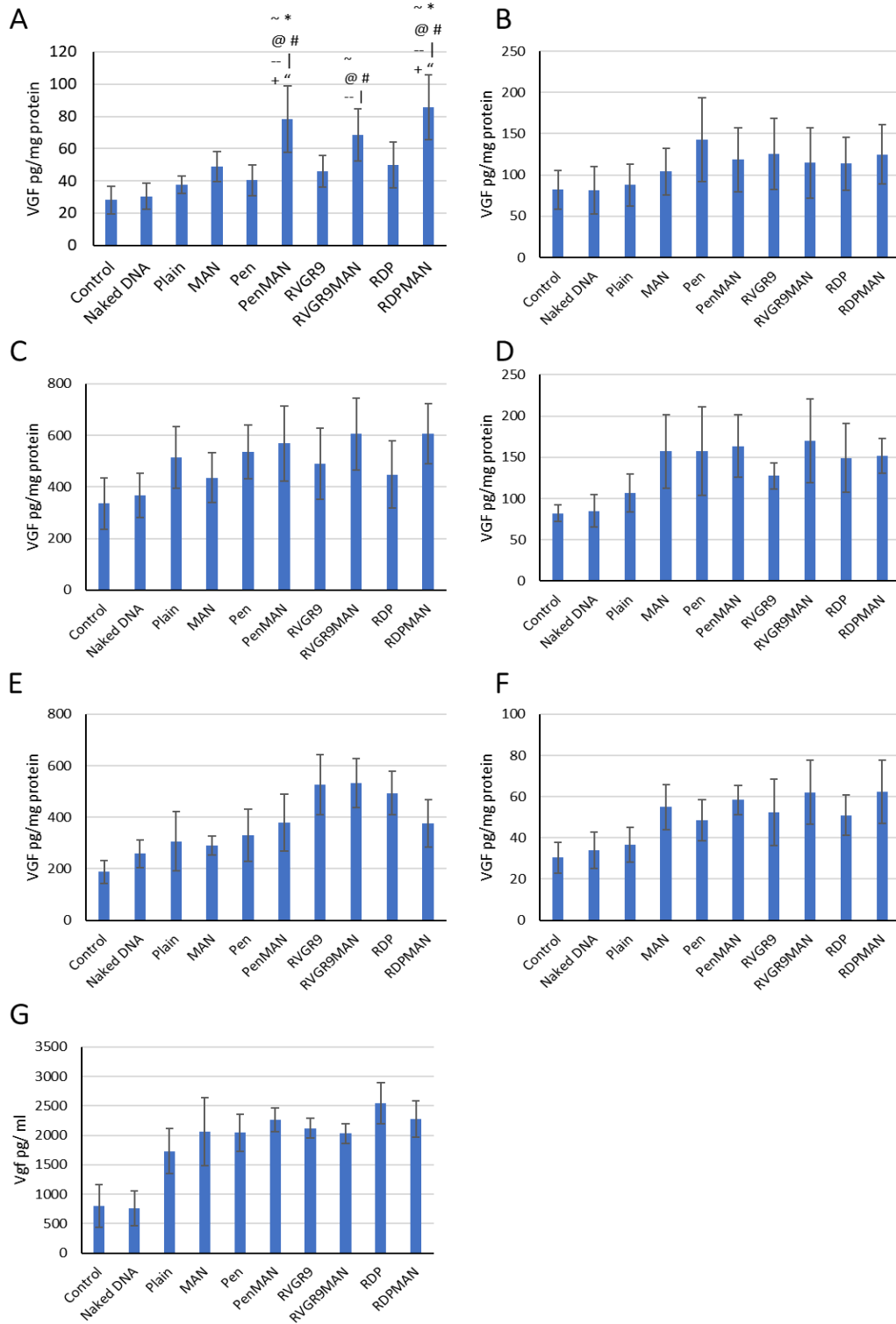


Figure 20. Vgf expression levels post 5 days after transfection *in-vivo* in different organs. A) Brain, B) Heart, C) Kidney, D) Lungs, E) Liver, F) Spleen, and G) Plasma. Data shown as mean (SD) with 6 repeats. ~, |, @, #, *, --, +, and “ shows statistical significance ($p < 0.05$) from control, naked DNA, plain, Pen, MAN, CGN, RVGR9 and RDP liposomes, respectively.

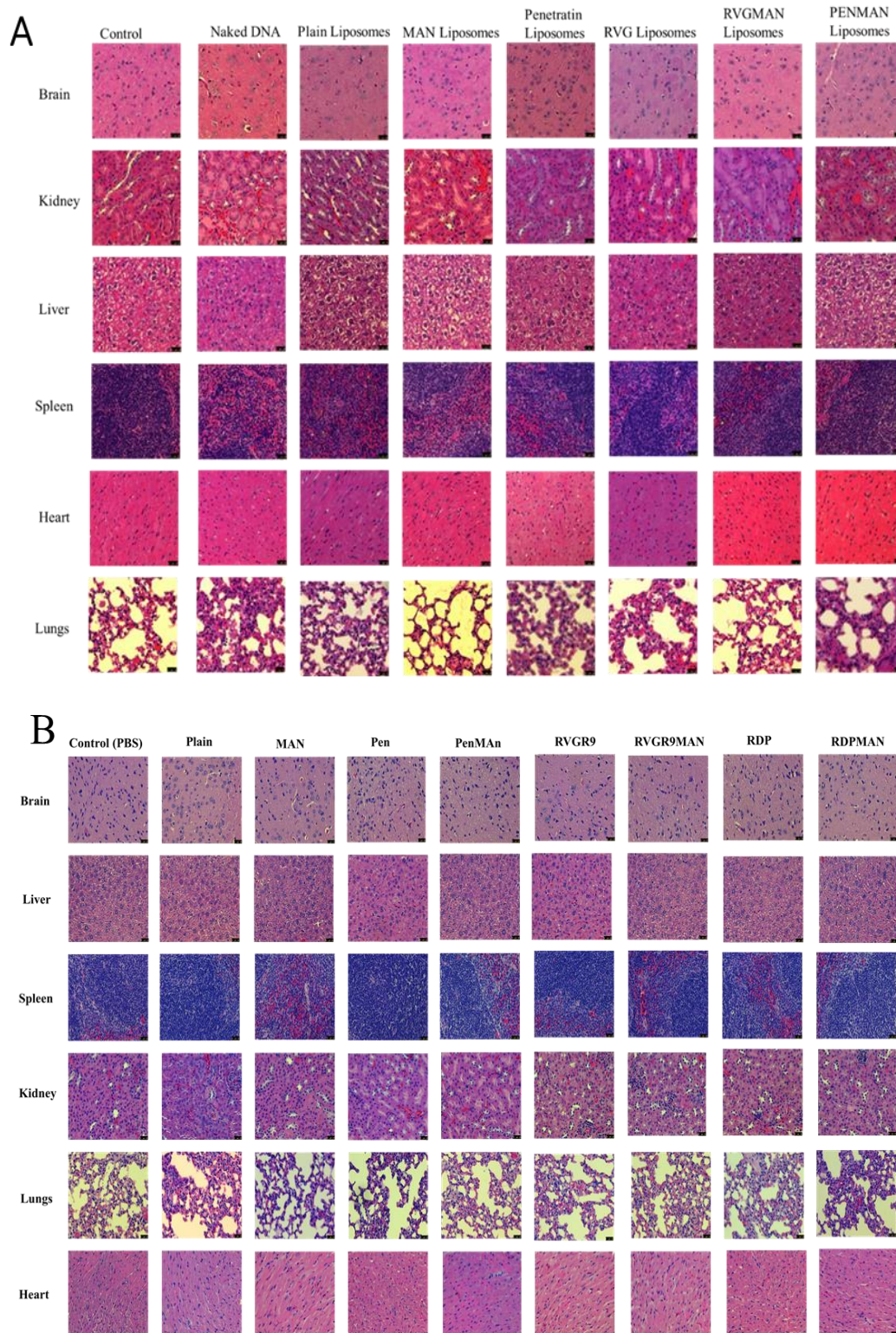


Figure 21. Biocompatibility analysis via H&E staining of tissue sections from different organs of C57BL/6 mice 5 days post treatment with various liposomal formulations entrapping A) chitosan-pApoE complexes, B) chitosan-pVGF complexes and C) chitosan-pBDNF complexes.

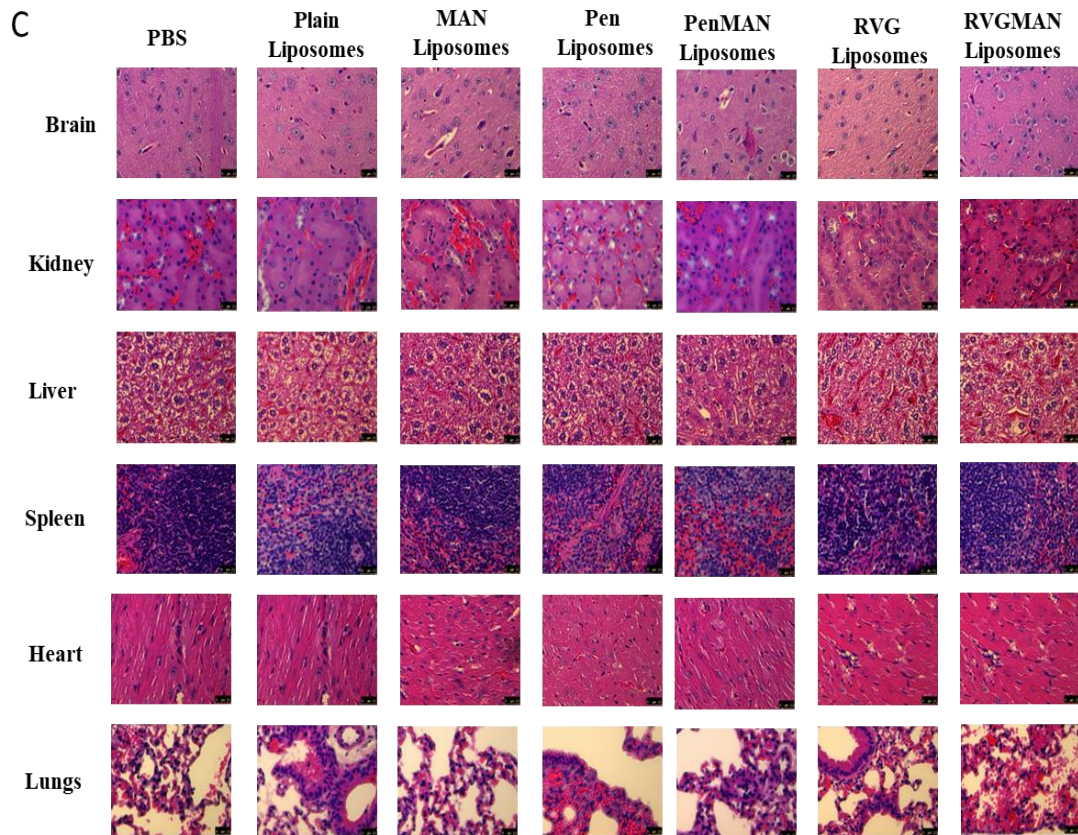


Figure 21. Biocompatibility analysis via H&E staining of tissue sections from different organs of C57BL/6 mice 5 days post treatment with various liposomal formulations entrapping A) chitosan-pApoE complexes, B) chitosan-pVGF complexes and C) chitosan-pBDNF complexes (continued).

3.13. BDNF Protein Transfection in AD Mice

Liposomal nanoparticles entrapping pBDNF/chitosan complexes were intravenously administered in 6- and 9-month-old APP/PS1 mice. Transfection ability of the liposomal nanoparticles was assessed in the brain tissue of these mice using BDNF ELISA. As expected, we observed ~35% reduction in the BDNF levels in the untreated transgenic mice in comparison to the wild-type age-matched controls in both 6- and 9-month-old APP/PS1 mice (**Figure 22**). BDNF protein was found to be increased in the treatment groups compared to the PBS-only treated AD mice. APP/PS1 mice treated with monofunctionalized (MAN, Pen, and RDP) liposomes demonstrated a ~60% increase in BDNF protein which was significantly higher ($p < 0.05$) from their age-matched PBS and naked DNA treated AD mice in 6- as well as in 9-month-old APP/PS1

mice age groups. Moreover, APP/PS1 AD mice treated with bifunctionalized (RDPMAN and MANPen) liposomes displayed ~95% increase in BDNF protein which was significantly higher ($p < 0.05$) compared to respective PBS treated AD mice control in both age groups (**Figure 22**). Transgenic mice treated with the bifunctionalized liposomal nanoparticles also demonstrated BDNF protein levels higher than their age-matched wild-type controls.

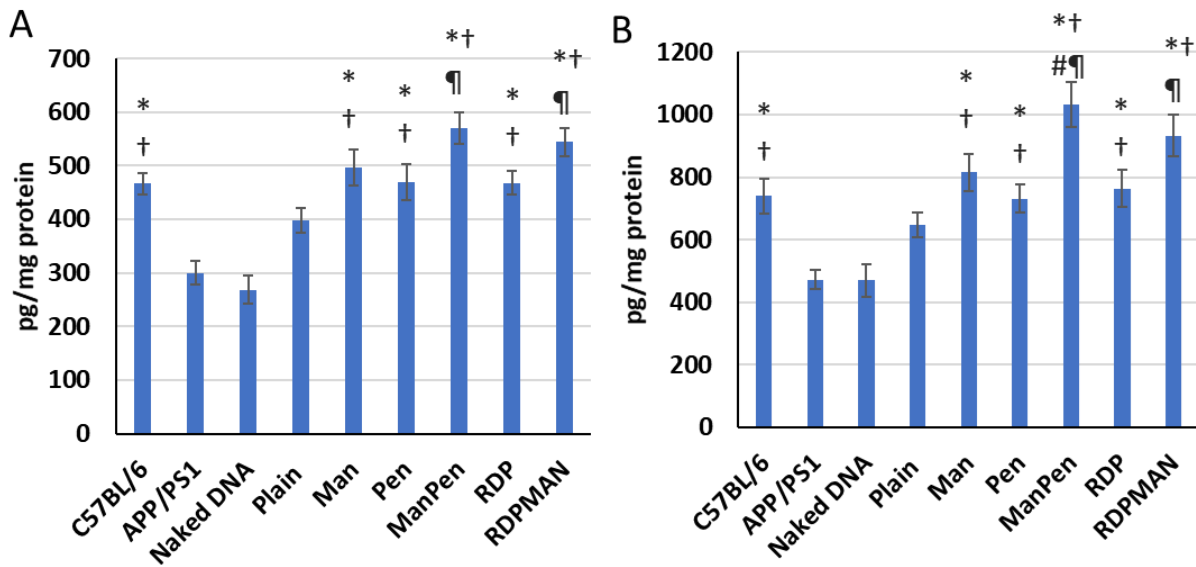


Figure 22. BDNF expression levels in A) 6-months and B) 9-months mice brain post four weekly intravenous administration of liposomes entrapping pBDNF/chitosan complexes. Data presents mean \pm SEM of 6 animals. Statistically significant difference ($p < 0.05$) is shown as (#) with C57BL/6, (*) with APP/PS1, (†) with naked DNA, and (¶) with Plain liposomes.

3.14. Quantification of Amyloid Beta Peptides

It has been demonstrated that disruption in the BDNF signaling results in the activation of the amyloidogenic pathway and increase in APP levels.¹⁸ Studies by various groups have shown the inhibitory effect of neurotrophic factors on abeta production.^{31,169} Amongst abeta isoforms, abeta 40 and 42 are believed to be the chief culprits for neurotoxic effects in AD. Also, abeta-42 has shown to have higher inclination for aggregation and cellular toxicity than abeta-40 isoform

in the brain.^{266,267} Therefore, effect of BDNF transfection in the brain was evaluated on abeta-40 and -42 fraction levels.

Investigation of the soluble (TBS fraction), membrane-associated (TBSX fraction), and insoluble abeta linked to the plaque deposition (GDN fraction) were performed in 6- and 9-month-old APP/PS1 mice treated with liposomal nanoparticles entrapping BDNF/chitosan complexes. All the fractions of the abeta-40 as well as abeta-42 were found to be significantly higher ($p < 0.05$) in APP/PS1 mice compared to their wild-type controls (**Figure 23, 24**). Additionally, higher levels of abeta-40 and -42 was observed in 9-month-old APP/PS1 mice compared to their 6-month-old counterparts. No statistically significant difference was observed between the naked DNA group and transgenic mice controls reaffirming incapability of naked DNA to bypass BBB and cellular membranes. However, bifunctionalized liposomal nanoparticles (RDPMAN and MANPen) demonstrated significant reduction ($p < 0.05$) in the fractions of the abeta-40 as well as abeta-42 in both 6- and 9-month-old transgenic mice.

In 6-month-old APP/PS1 mice, we observed more than 50% reduction in the levels of the abeta-40 fractions in transgenic mice following 4-week weekly treatment regimen with bifunctionalized (RDPMAN and MANPen) liposomes (**Figure 23 A, B, C**). Moreover, transgenic AD mice treated with bifunctionalized liposomes showed comparable abeta levels to healthy wild-type age-matched controls (no significant difference, $p > 0.05$) (**Figure 23 A, B**). Similarly, we observed more than 50% reduction in the levels of the abeta-42 fractions in transgenic AD mice treated with bifunctionalized (RDPMAN and MANPen) liposomes (**Figure 23 D, E, F**). RDPMAN and MANPen liposomal nanoparticles performed comparably in their efficacy to reduce abeta-40 and abeta-42 fractions.

In 9-month old APP/PS1 mice, bifunctionalized (RDPMAN and MANPen) liposomes also resulted in a significant reduction of abeta-40 and abeta-42 fractions compared to untreated control (**Figure 24**). TBS fraction of abeta peptides was observed to be reduced by ~25% and ~35% in APP/PS1 mice treated with RDPMAN and MANPen liposomes, respectively (**Figure 24 A, D**). Additionally, TBSX and GDN fractions of abeta peptides demonstrated 30-40% reduction following treatment with RDPMAN and MANPen liposomes (**Figure 24 B, C, E, F**). As observed in 6-month-old transgenic mice, RDPMAN and MANPen liposomal nanoparticles performed similarly in their efficacy to reduce abeta-40 and abeta-42 fractions in 9-month-old AD mice. Bifunctionalized nanoparticles fared better than monofunctionalized liposomes in reducing abeta peptides in both age groups.

These results have been in agreement with the previous studies demonstrating the altering effect of BDNF protein on abeta production.^{31,268-270} There is also enough evidence that abeta peptide production drives the amyloid deposition in the brain parenchyma. Additionally, recent study has shown association between BDNF downregulation and increased plaque deposition in the postmortem human brain tissues.²⁷¹ Suggesting, BDNF restoration *via* neurotrophin therapy may result in prevention and/or attenuation of amyloid pathology.^{30,270-272}

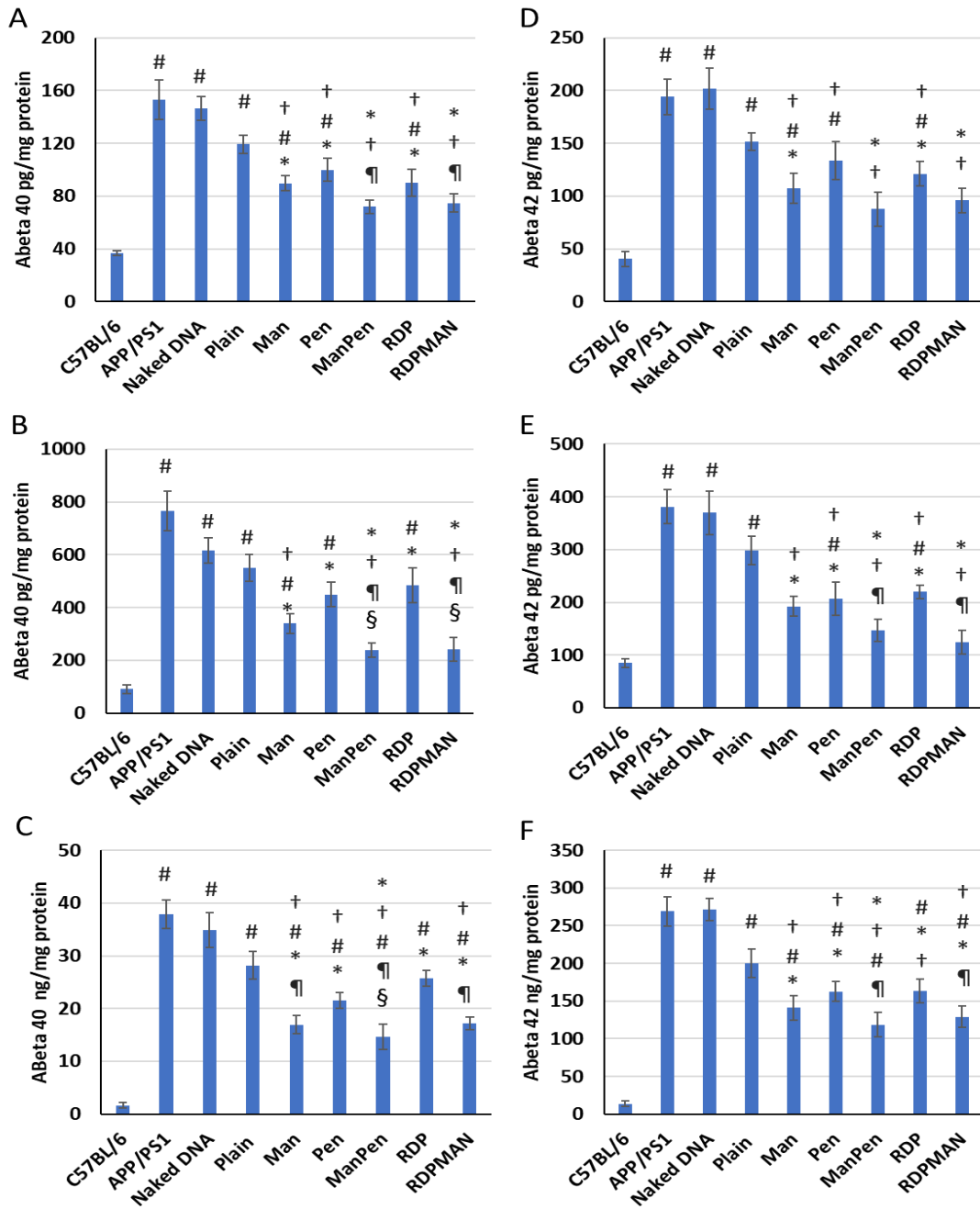


Figure 23. Levels of various fractions of abeta in 6-months old mice brain post four weekly intravenous administration of liposomes entrapping pBDNF/chitosan complexes. A,B,C) Abeta 40 and D,E,F) Abeta 42. A,D) TBS B,E) TBSX and C,F) GDN fraction. Data presents mean \pm SEM of 6 animals. Statistically significant difference ($p < 0.05$) is shown as (#) with C57BL/6, (*) with APP/PS1, (†) with naked DNA, (¶) with Plain liposomes and (§) with RDP liposomes.

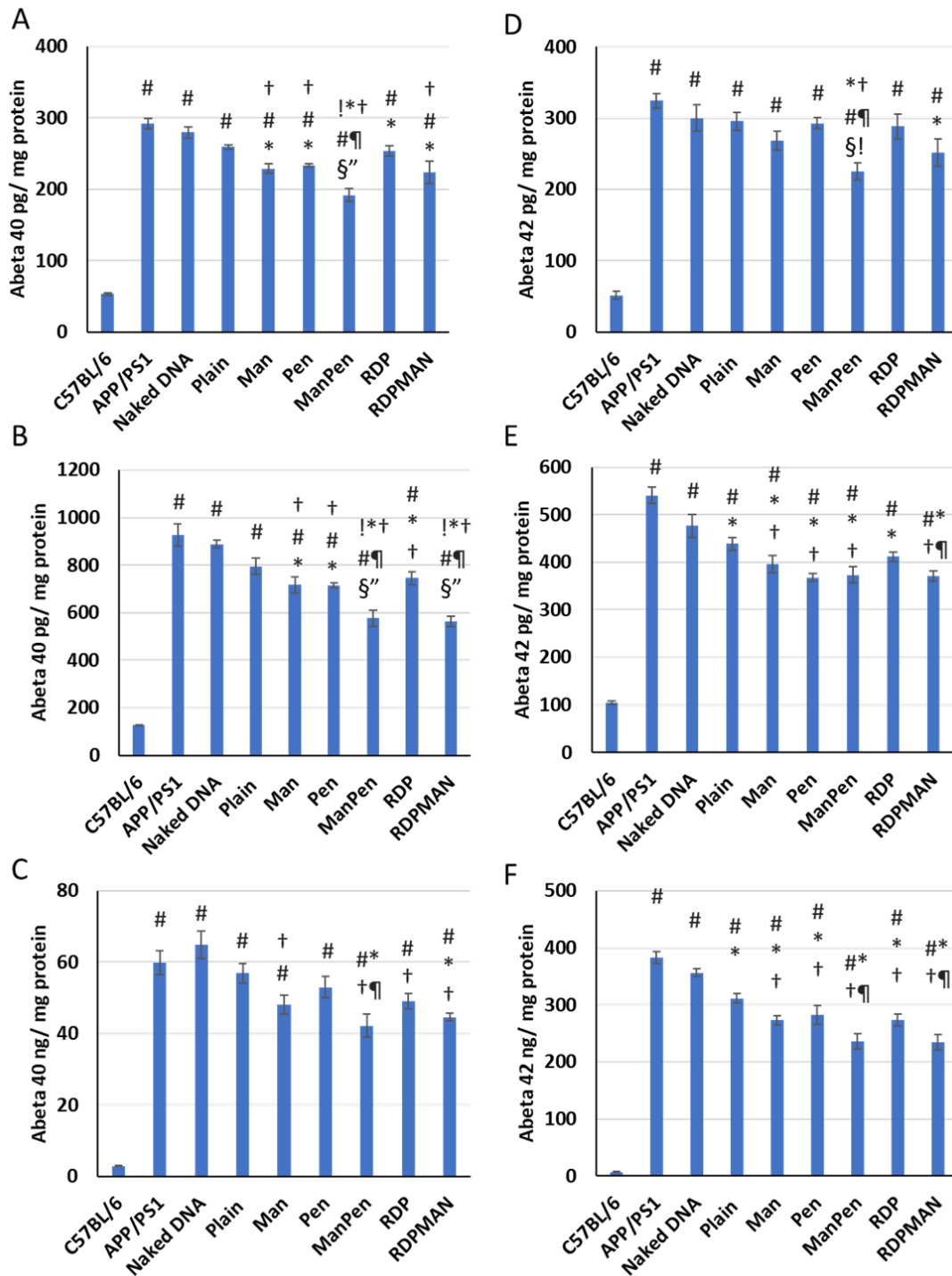


Figure 24. Levels of various fractions of abeta in 9-months old mice brain post four weekly intravenous administration of liposomes entrapping pBDNF/chitosan complexes. A,B,C) Abeta 40 and D,E,F) Abeta 42. A,D) TBS B,E) TBSX and C,F) GDN fraction. Data presents mean \pm SEM of 6 animals. Statistically significant difference ($p < 0.05$) is shown as (#) with C57BL/6, (*) with APP/PS1, (†) with naked DNA, (¶) with Plain liposomes, (†) with MAN liposomes, (!) with Pen liposomes and (§) with RDP liposomes.

3.15. Plaque Load

Quantitative analysis of the area occupied by the amyloid plaques in the brain was performed by calculating the ratio of plaque area to the total area of the region (**Figure 25, 26, 27**). This is expressed in percentages and referred to as plaque load. Plaque load was assessed in the cortex and hippocampus region of the 6- and 9-month-old APP/PS1 mice (**Figure 25**). Total plaque load (hippocampus + cortex) was also analyzed in these mice to better understand the efficacy of BDNF gene therapy. Sharp increase in plaque load was observed in advanced stage (9-month-old) APP/PS1 mice (~3 times) when compared to early stage (6-month-old) counterpart, in both hippocampus and cortex regions of the brain.

BDNF transfection following both monofunctionalized and bifunctionalized liposomal nanoparticles showed appreciable reduction in plaque load in the cortex and the hippocampus regions of the 6-month-old transgenic mice compared to their age-matched untreated control (**Figure 25 A, B, C**). Although, plain non-functionalized liposomes demonstrated a slight reduction in the plaque load, no significant difference ($p > 0.05$) was observed compared to the age-matched untreated control. Mice treated using bifunctionalized MANPen liposomes showed ~6 times plaque load reduction in the cortex region and ~10 times plaque load reduction in the hippocampus region, which was significantly lower ($p < 0.05$) compared to the plaque load in untreated APP/PS1 mice. Similarly, RDPMAN bifunctionalized liposomes displayed ~2 times and ~4 times reduction in the plaque load in the cortex and hippocampus region, respectively, in comparison ($p < 0.05$) to their age-matched untreated controls. A similar trend was observed in the total plaque load (hippocampus + cortex) for the bifunctionalized liposomal nanoparticles (**Figure 25 C**). Interestingly, monofunctionalized MAN-liposomes treated transgenic AD mice also

demonstrated significantly lower plaque load ($p < 0.05$) in the hippocampus area compared to untreated transgenic AD mice.

Similar observations were noted in the advanced stage 9-month-old transgenic AD mouse model. BDNF gene delivery in these mice using bifunctionalized MANPen liposomes resulted in ~2 times plaque load reduction in the cortex region and ~3 times plaque load reduction in the hippocampus region which was significantly improved ($p < 0.05$) compared to the plaque load in age-matched untreated transgenic control (**Figure 25 D, E, F**). Monofunctionalized nanoparticles MAN or Pen and bifunctionalized nanoparticles RDPMAN demonstrated some reduction in plaque load in the cortex and hippocampus regions, however, the difference was not statistically significant ($p > 0.05$) compared to their age-matched untreated transgenic mice control. These results suggest that BDNF restoration *via* neurotrophin therapy may result in the prevention and attenuation of amyloid pathology.^{30,270–272}

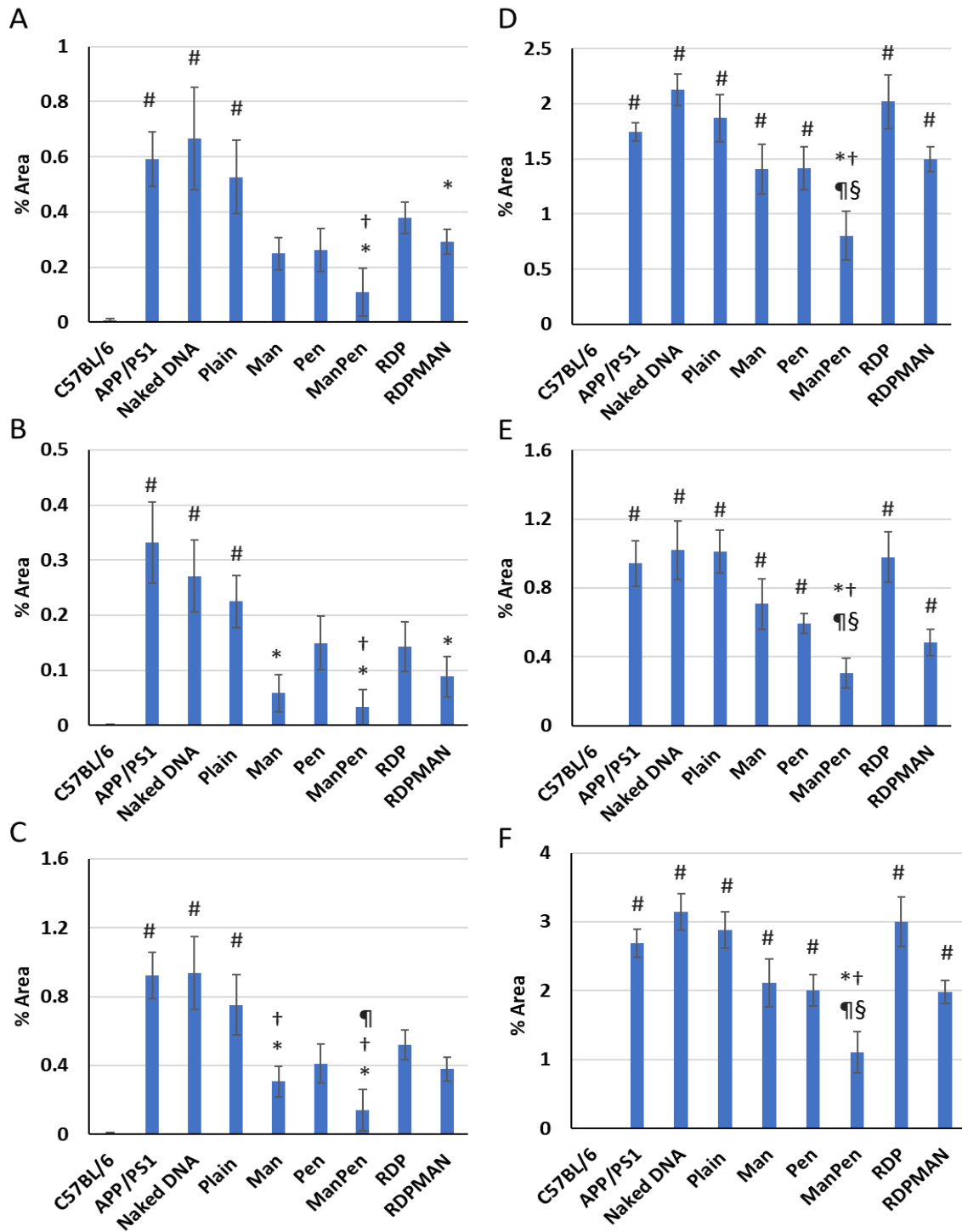


Figure 25. Plaque load in mice brain post four weekly intravenous administration of liposomes entrapping pBDNF/chitosan complexes. A,B,C) 6-months and D,E,F) 9-months. A,D) cortex B,E) hippocampus and C,F) total (cortex + hippocampus). Data presents mean \pm SEM of 6 animals. Statistically significant difference ($p < 0.05$) is shown as (#) with C57BL/6, (*) with APP/PS1, (†) with naked DNA, (¶) with Plain liposomes and (§) with RDP liposomes.

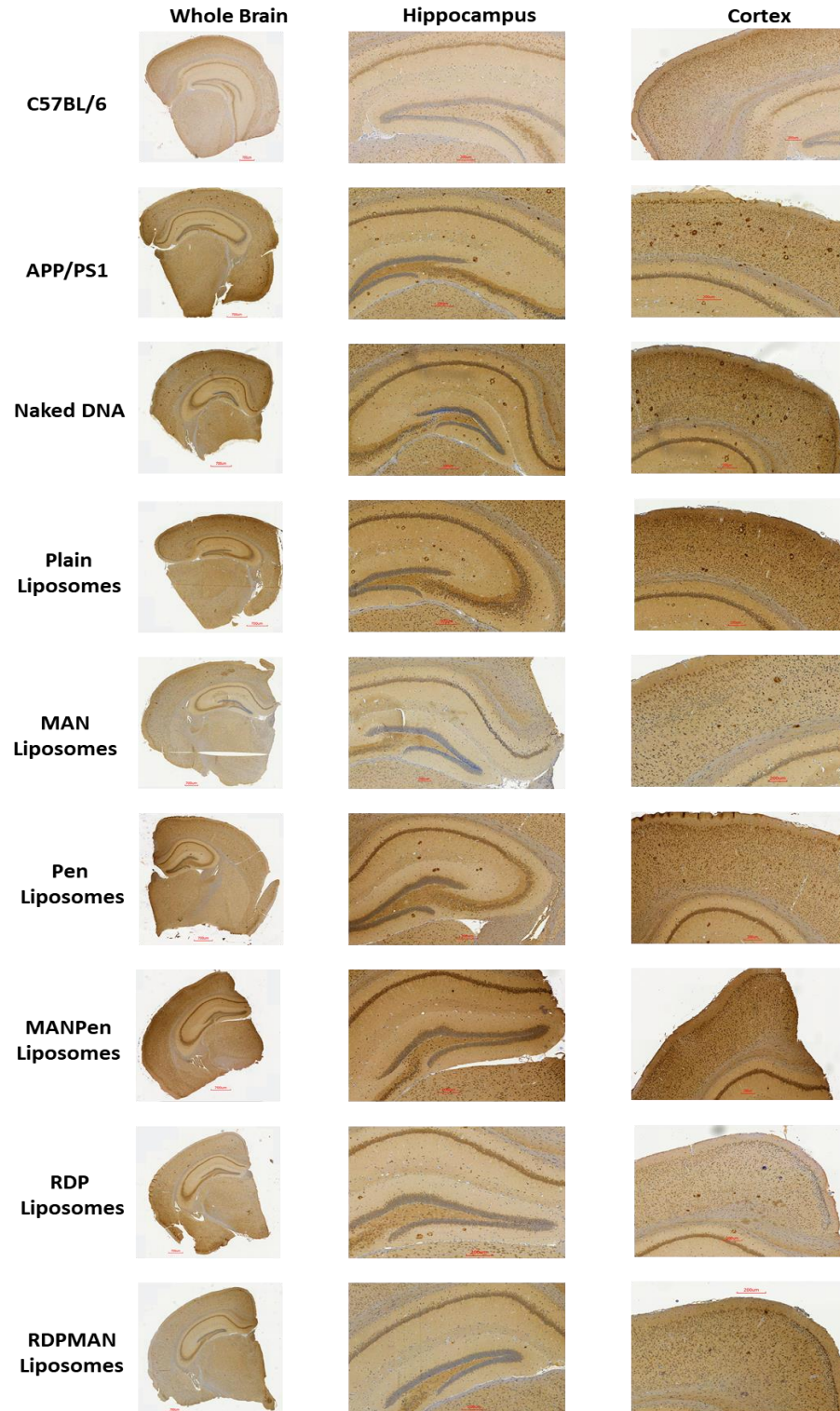


Figure 26. Anti-amyloid beta antibody stained brain sections of 6-months-old mice post four weekly intravenous administration of liposomes entrapping pBDNF/chitosan complexes. C57BL/6 and APP/PS1 represent untreated healthy and AD controls, respectively.

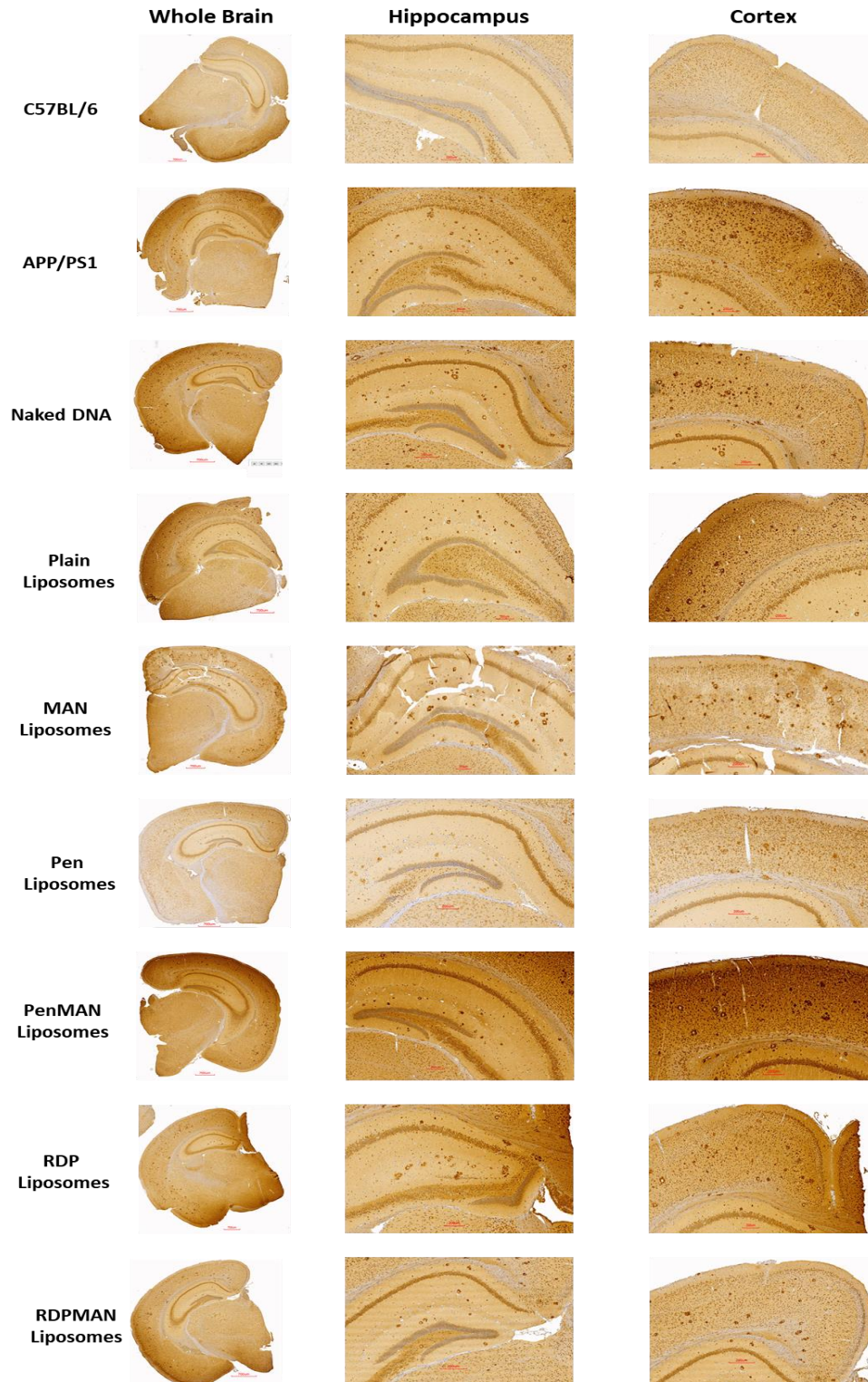


Figure 27. Anti-amyloid beta antibody stained brain sections of 9-months-old mice post four weekly intravenous administration of liposomes entrapping pBDNF/chitosan complexes. C57BL/6 and APP/PS1 represent untreated healthy and AD controls, respectively.

3.16. Cell Proliferation

The family of neurotrophic factors including BDNF, plays crucial part in the differentiation and proliferation of the brain cells during developmental phase and aids in cell survival and function post developmental phase.^{273–275} BDNF acts *via* its Trk receptors and activates various pathways including phosphatidylinositol-3-kinase (PI3K)/Akt pathway resulting in facilitation of survival, proliferation, and plasticity inside the brain.^{276,277} Hence, in this study, we elucidated the effects of BDNF gene therapy on cell proliferation in the brain of AD transgenic mice.

Ki-67 (cell proliferation marker) was utilized to assess the neurogenesis in the brains of 6- and 9-month-old APP/PS1 mice. As expected, in the early-stage AD mouse model (6-months old transgenic mice) we observed a significant lower ki-67 positive cells in untreated APP/PS1 mice as compared to healthy wild-type controls (**Figure 28 A**). BDNF transfection using liposomes modified with MANPen demonstrated a significant increase in ki-67 positive cells in 6-month-old APP/PS1 mice compared to their age-matched untreated controls. However, no significant difference was demonstrated with any of the monofunctionalized (MAN, Pen, and RDP) or RDPMAN functionalized liposomal nanoparticles. Additionally, in 9-month-old mice (wild type, transgenic, and treatment groups), we did not observe a significant number of ki-67 positive cells to infer our findings (data not shown).

These observations are consistent with the previously published reports indicating an age-related decline in proliferating cells in different regions of the brain.^{278–280} Accordingly, this indicates that BDNF gene therapy at current transfection levels may not be able to resurrect cell proliferation machinery; however, it may help prevent cell death against the toxic effect of the abeta plaques at early disease stages.^{272,281}

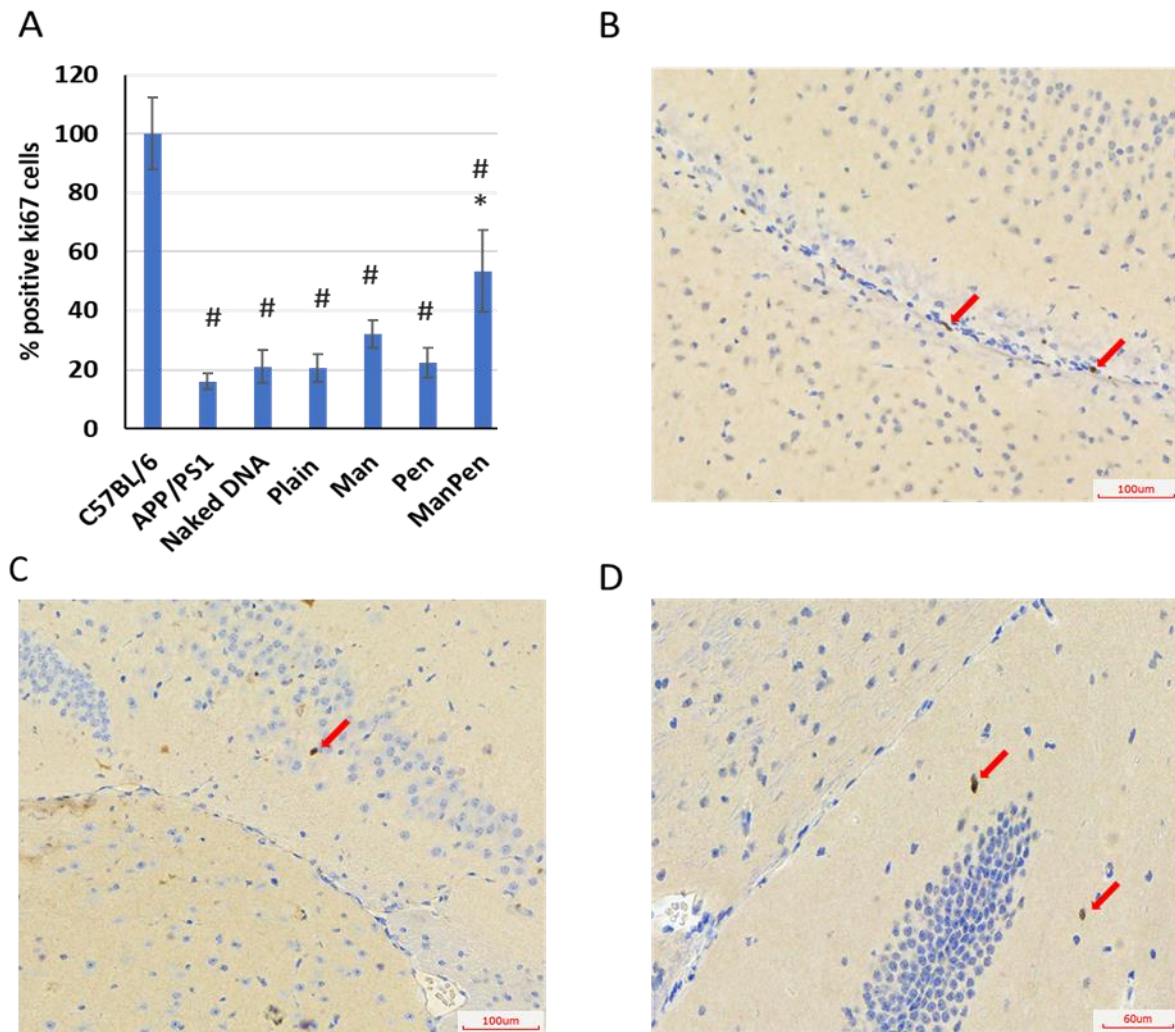


Figure 28. Cell proliferation in the brains of 6-month old mice post four weekly intravenous administration of liposomes entrapping pBDNF/chitosan complexes. A) percentage positive ki67 cells. Ki67 positive cells in the brain sections of B) C57BL/6, C) APP/PS1, and D) APP/PS1 treated with MANPen liposomes. Data presents mean \pm SEM of 6 animals. Statistically significant difference ($p < 0.05$) is shown as (#) with C57BL/6, and (*) with APP/PS1.

3.17. Synaptophysin and PSD-95 Protein Quantification

Dysregulation of the downstream pathways associated BDNF including Akt, PLC, and ERK, results in the alteration in the essential synaptic protein levels, synaptophysin and PSD-95.^{276,282,283} Depletion of synaptic proteins results in the loss of synapses, which is correlated with the degree of cognition impairment witnessed in the initial and later stages of the AD^{284,285}. Therefore, the modulation in the levels of synaptic proteins were examined post BDNF

transfection in the APP/PS1 mice. Levels of synaptophysin and PSD-95 protein were assessed in the brains of the AD transgenic mice. Synaptic protein levels were found to be reduced in the brains of both 6- and 9-month-old APP/PS1 mice in comparison to their healthy age-matched wild-type controls. Synaptophysin levels were found to be increased in the transgenic animals following BDNF gene delivery *via* biofunctionalized liposomal nanoparticles (**Figure 29**). Both MANPen and RDPMAN treated groups demonstrated more than 1.5 times increase in the levels of the synaptophysin protein in the 6- and 9-month-old APP/PS1 mice which was significantly higher compared to ($p < 0.05$) untreated control (**Figure 29 A, B**).

Similarly, PSD-95 protein was also found to be significantly reduced in the brains of 6- and 9-month-old APP/PS1 AD mice compared to their healthy wild-type controls. All treatment groups showed increase in PSD-95 protein level following BDNF transfection in APP/PS1 mice (**Figure 29 C, D**). BDNF transfection using bifunctionalized liposomes resulted in ~2 times increase in PSD-95 protein level which was significantly higher ($p < 0.05$) compared to the untreated transgenic controls in both age groups.

Thus, BDNF gene therapy was able to rescue this decline and bring the levels of these pre and post synaptic proteins comparable to the baseline levels. This was also in agreement with a recently published report demonstrating the positive therapeutic effect of BDNF on synapse proteins.²⁷⁰ Rescue of synaptic proteins aids in promoting and sustaining the appropriate functioning of the existing brain cells for synaptic plasticity processes.

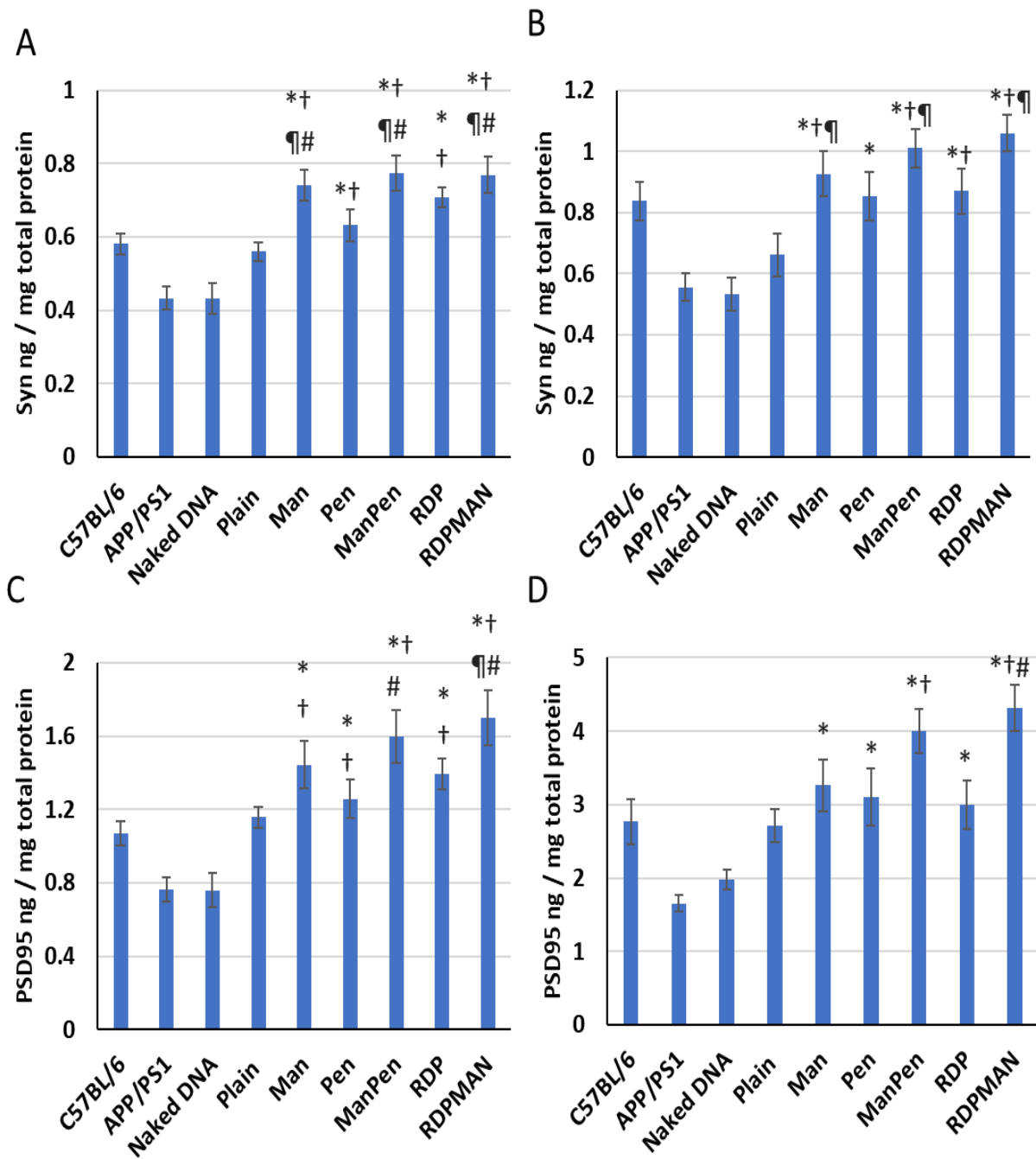


Figure 29. Levels of synaptic proteins in mice brain post four weekly intravenous administration of liposomes entrapping pBDNF/chitosan complexes. A,C) 6-months and B,D) 9-months. A,B) Synaptophysin C,D) PSD95. Data presents mean \pm SEM of 6 animals. Statistically significant difference ($p < 0.05$) is shown as (#) with C57BL/6, (*) with APP/PS1, (†) with naked DNA, and (¶) with Plain liposomes.

3.18. Nesting

The efficacy of BDNF gene therapy was evaluated *via* nesting behavior in the transgenic mice model of AD. Nest formation is a natural behavior in rodents as it is essential for shelter, thermoregulation, and reproduction. This behavior can be interpreted as activities of daily living in humans which is severely affected as AD progresses.²⁸⁶ This behavior is seen to be deteriorated significantly starting from 6 months of age in AD mice.^{226,287} Nest building behavior was assessed in AD mice with and without treatment using portion controlled and easy to dispense bedding material.

Transgenic AD mice displayed significant ($p < 0.05$) impairment in their nesting ability in comparison to their wild type controls in 6- and 9-months old age groups (**Figure 30, 31, 32**). Interestingly, the transgenic mice treated with the bifunctionalized (RDPMAN and MANPen) nanoparticles displayed overall improved nesting score based on their nest forming ability compared to their wild type controls (**Figure 30**). Moreover, APP/PS1 mice treated with the MAN functionalized liposomes also displayed superior nesting behavior compared to their wild type controls in both the age groups.

However, due to low number of animals in our present study significance was not observed ($p > 0.05$). Therefore, we will be performing power analysis on our current data and future studies will be performed with appropriate number of animals to achieve a good conclusion. In addition, other studies such as Morris water maze test exploration and anxiety assessments will be done for overall assessment of cognitive and behavioral improvements.

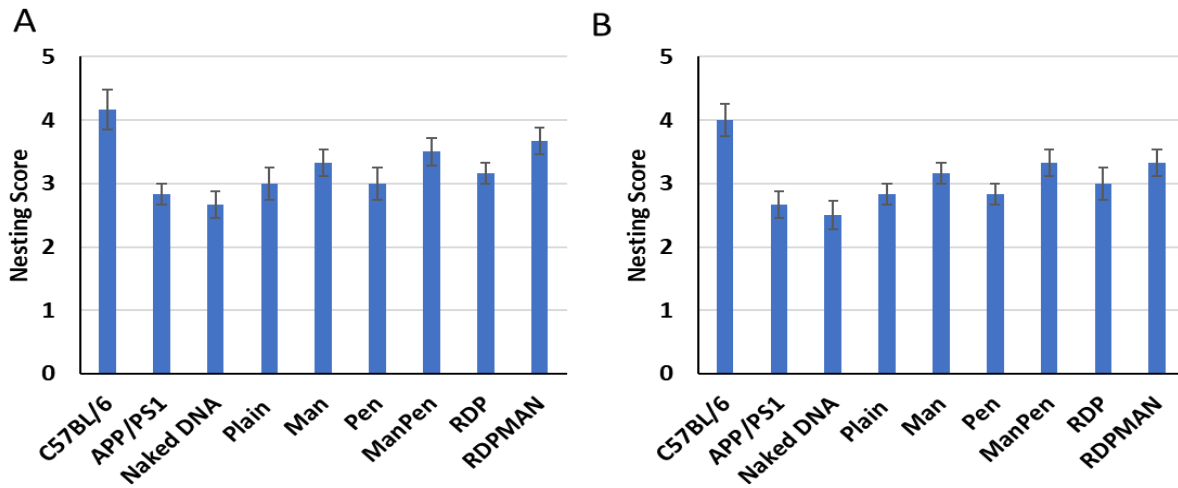


Figure 30. Nesting score in A) 6-month and B) 9-month old mice post four weekly intravenous administration of liposomes entrapping pBDNF/chitosan complexes. Data presents mean \pm SEM of 6 animals.

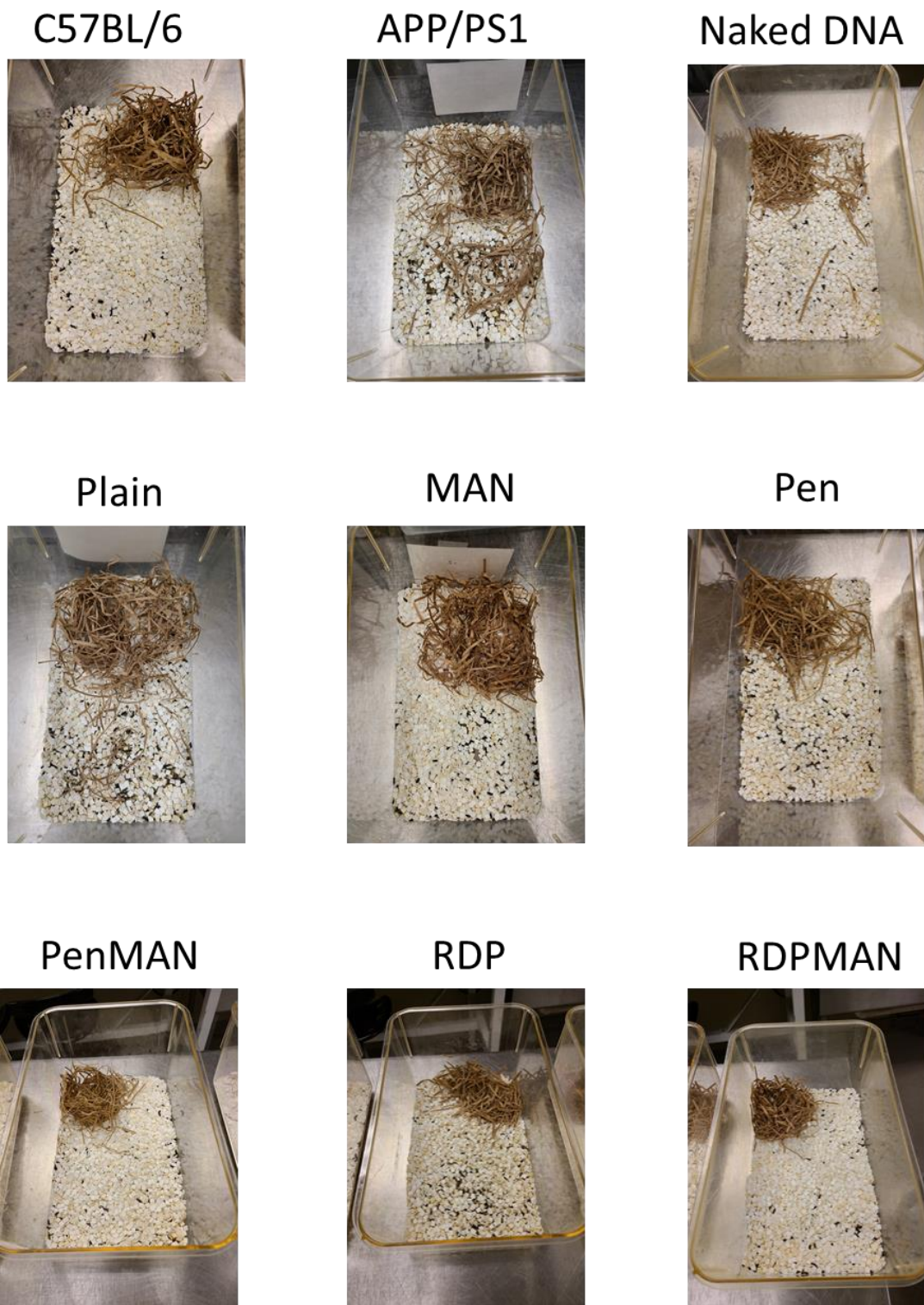


Figure 31. Nests built by 6-month-old mice post four weekly intravenous administration of liposomes entrapping pBDNF/chitosan complexes. C57BL/6 and APP/PS1 represent untreated healthy and AD controls, respectively.

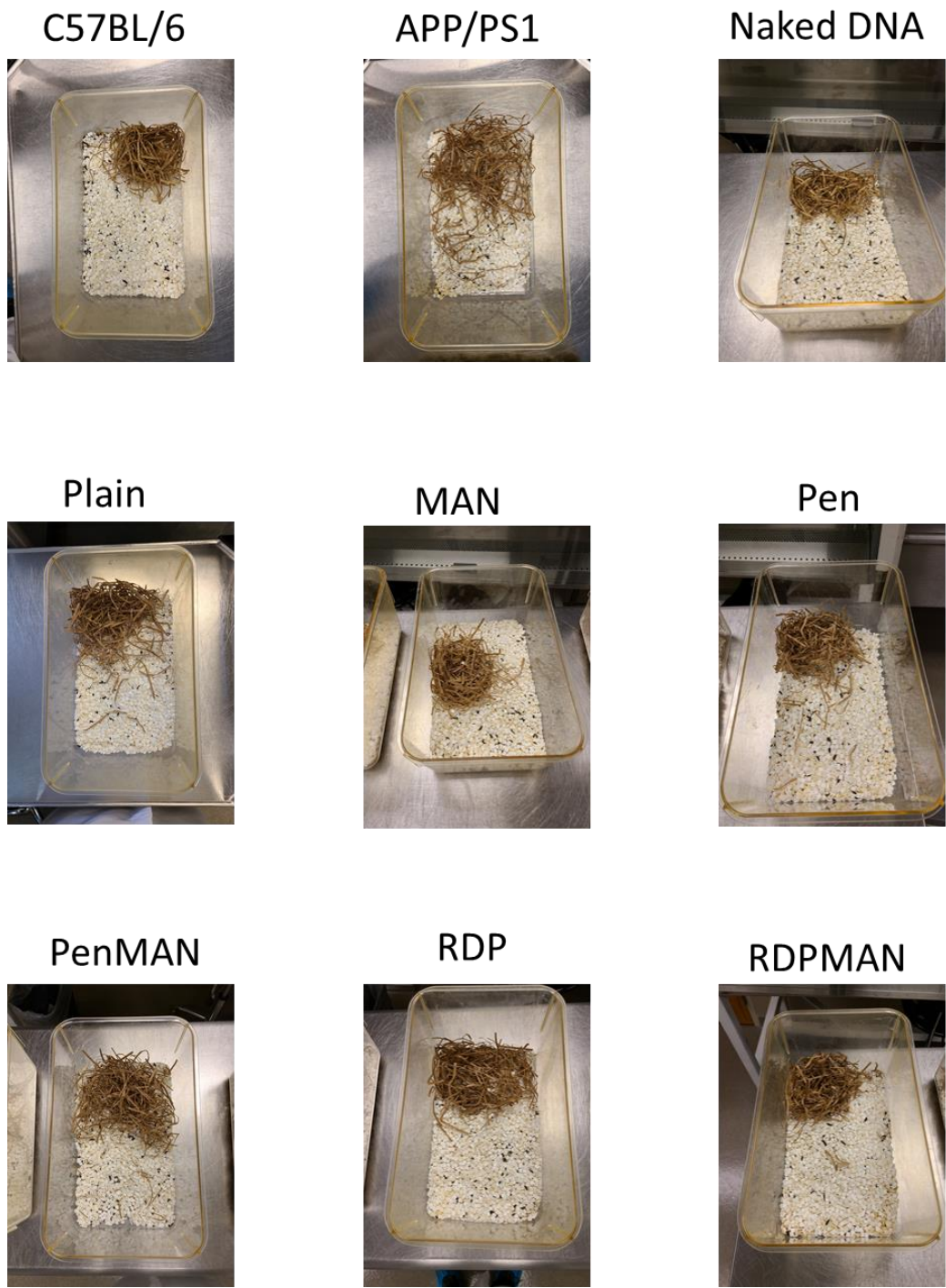


Figure 32. Nests built by 9-month-old mice post four weekly intravenous administration of liposomes entrapping pBDNF/chitosan complexes. C57BL/6 and APP/PS1 represent untreated healthy and AD controls, respectively.

4. SUMMARY AND CONCLUSION

One of the deadliest CNS disorders in elderly is Alzheimer's disease (AD), which results in loss of memory, cognitive ability and ability to function socially. Despite the recent developments in gene therapy technology, there is still a huge gap for brain targeted treatments for CNS disorders such as AD. Over the past decade, various delivery systems have been developed by utilizing numerous targeting ligands, however, due to the shortcomings of the current strategies, it is essential to develop innovative systems for the treatment of CNS diseases. Therefore, in our present study, we explored brain targeted liposomes which utilizes MAN in combination with CPPs to enhance the translocation across the BBB to transfect the cells in the brain. Plasmid encoding BDNF, ApoE2 or vgf protein was encapsulated inside these liposomes as it plays a critical role in learning and memory formation process, enhancing synaptic activity and neurogenesis, and found to be downregulated in the AD. Efficient transport of nanoparticles inside the brain requires uniformity in their hydrodynamic diameter and high entrapment efficiency of the therapeutic gene. The liposomal nanoparticles prepared in this study were homogeneous in their hydrodynamic diameter, as depicted by their low PDI, and demonstrated high entrapment efficiency. Moreover, a major concern for a delivery system is its biocompatibility. Therefore, in our formulation, low cytotoxicity and high transfection efficiency was promoted by incorporating cationic phospholipid DOTAP and helper phospholipid DOPE in equimolar ratios. Also, PEGylation was utilized on liposomal surface to assist shielding from opsonization, and accumulation, which aids in attenuating their clearance from the biological system. The cellular penetration aided by CPPs and endocytosis aided by GLUT-1 transporters, helped in the higher uptake of these nanoparticles as compared to plain liposomes. The internalization of the nanoparticles initiates with the activation of the cellular transport pathways upon interaction of

cell membrane and liposomes components. This results in either direct translocation or endocytosis across the cell membrane. Post internalization of the liposomes inside the cells, genetic payload should be transferred efficiently to the nucleus to induce transfection of the desired protein. The bifunctionalized liposomes encapsulating pDNA/chitosan complexes resulted in the enhanced transfection efficiency in comparison to the plain and single modified liposomes in all the cell lines tested.

In our study, BBB models were developed utilizing either murine cell lines. The co-cultured BBB model TEER and permeability was observed to be superior than the monolayer model. Thereafter, transport and transfection efficiency of liposomes were performed in the murine BBB model for better understanding of the delivery system. We observed higher transport and transfection efficiency by bifunctionalized liposomes, which can be rationalized *via* their dual transport mechanisms, leading to the enhanced transport of the therapeutic gene to the nucleus of cells. These observations advocate the effect of target ligands (MAN and CPP) on developing liposomal nanoparticles as suitable candidates for brain targeted gene therapy for treating AD.

The *in vivo* transfection in the brain confirms the ability of these liposomal nanoparticles to get transcytosed across the BBB and transfect the brain cells. The dual targeting effect with CPP and MAN aided the enhanced translocation of the bifunctionalized liposomes inside the brain cells, in comparison to other formulations, leading to superior transfection efficiency. Significant increase in transfection was found in the liver, spleen and kidney due to the presence of fenestrations in endothelial cells and reticuloendothelial system (RES), leading to accumulation of nanoparticles in these organs and nonspecific transfection. Histopathological analysis was performed in all vital tissues due the distribution of the liposomes in these organs and all nanoparticle formulations did not demonstrated any signs of pathology as observed previously.

Interestingly, reduction in BDNF protein levels have shown to be correlated with the impairment of brain functions in AD. This crucial protein is essential for synapse formation, neuronal plasticity, memory formation and learning inside the brain. Therefore, bifunctionalized (MANPen and RDPMAN) liposomes were assessed for their efficacy in AD transgenic mice model post transfection of BDNF protein inside the brain. In our current study, bifunctionalized liposomes demonstrated higher BDNF transfection than unmodified and monofunctionalized liposomes, which can be due to their higher transport levels inside the brain of APP/PS1 mice 6- and 9- months old. This helped in elevating the levels of this crucial protein BDNF in the brain to levels that were similar to their age-matched wild type controls. Moreover, these bifunctionalized liposomes demonstrated significant reduction of the various abeta 40 and 42 fractions in the 6- and 9-month old APP/PS1 mice post BDNF gene therapy using bifunctionalized liposomes (RDPMAN and MANPen). This resulted in the reduction of plaque load in the 6- and 9-months old AD transgenic mice treated with the bifunctionalized liposomes.

BDNF acts *via* its tropomyosin receptor kinase (Trk) receptors and activates various pathways including phosphatidylinositol-3-kinase (PI3K)/Akt pathway resulting in facilitation of survival, proliferation, and plasticity inside the brain. Hence, in this study, we elucidated the effects of BDNF gene therapy on cell proliferation in the brain of AD transgenic mice. Functionalized liposomal nanoparticles demonstrated increase in the number of ki-67 positive cells in the cortex and hippocampal regions of the 6-months old APP/PS1 mice. However, we hardly observed any ki-67 positive cells in the cortex and hippocampal regions of the brain of 9-months old wild type as well as in AD transgenic mice. Also, depletion of synaptic proteins results in the loss of synapses, which is correlated with the degree of cognition impairment witnessed in the initial and later stages of the AD. The depletion of these essential synaptic proteins was also observed in our

present study. Both PSD95 and synaptophysin were reduced by more than 30% by 9 months of age in transgenic mice in comparison to their wild type counterparts. However, BDNF gene therapy was able to rescue this decline and bring the levels of these pre and post synaptic proteins comparable to the baseline levels.

Finally, the efficacy of the BDNF gene therapy was evaluated utilizing nesting behavior in the transgenic mice model of AD. nest building behavior was assessed utilizing portion controlled and easy to dispense bedding material. BDNF gene therapy *via* liposomes was seemed to improve the nesting behavior in these animals. However, due to low number of animals in our present study significance was not observed. Therefore, we will be performing power analysis on our current data to achieve significance.

In conclusion, BDNF gene therapy *via* brain targeted liposomes has a strong potential to rescue AD pathology by elevating the levels of the essential synaptic proteins, alteration of abeta production, and improved cell survival and proliferation.

4.1. Future Directions

Our present study demonstrates the ability of surface modified liposomes to successfully transfect brain cells, resulting in the improvement of AD related pathology. However, we acknowledge some limitations in our present study which must be considered for future research work in this area. Firstly, although APP/PS1 model of AD mimics various hallmarks of AD pathology, this model lacks tauopathy or intracellular neurofibrillary tangles formation. Therefore, studies evaluating ApoE2, VGF and BDNF gene therapy in other models of AD with tauopathy are needed. Additionally, behavioral tests in different mouse models of AD will be pertinent in evaluating improvement in memory and cognitive functions following the treatment strategy presented in this study. Neuropsychological assessments will aid in better understanding of

liposomes on various cognitive domains such as semantic, episodic and working memory. Generally, it is hard to directly compare the therapeutic efficacy among various transgenic models due to the differences in the underlying variations among these animals. Thus, future studies encompassing these limitations will provide a robust understanding of this therapy to develop a clinically viable gene therapy for AD patients.

On the other hand, our current study utilized conventional plasmid DNA which plays a significant role in gene therapy. However, in clinical studies, these plasmids had shown to result in inflammatory reactions due to the presence of bacterial sequence in their structure. These bacterial sequences are necessary for maintaining and scaling up of the plasmid in the prokaryotes, resulting in its large size and compromised transfection. Therefore, incorporation of DNA ministrings encoding same sequence will be performed in future studies. DNA ministrings have shown to improve safety, transfection, and cytoplasmic kinetics in comparison to their conventional plasmid counterparts.

Finally, ApoE is well known to modulate the clearance of toxic amyloid beta plaques. These plaques are cleared from the brain in an isoform dependent manner (E3 > E4). E3 and E4 isoforms differ in only 1 amino acid from each other. Therefore, structural correcting small molecule PH002 can be employed to convert the structure of E4 isoform to E3 isoform. This strategy has shown to ameliorate the toxic effects of tauopathy and abeta production contributing to neuronal survival.

Overall, a combinational therapeutic approach using neurotrophic factor replenishing gene therapy along with ApoE structure corrector molecule using the optimized brain-targeted liposomal nanoparticles can help provide a much-needed treatment strategy for AD patients.

REFERENCES

- (1) Prince, M.; Wimo, A.; Guerchet, M.; Gemma-Claire, A.; Wu, Y.-T.; Prina, M. *Professional and Social Support in Dementia Care. : The Global Impact of Dementia - An Analysis of Prevalence, Incidence, Cost and Trends*; 2015.
- (2) 2020 Alzheimer's Disease Facts and Figures. *Alzheimer's Dement.* **2020**, *16* (3), 391–460.
- (3) Dubois, B.; Hampel, H.; Feldman, H. H.; Scheltens, P.; Aisen, P.; Andrieu, S.; Bakardjian, H.; Benali, H.; Bertram, L.; Blennow, K.; Broich, K.; Cavedo, E.; Crutch, S.; Dartigues, J. F.; Duyckaerts, C.; Epelbaum, S.; Frisoni, G. B.; Gauthier, S.; Genthon, R.; Gouw, A. A.; Habert, M. O.; Holtzman, D. M.; Kivipelto, M.; Lista, S.; Molinuevo, J. L.; O'Bryant, S. E.; Rabinovici, G. D.; Rowe, C.; Salloway, S.; Schneider, L. S.; Sperling, R.; Teichmann, M.; Carrillo, M. C.; Cummings, J.; Jack, C. R. Preclinical Alzheimer's Disease: Definition, Natural History, and Diagnostic Criteria. *Alzheimer's Dement.* **2016**, *12* (3), 292–323.
- (4) Mufson, E. J.; Ikonovic, M. D.; Counts, S. E.; Perez, S. E.; Malek-Ahmadi, M.; Scheff, S. W.; Ginsberg, S. D. Molecular and Cellular Pathophysiology of Preclinical Alzheimer's Disease. *Behav. Brain Res.* **2016**, *311*, 54–69.
- (5) Ali, A. A. Alzheimer's Disease: Pathophysiology, Hypotheses and Treatment Strategies. *Acta Psychopathol.* **2016**, *2* (3).
- (6) Terry, R. D.; Masliah, E.; Salmon, D. P.; Butters, N.; DeTeresa, R.; Hill, R.; Hansen, L. A.; Katzman, R. Physical Basis of Cognitive Alterations in Alzheimer's Disease: Synapse Loss Is the Major Correlate of Cognitive Impairment. *Ann. Neurol.* **1991**, *30* (4), 572–580.
- (7) Samuel, W.; Masliah, E.; Hill, L. R.; Butters, N.; Terry, R. Hippocampal Connectivity and Alzheimer's Dementia: Effects of Synapse Loss and Tangle Frequency in a Two-Component Model. *Neurology* **1994**, *44* (11), 2081–2088.
- (8) Morales, I.; Guzmán-Martínez, L.; Cerda-Troncoso, C.; Farías, G. A.; Maccioni, R. B. Neuroinflammation in the Pathogenesis of Alzheimer's Disease. A Rational Framework for the Search of Novel Therapeutic Approaches. *Front. Cell. Neurosci.* **2014**, *8* (1 APR).
- (9) Blurton-Jones, M.; Kitazawa, M.; Martínez-Coria, H.; Castello, N. A.; Müller, F. J.; Loring, J. F.; Yamasaki, T. R.; Poon, W. W.; Green, K. N.; LaFerla, F. M. Neural Stem Cells Improve Cognition via BDNF in a Transgenic Model of Alzheimer Disease. *Proc. Natl. Acad. Sci. U. S. A.* **2009**, *106* (32), 13594–13599.
- (10) Murer, M. G.; Yan, Q.; Raisman-Vozari, R. Brain-Derived Neurotrophic Factor in the Control Human Brain, and in Alzheimer's Disease and Parkinson's Disease. *Prog. Neurobiol.* **2001**, *63* (1), 71–124.
- (11) Phillips, H. S.; Hains, J. M.; Armanini, M.; Laramée, G. R.; Johnson, S. A.; Winslow, J. W. BDNF mRNA Is Decreased in the Hippocampus of Individuals with Alzheimer's Disease. *Neuron* **1991**, *7* (5), 695–702.
- (12) Nagahara, A. H.; Tuszynski, M. H. Potential Therapeutic Uses of BDNF in Neurological and Psychiatric Disorders. *Nat. Rev. Drug Discov.* **2011**, *10*, 209–219.
- (13) Chao, M. V. Neurotrophins and Their Receptors: A Convergence Point for Many Signalling Pathways. *Nat. Rev. Neurosci.* **2003**, *4*, 299–309.
- (14) Zhang, G.; Bowling, H.; Hom, N.; Kirshenbaum, K.; Klann, E.; Chao, M. V.; Neubert, T. A. In-Depth Quantitative Proteomic Analysis of de Novo Protein Synthesis Induced by Brain-Derived Neurotrophic Factor. *J. Proteome Res.* **2014**, *13* (12), 5707–5714.

- (15) Peng, S.; Garzon, D. J.; Marchese, M.; Klein, W.; Ginsberg, S. D.; Francis, B. M.; Mount, H. T. J.; Mufson, E. J.; Salehi, A.; Fahnstock, M. Decreased Brain-Derived Neurotrophic Factor Depends on Amyloid Aggregation State in Transgenic Mouse Models of Alzheimer's Disease. *J. Neurosci.* **2009**, *29* (29), 9321–9329.
- (16) Peng, S.; Wu, J.; Mufson, E. J.; Fahnstock, M. Precursor Form of Brain-Derived Neurotrophic Factor and Mature Brain-Derived Neurotrophic Factor Are Decreased in the Pre-Clinical Stages of Alzheimer's Disease. *J. Neurochem.* **2005**, *93* (6), 1412–1421.
- (17) Connor, B.; Young, D.; Yan, Q.; Faull, R. L. M.; Synek, B.; Dragunow, M. Brain-Derived Neurotrophic Factor Is Reduced in Alzheimer's Disease. *Mol. Brain Res.* **1997**, *49* (1–2), 71–81.
- (18) Matrone, C.; Ciotti, M. T.; Mercanti, D.; Marolda, R.; Calissano, P. NGF and BDNF Signaling Control Amyloidogenic Route and A β Production in Hippocampal Neurons. *Proc. Natl. Acad. Sci. U. S. A.* **2008**, *105* (35), 13139–13144.
- (19) Alder, J.; Thakker-Varia, S.; Bangasser, D. A.; Kuroiwa, M.; Plummer, M. R.; Shors, T. J.; Black, I. B. Brain-Derived Neurotrophic Factor-Induced Gene Expression Reveals Novel Actions of VGF in Hippocampal Synaptic Plasticity. *J. Neurosci.* **2003**, *23* (34), 10800–10808.
- (20) Snyder, S. E.; Cheng, H. W.; Murray, K. D.; Isackson, P. J.; McNeill, T. H.; Salton, S. R. J. The Messenger RNA Encoding VGF, a Neuronal Peptide Precursor, Is Rapidly Regulated in the Rat Central Nervous System by Neuronal Activity, Seizure and Lesion. *Neuroscience* **1997**, *82* (1), 7–19.
- (21) Bozdagi, O.; Rich, E.; Tronel, S.; Sadahiro, M.; Patterson, K.; Shapiro, M. L.; Alberini, C. M.; Huntley, G. W.; Salton, S. R. J. The Neurotrophin-Inducible Gene *Vgf* Regulates Hippocampal Function and Behavior through a Brain-Derived Neurotrophic Factor-Dependent Mechanism. *J. Neurosci.* **2008**, *28* (39), 9857–9869.
- (22) Thakker-Varia, S.; Behnke, J.; Doobin, D.; Dalal, V.; Thakkar, K.; Khadim, F.; Wilson, E.; Palmieri, A.; Antila, H.; Rantamaki, T.; Alder, J. VGF (TLQP-62)-Induced Neurogenesis Targets Early Phase Neural Progenitor Cells in the Adult Hippocampus and Requires Glutamate and BDNF Signaling. *Stem Cell Res.* **2014**, *12* (3), 762–777.
- (23) Carrette, O.; Demalte, I.; Scherl, A.; Yalkinoglu, O.; Corthals, G.; Burkhard, P.; Hochstrasser, D. F.; Sanchez, J. C. A Panel of Cerebrospinal Fluid Potential Biomarkers for the Diagnosis of Alzheimer's Disease. In *Proteomics*; 2003; Vol. 3, pp 1486–1494.
- (24) Rüetschi, U.; Zetterberg, H.; Podust, V. N.; Gottfries, J.; Li, S.; Hviid Simonsen, A.; McGuire, J.; Karlsson, M.; Rymo, L.; Davies, H.; Minthon, L.; Blennow, K. Identification of CSF Biomarkers for Frontotemporal Dementia Using SELDI-TOF. *Exp. Neurol.* **2005**, *196* (2), 273–281.
- (25) Selle, H.; Lamerz, J.; Buerger, K.; Dessauer, A.; Hager, K.; Hampel, H.; Karl, J.; Kellmann, M.; Lannfelt, L.; Louhija, J.; Riepe, M.; Rollinger, W.; Tumani, H.; Schrader, M.; Zucht, H.-D. Identification of Novel Biomarker Candidates by Differential Peptidomics Analysis of Cerebrospinal Fluid in Alzheimers Disease. *Comb. Chem. High Throughput Screen.* **2005**, *8* (8), 801–806.
- (26) Cocco, C.; D'Amato, F.; Noli, B.; Ledda, A.; Brancia, C.; Bongioanni, P.; Ferri, G. L. Distribution of VGF Peptides in the Human Cortex and Their Selective Changes in Parkinson's and Alzheimer's Diseases. *J. Anat.* **2010**, *217* (6), 683–693.
- (27) Levi, A.; Eldridge, J. D.; Paterson, B. M. Molecular Cloning of a Gene Sequence Regulated by Nerve Growth Factor. *Science (80-.)*. **1985**, *229* (4711), 393–395.

- (28) Bonni, A.; Ginty, D. D.; Dudek, H.; Greenberg, M. E. Serine 133-Phosphorylated CREB Induces Transcription via a Cooperative Mechanism That May Confer Specificity to Neurotrophin Signals. *Mol. Cell. Neurosci.* **1995**, *6* (2), 168–183.
- (29) Nagahara, A. H.; Mateling, M.; Kovacs, I.; Wang, L.; Eggert, S.; Rockenstein, E.; Koo, E. H.; Masliah, E.; Tuszynski, M. H. Early BDNF Treatment Ameliorates Cell Loss in the Entorhinal Cortex of APP Transgenic Mice. *J. Neurosci.* **2013**, *33* (39), 15596–15602.
- (30) Nagahara, A. H.; Merrill, D. A.; Coppola, G.; Tsukada, S.; Schroeder, B. E.; Shaked, G. M.; Wang, L.; Blesch, A.; Kim, A.; Conner, J. M.; Rockenstein, E.; Chao, M. V.; Koo, E. H.; Geschwind, D.; Masliah, E.; Chiba, A. A.; Tuszynski, M. H. Neuroprotective Effects of Brain-Derived Neurotrophic Factor in Rodent and Primate Models of Alzheimer’s Disease. *Nat. Med.* **2009**, *15* (3), 331–337.
- (31) Rohe, M.; Synowitz, M.; Glass, R.; Paul, S. M.; Nykjaer, A.; Willnow, T. E. Brain-Derived Neurotrophic Factor Reduces Amyloidogenic Processing through Control of SORLA Gene Expression. *J. Neurosci.* **2009**, *29* (49), 15472–15478.
- (32) El Gaamouch, F.; Audrain, M.; Lin, W. J.; Beckmann, N.; Jiang, C.; Hariharan, S.; Heeger, P. S.; Schadt, E. E.; Gandy, S.; Ehrlich, M. E.; Salton, S. R. VGF-Derived Peptide TLQP-21 Modulates Microglial Function through C3aR1 Signaling Pathways and Reduces Neuropathology in 5xFAD Mice. *Mol. Neurodegener.* **2020**, *15* (1).
- (33) Lin, W. J.; Jiang, C.; Sadahiro, M.; Bozdagi, O.; Vulchanova, L.; Alberini, C. M.; Salton, S. R. VGF and Its C-Terminal Peptide TLQP-62 Regulate Memory Formation in Hippocampus via a BDNF-TrkB-Dependent Mechanism. *J. Neurosci.* **2015**, *35* (28), 10343–10356.
- (34) Corder, E. H.; Saunders, A. M.; Strittmatter, W. J.; Schmechel, D. E.; Gaskell, P. C.; Small, G. W.; Roses, A. D.; Haines, J. L.; Pericak-Vance, M. A. Gene Dose of Apolipoprotein E Type 4 Allele and the Risk of Alzheimer’s Disease in Late Onset Families. *Science* (80-.). **1993**, *261* (5123), 921–923.
- (35) Sadigh-Eteghad, S.; Talebi, M.; Farhoudi, M. Association of Apolipoprotein E Epsilon 4 Allele with Sporadic Late Onset Alzheimer’s Disease: A Meta-Analysis. *Neurosciences* **2012**, *17* (4), 321–326.
- (36) Farrer, L. A.; Cupples, L. A.; Haines, J. L.; Hyman, B.; Kukull, W. A.; Mayeux, R.; Myers, R. H.; Pericak-Vance, M. A.; Risch, N.; Van Duijn, C. M. Effects of Age, Sex, and Ethnicity on the Association between Apolipoprotein E Genotype and Alzheimer Disease: A Meta-Analysis. *J. Am. Med. Assoc.* **1997**, *278* (16), 1349–1356.
- (37) Kanekiyo, T.; Xu, H.; Bu, G. ApoE and A?? In Alzheimer’s Disease: Accidental Encounters or Partners? *Neuron* **2014**, *81* (4), 740–754.
- (38) Mayeux, R.; Stern, Y. Epidemiology of Alzheimer Disease. *Cold Spring Harb. Perspect. Med.* **2012**, *2* (8).
- (39) Cogley, J. N.; Fiorello, M. L.; Bailey, D. M. 13 Reasons Why the Brain Is Susceptible To Oxidative Stress. *Redox Biol.* **2018**, *15*, 490–503.
- (40) Aliev, G.; Palacios, H. H.; Walrafen, B.; Lipsitt, A. E.; Obrenovich, M. E.; Morales, L. Brain Mitochondria as a Primary Target in the Development of Treatment Strategies for Alzheimer Disease. *Int. J. Biochem. Cell Biol.* **2009**, *41* (10), 1989–2004.
- (41) Mohsenzadegan, M.; Mirshafiey, A. The Immunopathogenic Role of Reactive Oxygen Species in Alzheimer Disease. *Iranian Journal of Allergy, Asthma and Immunology.* 2012.
- (42) Huang, W. J.; Zhang, X.; Chen, W. W. Role of Oxidative Stress in Alzheimer’s Disease (Review). *Biomed. Reports* **2016**, *4* (5), 519–522.

- (43) Brandt, R.; Bakota, L. Microtubule Dynamics and the Neurodegenerative Triad of Alzheimer's Disease: The Hidden Connection. *J. Neurochem.* **2017**, *143* (4), 409–417.
- (44) Van Cauwenberghe, C.; Van Broeckhoven, C.; Sleegers, K. The Genetic Landscape of Alzheimer Disease: Clinical Implications and Perspectives. *Genetics in Medicine.* 2016.
- (45) Kawabata, K.; Takakura, Y.; Hashida, M. The Fate of Plasmid DNA After Intravenous Injection in Mice: Involvement of Scavenger Receptors in Its Hepatic Uptake. *Pharm. Res. An Off. J. Am. Assoc. Pharm. Sci.* **1995**.
- (46) Hu, Y.; Haynes, M. T.; Wang, Y.; Liu, F.; Huang, L. A Highly Efficient Synthetic Vector: Nonhydrodynamic Delivery of DNA to Hepatocyte Nuclei in Vivo. *ACS Nano* **2013**, *7* (6), 5376–5384.
- (47) Kim, Y. H.; Park, J. H.; Lee, M.; Kim, Y. H.; Park, T. G.; Kim, S. W. Polyethylenimine with Acid-Labile Linkages as a Biodegradable Gene Carrier. *J. Control. Release* **2005**, *103* (1), 209–219.
- (48) Mao, H. Q.; Roy, K.; Troung-Le, V. L.; Janes, K. A.; Lin, K. Y.; Wang, Y.; August, J. T.; Leong, K. W. Chitosan-DNA Nanoparticles as Gene Carriers: Synthesis, Characterization and Transfection Efficiency. *J. Control. Release* **2001**, *70* (3), 399–421.
- (49) Park, S.; Healy, K. E. Nanoparticulate DNA Packaging Using Terpolymers of Poly (Lysine-g-(Lactide-b-Ethylene Glycol)). *Bioconjug. Chem.* **2003**, *14* (2), 311–319.
- (50) Yang, Y.; Park, Y.; Man, S.; Liu, Y.; Rice, K. G. Cross-Linked Low Molecular Weight Glycopeptide-Mediated Gene Delivery: Relationship between DNA Metabolic Stability and the Level of Transient Gene Expression in Vivo. *J. Pharm. Sci.* **2001**, *90* (12), 2010–2022.
- (51) Nayerossadat, N.; Ali, P.; Maedeh, T. Viral and Nonviral Delivery Systems for Gene Delivery. *Adv. Biomed. Res.* **2012**, *1* (27), 1–11.
- (52) Kursu, M.; Walker, G. F.; Roessler, V.; Ogris, M.; Roedl, W.; Kircheis, R.; Wagner, E. Novel Shielded Transferrin-Polyethylene Glycol-Polyethylenimine/DNA Complexes for Systemic Tumor-Targeted Gene Transfer. *Bioconjug. Chem.* **2003**, *14* (1), 222–231.
- (53) Layek, B.; Haldar, M. K.; Sharma, G.; Lipp, L.; Mallik, S.; Singh, J. Hexanoic Acid and Polyethylene Glycol Double Grafted Amphiphilic Chitosan for Enhanced Gene Delivery: Influence of Hydrophobic and Hydrophilic Substitution Degree. *Mol. Pharm.* **2014**, *11* (3), 982–994.
- (54) Chan, C. L.; Ewert, K. K.; Majzoub, R. N.; Hwu, Y. K.; Liang, K. S.; Leal, C.; Safinya, C. R. Optimizing Cationic and Neutral Lipids for Efficient Gene Delivery at High Serum Content. *J. Gene Med.* **2014**, *16* (3–4), 84–96.
- (55) Ruponen, M.; Ylä-Herttuala, S.; Urtili, A. Interactions of Polymeric and Liposomal Gene Delivery Systems with Extracellular Glycosaminoglycans: Physicochemical and Transfection Studies. *Biochim. Biophys. Acta - Biomembr.* **1999**, *1415* (2), 331–341.
- (56) Takakura, Y.; Mahato, R. I.; Hashida, M. Extravasation of Macromolecules. *Adv. Drug Deliv. Rev.* **1998**, *34* (1), 93–108.
- (57) Thibault, M.; Nimesh, S.; Lavertu, M.; Buschmann, M. D. Intracellular Trafficking and Decondensation Kinetics of Chitosan-PDNA Polyplexes. *Mol. Ther.* **2010**.
- (58) Dallüge, R.; Haberland, A.; Zaitsev, S.; Schneider, M.; Zastrow, H.; Sukhorukov, G.; Böttger, M. Characterization of Structure and Mechanism of Transfection-Active Peptide-DNA Complexes. *Biochim. Biophys. Acta - Gene Struct. Expr.* **2002**, *1576* (1–2), 45–52.

- (59) Koltover, I.; Salditt, T.; Rädler, J. O.; Safinya, C. R. An Inverted Hexagonal Phase of Cationic Liposome-DNA Complexes Related to DNA Release and Delivery. *Science* (80-.). **1998**, *281* (5373), 78–81.
- (60) Lechardeur, D.; Sohn, K. J.; Haardt, M.; Joshi, P. B.; Monck, M.; Graham, R. W.; Beatty, B.; Squire, J.; O’Brodivich, H.; Lukacs, G. L. Metabolic Instability of Plasmid DNA in the Cytosol: A Potential Barrier to Gene Transfer. *Gene Ther.* **1999**, *6* (4), 482–497.
- (61) Rehman, Z. U.; Hoekstra, D.; Zuhorn, I. S. Mechanism of Polyplex- and Lipoplex-Mediated Delivery of Nucleic Acids: Real-Time Visualization of Transient Membrane Destabilization without Endosomal Lysis. *ACS Nano* **2013**, *7* (5), 3767–3777.
- (62) Vaughan, E. E.; Geiger, C. R.; Miller, A. M.; Loh-Marley, P. L.; Suzuki, T.; Miyata, N.; Dean, D. A. Microtubule Acetylation through HDAC6 Inhibition Results in Increased Transfection Efficiency. *Mol. Ther.* **2008**, *16* (11), 1841–1847.
- (63) Mesika, A.; Kiss, V.; Brumfeld, V.; Ghosh, G.; Reich, Z. Enhanced Intracellular Mobility and Nuclear Accumulation of DNA Plasmids Associated with a Karyophilic Protein. *Hum. Gene Ther.* **2005**, *16* (2), 200–208.
- (64) Vaughan, E. E.; Dean, D. A. Intracellular Trafficking of Plasmids during Transfection Is Mediated by Microtubules. *Mol. Ther.* **2006**, *13* (2), 422–428.
- (65) Badding, M. A.; Vaughan, E. E.; Dean, D. A. Transcription Factor Plasmid Binding Modulates Microtubule Interactions and Intracellular Trafficking during Gene Transfer. *Gene Ther.* **2012**, *19* (3), 338–346.
- (66) Pérez-Martínez, F. C.; Guerra, J.; Posadas, I.; Ceña, V. Barriers to Non-Viral Vector-Mediated Gene Delivery in the Nervous System. *Pharm. Res.* **2011**, *28* (8), 1843–1858.
- (67) Wiethoff, C. M.; Middaugh, C. R. Barriers to Nonviral Gene Delivery. *J. Pharm. Sci.* **2003**, *92* (2), 203–217.
- (68) Barua, S.; Mitragotri, S. Challenges Associated with Penetration of Nanoparticles across Cell and Tissue Barriers: A Review of Current Status and Future Prospects. *Nano Today* **2014**, *9* (2), 223–243.
- (69) Pardridge, W. M. Drug Transport across the Blood-Brain Barrier. *J. Cereb. Blood Flow Metab.* **2012**, *32* (11), 1959–1972.
- (70) Saraiva, C.; Praça, C.; Ferreira, R.; Santos, T.; Ferreira, L.; Bernardino, L. Nanoparticle-Mediated Brain Drug Delivery: Overcoming Blood-Brain Barrier to Treat Neurodegenerative Diseases. *J. Control. Release* **2016**, *235*, 34–47.
- (71) Marroni, M.; Kight, K. M.; Hossain, M.; Cucullo, L.; Desai, S. Y.; Janigro, D. Dynamic in Vitro Model of the Blood-Brain Barrier. Gene Profiling Using CDNA Microarray Analysis. *Methods Mol. Med.* **2003**, *89*, 419–434.
- (72) Eigenmann, D. E.; Xue, G.; Kim, K. S.; Moses, A. V.; Hamburger, M.; Oufir, M. Comparative Study of Four Immortalized Human Brain Capillary Endothelial Cell Lines, HCMEC/D3, HBMEC, TY10, and BB19, and Optimization of Culture Conditions, for an in Vitro Blood-Brain Barrier Model for Drug Permeability Studies. *Fluids Barriers CNS* **2013**, *10* (1).
- (73) Rahman, N. A.; Rasil, A. N. ain H. M.; Meyding-Lamade, U.; Craemer, E. M.; Diah, S.; Tuah, A. A.; Muharram, S. H. Immortalized Endothelial Cell Lines for in Vitro Blood-Brain Barrier Models: A Systematic Review. *Brain Research.* 2016, pp 532–545.
- (74) Kaisar, M. A.; Sajja, R. K.; Prasad, S.; Abhyankar, V. V.; Liles, T.; Cucullo, L. New Experimental Models of the Blood-Brain Barrier for CNS Drug Discovery. *Expert Opinion on Drug Discovery.* 2017.

- (75) Gastfriend, B. D.; Palecek, S. P.; Shusta, E. V. Modeling the Blood–Brain Barrier: Beyond the Endothelial Cells. *Curr. Opin. Biomed. Eng.* **2018**, *5*, 6–12.
- (76) Salvador, E.; Shityakov, S.; Förster, C. Glucocorticoids and Endothelial Cell Barrier Function. *Cell Tissue Res.* **2014**, *355* (3), 597–605.
- (77) Romero, I. A.; Radewicz, K.; Jubin, E.; Michel, C. C.; Greenwood, J.; Couraud, P. O.; Adamson, P. Changes in Cytoskeletal and Tight Junctional Proteins Correlate with Decreased Permeability Induced by Dexamethasone in Cultured Rat Brain Endothelial Cells. *Neurosci. Lett.* **2003**, *344* (2), 112–116.
- (78) Calabria, A. R.; Weidenfeller, C.; Jones, A. R.; De Vries, H. E.; Shusta, E. V. Puromycin-Purified Rat Brain Microvascular Endothelial Cell Cultures Exhibit Improved Barrier Properties in Response to Glucocorticoid Induction. *J. Neurochem.* **2006**, *97* (4), 922–933.
- (79) Förster, C.; Silwedel, C.; Golenhofen, N.; Burek, M.; Kietz, S.; Mankertz, J.; Drenckhahn, D. Occludin as Direct Target for Glucocorticoid-Induced Improvement of Blood-Brain Barrier Properties in a Murine in Vitro System. *J. Physiol.* **2005**, *565* (2), 475–486.
- (80) Förster, C.; Waschke, J.; Burek, M.; Leers, J.; Drenckhahn, D. Glucocorticoid Effects on Mouse Microvascular Endothelial Barrier Permeability Are Brain Specific. *J. Physiol.* **2006**, *573* (2), 413–425.
- (81) Förster, C. Tight Junctions and the Modulation of Barrier Function in Disease. *Histochem. Cell Biol.* **2008**, *130* (1), 55–70.
- (82) Sweeney, M. D.; Sagare, A. P.; Zlokovic, B. V. Blood-Brain Barrier Breakdown in Alzheimer Disease and Other Neurodegenerative Disorders. *Nat. Rev. Neurol.* **2018**, *14* (3), 133–150.
- (83) Stam, R. Electromagnetic Fields and the Blood-Brain Barrier. *Brain Res. Rev.* **2010**, *65* (1), 80–97.
- (84) Hynynen, K. Ultrasound for Drug and Gene Delivery to the Brain. *Adv. Drug Deliv. Rev.* **2008**, *60* (10), 1209–1217.
- (85) Razzak, R. A.; Florence, G. J.; Gunn-Moore, F. J. Approaches to Cns Drug Delivery with a Focus on Transporter-Mediated Transcytosis. *Int. J. Mol. Sci.* **2019**, *20* (12).
- (86) Choudhury, S. R.; Hudry, E.; Maguire, C. A.; Sena-Esteves, M.; Breakefield, X. O.; Grandi, P. Viral Vectors for Therapy of Neurologic Diseases. *Neuropharmacology*. 2017.
- (87) Vite, C. H.; Passini, M. A.; Haskins, M. E.; Wolfe, J. H. Adeno-Associated Virus Vector-Mediated Transduction in the Cat Brain. *Gene Ther.* **2003**, *10* (22), 1874–1881.
- (88) Kim, J. Y.; Grunke, S. D.; Levites, Y.; Golde, T. E.; Jankowsky, J. L. Intracerebroventricular Viral Injection of the Neonatal Mouse Brain for Persistent and Widespread Neuronal Transduction. *J. Vis. Exp.* **2014**, No. 91.
- (89) Snyder, B. R.; Gray, S. J.; Quach, E. T.; Huang, J. W.; Leung, C. H.; Samulski, R. J.; Boulis, N. M.; Federici, T. Comparison of Adeno-Associated Viral Vector Serotypes for Spinal Cord and Motor Neuron Gene Delivery. *Hum. Gene Ther.* **2011**, *22* (9), 1129–1135.
- (90) Yang, B.; Li, S.; Wang, H.; Guo, Y.; Gessler, D. J.; Cao, C.; Su, Q.; Kramer, J.; Zhong, L.; Ahmed, S. S.; Zhang, H.; He, R.; Desrosiers, R. C.; Brown, R.; Xu, Z.; Gao, G. Global CNS Transduction of Adult Mice by Intravenously Delivered RAAVrh.8 and RAAVrh.10 and Nonhuman Primates by RAAVrh.10. *Mol. Ther.* **2014**, *22* (7), 1299–1309.
- (91) Wong, A. D.; Ye, M.; Levy, A. F.; Rothstein, J. D.; Bergles, D. E.; Searson, P. C. The Blood-Brain Barrier: An Engineering Perspective. *Front. Neuroeng.* **2013**, No. JUL.

- (92) Schuster, D. J.; Dykstra, J. A.; Riedl, M. S.; Kitto, K. F.; Belur, L. R.; Scott McIvor, R.; Elde, R. P.; Fairbanks, C. A.; Vulchanova, L. Biodistribution of Adeno-Associated Virus Serotype 9 (AAV9) Vector after Intrathecal and Intravenous Delivery in Mouse. *Front. Neuroanat.* **2014**, *8* (JUN).
- (93) Samaranch, L.; Salegio, E. A.; San Sebastian, W.; Kells, A. P.; Foust, K. D.; Bringas, J. R.; Lamarre, C.; Forsayeth, J.; Kaspar, B. K.; Bankiewicz, K. S. Adeno-Associated Virus Serotype 9 Transduction in the Central Nervous System of Nonhuman Primates. *Hum. Gene Ther.* **2011**, *23* (4), 382–389.
- (94) Wilson, J. M. Lessons Learned from the Gene Therapy Trial for Ornithine Transcarbamylase Deficiency. *Get. to Good Res. Integr. Biomed. Sci.* **2018**, 490–497.
- (95) Foldvari, M.; Chen, D. W.; Nafissi, N.; Calderon, D.; Narsineni, L.; Rafiee, A. Non-Viral Gene Therapy: Gains and Challenges of Non-Invasive Administration Methods. *J. Control. Release* **2016**, *240*, 165–190.
- (96) Ginn, S. L.; Amaya, A. K.; Alexander, I. E.; Edelstein, M.; Abedi, M. R. Gene Therapy Clinical Trials Worldwide to 2017: An Update. *J. Gene Med.* **2018**, *20* (5).
- (97) Kamimura, K.; Liu, D. Physical Approaches for Nucleic Acid Delivery to Liver. *AAPS J.* **2008**, *10* (4), 589–595.
- (98) Neumann, E.; Schaefer-Ridder, M.; Wang, Y.; Hofschneider, P. H. Gene Transfer into Mouse Lyoma Cells by Electroporation in High Electric Fields. *EMBO J.* **1982**, *1* (7), 841–845.
- (99) Rigby, P. G. Prolongation of Survival of Tumour-Bearing Animals by Transfer of “Immune” RNA with DEAE Dextran [21]. *Nature* **1969**, *221* (5184), 968–969.
- (100) Titomirov, A. V.; Sukharev, S.; Kistanova, E. In Vivo Electroporation and Stable Transformation of Skin Cells of Newborn Mice by Plasmid DNA. *BBA - Gene Struct. Expr.* **1991**, *1088* (1), 131–134.
- (101) Bodles-Brakhop, A. M.; Heller, R.; Draghia-Akli, R. Electroporation for the Delivery of DNA-Based Vaccines and Immunotherapeutics: Current Clinical Developments. *Mol. Ther.* **2009**, *17* (4), 585–592.
- (102) Heller, R.; Heller, L. C. Gene Electrotransfer Clinical Trials. *Adv. Genet.* **2015**, *89*, 235–262.
- (103) Sardesai, N. Y.; Weiner, D. B. Electroporation Delivery of DNA Vaccines: Prospects for Success. *Curr. Opin. Immunol.* **2011**, *23* (3), 421–429.
- (104) Otten, G.; Schaefer, M.; Doe, B.; Liu, H.; Srivastava, I.; Zur Megede, J.; O’Hagan, D.; Donnelly, J.; Widera, G.; Rabussay, D.; Lewis, M. G.; Barnett, S.; Ulmer, J. B. Enhancement of DNA Vaccine Potency in Rhesus Macaques by Electroporation. *Vaccine* **2004**, *22* (19), 2489–2493.
- (105) Sha, S.; Xing, X. N.; Guo, W. S.; Li, Y.; Zong, L. X.; Guo, R.; Cao, Y. P. In Vivo Electroporation of a New Gene Vaccine Encoding Ten Repeats of A β 3-10 Prevents Brain A β Deposition and Delays Cognitive Impairment in Young Tg-APP^{swe}/PSEN1^{dE9} Mice. *Neurochem. Res.* **2012**, *37* (7), 1534–1544.
- (106) Xing, X. N.; Sha, S.; Chen, X. H.; Guo, W. S.; Guo, R.; Jiang, T. Z.; Cao, Y. P. Active Immunization with DNA Vaccine Reduced Cerebral Inflammation and Improved Cognitive Ability in APP/PS1 Transgenic Mice by In Vivo Electroporation. *Neurochem. Res.* **2015**, *40* (5), 1032–1041.
- (107) Evans, C. F.; Davtyan, H.; Petrushina, I.; Hovakimyan, A.; Davtyan, A.; Hannaman, D.; Cribbs, D. H.; Agadjanyan, M. G.; Ghochikyan, A. Epitope-Based DNA Vaccine for

- Alzheimer's Disease: Translational Study in Macaques. *Alzheimer's Dement.* **2014**, *10* (3), 284–295.
- (108) Ghochikyan, A.; Davtyan, H.; Petrushina, I.; Hovakimyan, A.; Movsesyan, N.; Davtyan, A.; Kiyatkin, A.; Cribbs, D. H.; Agadjanyan, M. G. Refinement of a DNA Based Alzheimer Disease Epitope Vaccine in Rabbits. *Hum. Vaccines Immunother.* **2013**, *9* (5), 1002–1010.
- (109) Klein, T. M.; Sanford, J. C.; Wolf, E. D.; Wu, R. High-Velocity Microprojectiles for Delivering Nucleic Acids into Living Cells. *Nature* **1987**, *327* (6117), 70–73.
- (110) Yang, N. S.; Burkholder, J.; Roberts, B.; Martinell, B.; McCabe, D. In Vivo and in Vitro Gene Transfer to Mammalian Somatic Cells by Particle Bombardment. *Proc. Natl. Acad. Sci. U. S. A.* **1990**, *87* (24), 9568–9572.
- (111) Williams, R. S.; Johnston, S. A.; Riedy, M.; DeVit, M. J.; McElligott, S. G.; Sanford, J. C. Introduction of Foreign Genes into Tissues of Living Mice by DNA-Coated Microprojectiles. *Proc. Natl. Acad. Sci. U. S. A.* **1991**, *88* (7), 2726–2730.
- (112) Qu, B.; Boyer, P. J.; Johnston, S. A.; Hynan, L. S.; Rosenberg, R. N. A β 42 Gene Vaccination Reduces Brain Amyloid Plaque Burden in Transgenic Mice. *J. Neurol. Sci.* **2006**, *244* (1–2), 151–158.
- (113) Ghochikyan, A.; Vasilevko, V.; Petrushina, I.; Movsesyan, N.; Babikyan, D.; Tian, W.; Sadzikava, N.; Ross, T. M.; Head, E.; Cribbs, D. H.; Agadjanyan, M. G. Generation and Characterization of the Humoral Immune Response to DNA Immunization with a Chimeric β -Amyloid-Interleukin-4 Minigene. *Eur. J. Immunol.* **2003**, *33* (12), 3232–3241.
- (114) Movsesyan, N.; Ghochikyan, A.; Mkrtychyan, M.; Petrushina, I.; Davtyan, H.; Olkhanud, P. B.; Head, E.; Biragyn, A.; Cribbs, D. H.; Agadjanyan, M. G. Reducing AD-like Pathology in 3xTg-AD Mouse Model by DNA Epitope Vaccine - A Novel Immunotherapeutic Strategy. *PLoS One* **2008**, *3* (5).
- (115) Qu, B. X.; Lambracht-Washington, D.; Fu, M.; Eagar, T. N.; Stüve, O.; Rosenberg, R. N. Analysis of Three Plasmid Systems for Use in DNA A β 42 Immunization as Therapy for Alzheimer's Disease. *Vaccine* **2010**, *28* (32), 5280–5287.
- (116) Davtyan, H.; Ghochikyan, A.; Movsesyan, N.; Ellefsen, B.; Petrushina, I.; Cribbs, D. H.; Hannaman, D.; Evans, C. F.; Agadjanyan, M. G. Delivery of a DNA Vaccine for Alzheimer's Disease by Electroporation versus Gene Gun Generates Potent and Similar Immune Responses. *Neurodegener. Dis.* **2012**, *10* (1–4), 261–264.
- (117) Lambracht-Washington, D.; Rosenberg, R. N. Co-Stimulation with TNF Receptor Superfamily 4/25 Antibodies Enhances in-Vivo Expansion of CD4+CD25+Foxp3+ T Cells (Tregs) in a Mouse Study for Active DNA A β 42 Immunotherapy. *J. Neuroimmunol.* **2015**, *278*, 90–99.
- (118) Lambracht-Washington, D.; Qu, B. X.; Fu, M.; Anderson, L. D.; Eagar, T. N.; Stüve, O.; Rosenberg, R. N. A Peptide Prime-DNA Boost Immunization Protocol Provides Significant Benefits as a New Generation A β 42 DNA Vaccine for Alzheimer Disease. *J. Neuroimmunol.* **2013**, *254* (1–2), 63–68.
- (119) Lambracht-Washington, D.; Qu, B. X.; Fu, M.; Anderson, L. D.; Stüve, O.; Eagar, T. N.; Rosenberg, R. N. DNA Immunization against Amyloid Beta 42 Has High Potential as Safe Therapy for Alzheimer's Disease as It Diminishes Antigen-Specific Th1 and Th17 Cell Proliferation. *Cell. Mol. Neurobiol.* **2011**, *31* (6), 867–874.

- (120) Rosenberg, R. N.; Fu, M.; Lambracht-Washington, D. Intradermal Active Full-Length DNA A β 42 Immunization via Electroporation Leads to High Anti-A β Antibody Levels in Wild-Type Mice. *J. Neuroimmunol.* **2018**, *322*, 15–25.
- (121) Qu, B. X.; Xiang, Q.; Li, L.; Johnston, S. A.; Hynan, L. S.; Rosenberg, R. N. A β 42 Gene Vaccine Prevents A β 42 Deposition in Brain of Double Transgenic Mice. *J. Neurol. Sci.* **2007**.
- (122) DaSilva, K. A.; Brown, M. E.; McLaurin, J. A. Reduced Oligomeric and Vascular Amyloid- β Following Immunization of TgCRND8 Mice with an Alzheimer's DNA Vaccine. *Vaccine* **2009**, *27* (9), 1365–1376.
- (123) Lambracht-Washington, D.; Rosenberg, R. N. Advances in the Development of Vaccines for Alzheimer's Disease. *Discov. Med.* **2013**, *15* (84), 319–326.
- (124) Lambracht-Washington, D.; Fu, M.; Wight-Carter, M.; Riegel, M.; Rosenberg, R. N. Evaluation of a DNA A β 42 Vaccine in Aged NZW Rabbits: Antibody Kinetics and Immune Profile after Intradermal Immunization with Full-Length DNA A β 42 Trimer. *J. Alzheimer's Dis.* **2017**, *57* (1), 97–112.
- (125) Lambracht-Washington, D.; Fu, M.; Frost, P.; Rosenberg, R. N. Evaluation of a DNA A β 42 Vaccine in Adult Rhesus Monkeys (*Macaca Mulatta*): Antibody Kinetics and Immune Profile after Intradermal Immunization with Full-Length DNA A β 42 Trimer. *Alzheimer's Res. Ther.* **2017**, *9* (1).
- (126) Tomalia, D. A.; Fréchet, J. M. J. Discovery of Dendrimers and Dendritic Polymers: A Brief Historical Perspective. *J. Polym. Sci. Part A Polym. Chem.* **2002**, *40* (16), 2719–2728.
- (127) Xiong, Z.; Shen, M.; Shi, X. Dendrimer-Based Strategies for Cancer Therapy: Recent Advances and Future Perspectives. *Sci. China Mater.* **2018**, *61* (11), 1387–1403.
- (128) Eichman, J. D.; Bielinska, A. U.; Kukowska-Latallo, J. F.; Baker, J. R. The Use of PAMAM Dendrimers in the Efficient Transfer of Genetic Material into Cells. *Pharm. Sci. Technol. Today* **2000**, *3* (7), 232–245.
- (129) Qamhieh, K.; Nylander, T.; Black, C. F.; Attard, G. S.; Dias, R. S.; Ainalem, M. L. Complexes Formed between DNA and Poly(Amido Amine) Dendrimers of Different Generations-Modelling DNA Wrapping and Penetration. *Phys. Chem. Chem. Phys.* **2014**, *16* (26), 13112–13122.
- (130) Pavan, G. M.; Danani, A.; Pricl, S.; Smith, D. K. Modeling the Multivalent Recognition between Dendritic Molecules and DNA: Understanding How Ligand “Sacrifice” and Screening Can Enhance Binding. *J. Am. Chem. Soc.* **2009**.
- (131) Shcharbin, D.; Pedziwiatr, E.; Bryszewska, M. How to Study Dendriplexes I: Characterization. *J. Control. Release* **2009**, *135* (3), 186–197.
- (132) Liu, Y.; An, S.; Li, J.; Kuang, Y.; He, X.; Guo, Y.; Ma, H.; Zhang, Y.; Ji, B.; Jiang, C. Brain-Targeted Co-Delivery of Therapeutic Gene and Peptide by Multifunctional Nanoparticles in Alzheimer's Disease Mice. *Biomaterials* **2016**, *80*, 33–45.
- (133) Jiang, Y.; Mullaney, K. A.; Peterhoff, C. M.; Che, S.; Schmidt, S. D.; Boyer-Boiteau, A.; Ginsberg, S. D.; Cataldo, A. M.; Mathews, P. M.; Nixon, R. A. Alzheimer's-Related Endosome Dysfunction in Down Syndrome Is A β -Independent but Requires APP and Is Reversed by BACE-1 Inhibition. *Proc. Natl. Acad. Sci. U. S. A.* **2010**, *107* (4), 1630–1635.

- (134) Lee, E. B.; Zhang, B.; Liu, K.; Greenbaum, E. A.; Doms, R. W.; Trojanowski, J. Q.; Lee, V. M. Y. BACE Overexpression Alters the Subcellular Processing of APP and Inhibits A β Deposition in Vivo. *J. Cell Biol.* **2005**, *168* (2), 291–302.
- (135) Kumar, P.; Wu, H.; McBride, J. L.; Jung, K. E.; Hee Kim, M.; Davidson, B. L.; Kyung Lee, S.; Shankar, P.; Manjunath, N. Transvascular Delivery of Small Interfering RNA to the Central Nervous System. *Nature* **2007**, *448* (7149), 39–43.
- (136) Evin, G.; Barakat, A.; Masters, C. L. BACE: Therapeutic Target and Potential Biomarker for Alzheimer's Disease. *Int. J. Biochem. Cell Biol.* **2010**, *42* (12), 1923–1926.
- (137) Zhang, C.; Gu, Z.; Shen, L.; Liu, X.; Lin, H. A Dual Targeting Drug Delivery System for Penetrating Blood Brain Barrier and Selectively Delivering SiRNA to Neurons for Alzheimer's Disease Treatment. *Curr. Pharm. Biotechnol.* **2018**, *19*.
- (138) Zhang, C.; Gu, Z.; Shen, L.; Liu, X.; Lin, H. In Vivo Evaluation and Alzheimer's Disease Treatment Outcome of SiRNA Loaded Dual Targeting Drug Delivery System. *Curr. Pharm. Biotechnol.* **2019**, *20* (1), 56–62.
- (139) Pack, D. W.; Hoffman, A. S.; Pun, S.; Stayton, P. S. Design and Development of Polymers for Gene Delivery. *Nat. Rev. Drug Discov.* **2005**, *4* (7), 581–593.
- (140) Sharma, D.; Arora, S.; dos Santos Rodrigues, B.; Lakkadwala, S.; Banerjee, A.; Singh, J. Chitosan-Based Systems for Gene Delivery - Functional Chitosan: Drug Delivery and Biomedical Applications. In *Functional Chitosan*; Jana, S., Jana, S., Eds.; Springer Singapore: Singapore, 2019; pp 229–267.
- (141) Liang, Y.; Liu, Z.; Shuai, X.; Wang, W.; Liu, J.; Bi, W.; Wang, C.; Jing, X.; Liu, Y.; Tao, E. Delivery of Cationic Polymer-SiRNA Nanoparticles for Gene Therapies in Neural Regeneration. *Biochem. Biophys. Res. Commun.* **2012**, *421* (4), 690–695.
- (142) Wen, X.; Wang, L.; Liu, Z.; Liu, Y.; Hu, J. Intracranial Injection of PEG-PEI/ROCK II-SiRNA Improves Cognitive Impairment in a Mouse Model of Alzheimer's Disease. *Int. J. Neurosci.* **2014**, *124* (9), 697–703.
- (143) Shyam, R.; Ren, Y.; Lee, J.; Braunstein, K. E.; Mao, H. Q.; Wong, P. C. Intraventricular Delivery of SiRNA Nanoparticles to the Central Nervous System. *Mol. Ther. - Nucleic Acids* **2015**, *4* (5), e242.
- (144) Guo, Q.; Zheng, X.; Yang, P.; Pang, X.; Qian, K.; Wang, P.; Xu, S.; Sheng, D.; Wang, L.; Cao, J.; Lu, W.; Zhang, Q.; Jiang, X. Small Interfering RNA Delivery to the Neurons near the Amyloid Plaques for Improved Treatment of Alzheimer's Disease. *Acta Pharm. Sin. B* **2019**, *9* (3), 590–603.
- (145) Wiesehan, K.; Buder, K.; Linke, R. P.; Patt, S.; Stoldt, M.; Unger, E.; Schmitt, B.; Bucci, E.; Willbold, D. Selection of D-Amino-Acid Peptides That Bind to Alzheimer's Disease Amyloid Peptide A β 1-42 by Mirror Image Phage Display. *ChemBioChem* **2003**, *4* (8), 748–753.
- (146) Tagalakis, A. D.; Lee, D. H. D.; Bienemann, A. S.; Zhou, H.; Munye, M. M.; Saraiva, L.; McCarthy, D.; Du, Z.; Vink, C. A.; Maeshima, R.; White, E. A.; Gustafsson, K.; Hart, S. L. Multifunctional, Self-Assembling Anionic Peptide-Lipid Nanocomplexes for Targeted SiRNA Delivery. *Biomaterials* **2014**, *35* (29), 8406–8415.
- (147) Rassu, G.; Soddu, E.; Posadino, A. M.; Pintus, G.; Sarmiento, B.; Giunchedi, P.; Gavini, E. Nose-to-Brain Delivery of BACE1 SiRNA Loaded in Solid Lipid Nanoparticles for Alzheimer's Therapy. *Colloids Surfaces B Biointerfaces* **2017**, *152*, 296–301.

- (148) Sampaio, T. B.; Savall, A. S.; Gutierrez, M. E. Z.; Pinton, S. Neurotrophic Factors in Alzheimer's and Parkinson's Diseases: Implications for Pathogenesis and Therapy. *Neural Regen. Res.* **2017**, *12* (4), 549–557.
- (149) dos Santos Rodrigues, B.; Kanekiyo, T.; Singh, J. ApoE-2 Brain-Targeted Gene Therapy Through Transferrin and Penetratin Tagged Liposomal Nanoparticles. *Pharm. Res.* **2019**, *36* (11), 1–11.
- (150) Banerjee, A.; Sharma, D.; Trivedi, R.; Singh, J. Treatment of Insulin Resistance in Obesity-Associated Type 2 Diabetes Mellitus through Adiponectin Gene Therapy. *Int. J. Pharm.* **2020**, *583*, 119357.
- (151) dos Santos Rodrigues, B.; Lakkadwala, S.; Sharma, D.; Singh, J. Chitosan for Gene, DNA Vaccines, and Drug Delivery. In *Materials for Biomedical Engineering*; Elsevier, 2019; pp 515–550.
- (152) Sharma, D.; Singh, J. Synthesis and Characterization of Fatty Acid Grafted Chitosan Polymer and Their Nanomicelles for Nonviral Gene Delivery Applications. *Bioconjug. Chem.* **2017**.
- (153) Rodrigues, B. D. S.; Kanekiyo, T.; Singh, J. Nerve Growth Factor Gene Delivery across the Blood-Brain Barrier to Reduce Beta Amyloid Accumulation in AD Mice. *Mol. Pharm.* **2020**, *17* (6), 2054–2063.
- (154) dos Santos Rodrigues, B.; Oue, H.; Banerjee, A.; Kanekiyo, T.; Singh, J. Dual Functionalized Liposome-Mediated Gene Delivery across Triple Co-Culture Blood Brain Barrier Model and Specific in Vivo Neuronal Transfection. *J. Control. Release* **2018**, *286*, 264–278.
- (155) dos Santos Rodrigues, B.; Arora, S.; Kanekiyo, T.; Singh, J. Efficient Neuronal Targeting and Transfection Using RVG and Transferrin-Conjugated Liposomes. *Brain Res.* **2020**, *1734*, 146738.
- (156) Rodrigues, B. dos S.; Kanekiyo, T.; Singh, J. Nerve Growth Factor Gene Delivery across the Blood-Brain Barrier to Reduce Beta Amyloid Accumulation in AD Mice. *Mol. Pharm.* **2020**.
- (157) Li, Y.; Wang, J.; Liu, J.; Liu, F. A Novel System for in Vivo Neprilysin Gene Delivery Using a Syringe Electrode. *J. Neurosci. Methods* **2010**, *193* (2), 226–231.
- (158) Park, T. E.; Singh, B.; Li, H.; Lee, J. Y.; Kang, S. K.; Choi, Y. J.; Cho, C. S. Enhanced BBB Permeability of Osmotically Active Poly(Mannitol-Co-PEI) Modified with Rabies Virus Glycoprotein via Selective Stimulation of Caveolar Endocytosis for RNAi Therapeutics in Alzheimer's Disease. *Biomaterials* **2015**, *38*, 61–71.
- (159) Sato, A. K.; Viswanathan, M.; Kent, R. B.; Wood, C. R. Therapeutic Peptides: Technological Advances Driving Peptides into Development. *Curr. Opin. Biotechnol.* **2006**, *17* (6), 638–642.
- (160) Hoyer, J.; Neundorff, I. Peptide Vectors for the Nonviral Delivery of Nucleic Acids. *Acc. Chem. Res.* **2012**, *45* (7), 1048–1056.
- (161) Kang, Z.; Meng, Q.; Liu, K. Peptide-Based Gene Delivery Vectors. *J. Mater. Chem. B* **2019**, *7* (11), 1824–1841.
- (162) Kristensen, M.; Birch, D.; Nielsen, H. M. Applications and Challenges for Use of Cell-Penetrating Peptides as Delivery Vectors for Peptide and Protein Cargos. *Int. J. Mol. Sci.* **2016**, *17* (2).
- (163) Park, H.; Oh, J.; Shim, G.; Cho, B.; Chang, Y.; Kim, S.; Baek, S.; Kim, H.; Shin, J.; Choi, H.; Yoo, J.; Kim, J.; Jun, W.; Lee, M.; Lengner, C. J.; Oh, Y. K.; Kim, J. In Vivo

- Neuronal Gene Editing via CRISPR–Cas9 Amphiphilic Nanocomplexes Alleviates Deficits in Mouse Models of Alzheimer’s Disease. *Nat. Neurosci.* **2019**, *22* (4), 524–528.
- (164) Youn, P.; Chen, Y.; Furgeson, D. Y. A Myristoylated Cell-Penetrating Peptide Bearing a Transferrin Receptor-Targeting Sequence for Neuro-Targeted SiRNA Delivery. *Mol. Pharm.* **2014**, *11* (2), 486–495.
- (165) Gatz, M.; Reynolds, C. A.; Fratiglioni, L.; Johansson, B.; Mortimer, J. A.; Berg, S.; Fiske, A.; Pedersen, N. L. Role of Genes and Environments for Explaining Alzheimer Disease. *Arch. Gen. Psychiatry* **2006**.
- (166) Sala Frigerio, C.; De Strooper, B. Alzheimer’s Disease Mechanisms and Emerging Roads to Novel Therapeutics. *Annu. Rev. Neurosci.* **2016**.
- (167) Huang, Y.; Mucke, L. Alzheimer Mechanisms and Therapeutic Strategies. *Cell.* 2012, pp 1204–1222.
- (168) Saunders, A. M.; Strittmatter, W. J.; Schmechel, D.; St. George-Hyslop, P. H.; Pericak-Vance, M. A.; Joo, S. H.; Rosi, B. L.; Gusella, J. F.; Crapper-Mac Lachlan, D. R.; Alberts, M. J.; Hulette, C.; Crain, B.; Goldgaber, D.; Roses, A. D. Association of Apolipoprotein E Allele E4 with Late-Onset Familial and Sporadic Alzheimer’s Disease. *Neurology* **1993**, *43* (8), 1467–1472.
- (169) Nagahara, A. H.; Mateling, M.; Kovacs, I.; Wang, L.; Eggert, S.; Rockenstein, E.; Koo, E. H.; Masliah, E.; Tuszynski, M. H. Early BDNF Treatment Ameliorates Cell Loss in the Entorhinal Cortex of APP Transgenic Mice. *J. Neurosci.* **2013**.
- (170) Angelova, A.; Angelov, B.; Drechsler, M.; Lesieur, S. Neurotrophin Delivery Using Nanotechnology. *Drug Discov. Today* **2013**, *18* (23–24), 1263–1271.
- (171) Verghese, P. B.; Castellano, J. M.; Holtzman, D. M. Apolipoprotein E in Alzheimer’s Disease and Other Neurological Disorders. *Lancet Neurol.* **2011**, *10* (3), 241–252.
- (172) Mahley, R. W. Apolipoprotein E: Remarkable Protein Sheds Light on Cardiovascular and Neurological Diseases. *Clin. Chem.* **2017**, *63* (1), 14–20.
- (173) Mahley, R. W.; Weisgraber, K. H.; Huang, Y. Apolipoprotein E4: A Causative Factor and Therapeutic Target in Neuropathology, Including Alzheimer’s Disease. *Proc. Natl. Acad. Sci. U. S. A.* **2006**, *103* (15), 5644–5651.
- (174) Genin, E.; Hannequin, D.; Wallon, D.; Sleegers, K.; Hiltunen, M.; Combarros, O.; Bullido, M. J.; Engelborghs, S.; De Deyn, P.; Berr, C.; Pasquier, F.; Dubois, B.; Tognoni, G.; Fiévet, N.; Brouwers, N.; Bettens, K.; Arosio, B.; Coto, E.; Del Zompo, M.; Mateo, I.; Epelbaum, J.; Frank-Garcia, A.; Helisalmi, S.; Porcellini, E.; Pilotto, A.; Forti, P.; Ferri, R.; Scarpini, E.; Siciliano, G.; Solfrizzi, V.; Sorbi, S.; Spalletta, G.; Valdivieso, F.; Veepsäläinen, S.; Alvarez, V.; Bosco, P.; Mancuso, M.; Panza, F.; Nacmias, B.; Boss, P.; Hanon, O.; Piccardi, P.; Annoni, G.; Seripa, D.; Galimberti, D.; Licastro, F.; Soininen, H.; Dartigues, J. F.; Kamboh, M. I.; Van Broeckhoven, C.; Lambert, J. C.; Amouyel, P.; Campion, D. APOE and Alzheimer Disease: A Major Gene with Semi-Dominant Inheritance. *Mol. Psychiatry* **2011**, *16* (9), 903–907.
- (175) Sando, S. B.; Melquist, S.; Cannon, A.; Hutton, M. L.; Sletvold, O.; Saltvedt, I.; White, L. R.; Lydersen, S.; Aasly, J. O. APOE E4 Lowers Age at Onset and Is a High Risk Factor for Alzheimer’s Disease; A Case Control Study from Central Norway. *BMC Neurol.* **2008**, *8*, 1–7.
- (176) Conejero-Goldberg, C.; Gomar, J. J.; Bobes-Bascaran, T.; Hyde, T. M.; Kleinman, J. E.; Herman, M. M.; Chen, S.; Davies, P.; Goldberg, T. E. APOE2 Enhances Neuroprotection

- against Alzheimer's Disease through Multiple Molecular Mechanisms. *Mol. Psychiatry* **2014**, *19*, 1243–1250.
- (177) Nagy, Z. S.; Esiri, M. M.; Jobst, K. A.; Johnston, C.; Litchfield, S.; Sim, E.; Smith, A. D. Influence of the Apolipoprotein E Genotype on Amyloid Deposition and Neurofibrillary Tangle Formation in Alzheimer's Disease. *Neuroscience* **1995**, *69* (3), 757–761.
- (178) Liu, C.-C.; Liu, C.-C.; Kanekiyo, T.; Xu, H.; Bu, G. Apolipoprotein E and Alzheimer Disease: Risk, Mechanisms and Therapy. *Nat. Rev. Neurol.* **2013**, *9* (2), 106–118.
- (179) Castellano, J. M.; Kim, J.; Stewart, F. R.; Jiang, H.; DeMattos, R. B.; Patterson, B. W.; Fagan, A. M.; Morris, J. C.; Mawuenyega, K. G.; Cruchaga, C.; Goate, A. M.; Bales, K. R.; Paul, S. M.; Bateman, R. J.; Holtzman, D. M. Human ApoE Isoforms Differentially Regulate Brain Amyloid- β Peptide Clearance. *Sci. Transl. Med.* **2011**, *3* (89), 89ra57.
- (180) Deane, R.; Sagare, A.; Hamm, K.; Parisi, M.; Lane, S.; Finn, M. B.; Holtzman, D. M.; Zlokovic, B. V. ApoE Isoform-Specific Disruption of Amyloid β Peptide Clearance from Mouse Brain. *J. Clin. Invest.* **2008**, *118* (12), 4002–4013.
- (181) Aleshkov, S.; Abraham, C. R.; Zannis, V. I. Interaction of Nascent Apoe2, Apoe3, and Apoe4 Isoforms Expressed in Mammalian Cells with Amyloid Peptide β (1–40). Relevance to Alzheimer's Disease. *Biochemistry* **1997**, *36* (34), 10571–10580.
- (182) Jiang, Q.; Lee, C. Y. D.; Mandrekar, S.; Wilkinson, B.; Cramer, P.; Zelcer, N.; Mann, K.; Lamb, B.; Willson, T. M.; Collins, J. L.; Richardson, J. C.; Smith, J. D.; Comery, T. A.; Riddell, D.; Holtzman, D. M.; Tontonoz, P.; Landreth, G. E. ApoE Promotes the Proteolytic Degradation of A β . *Neuron* **2008**, *58* (5), 681–693.
- (183) Bour, A.; Grootendorst, J.; Vogel, E.; Kelche, C.; Dodart, J. C.; Bales, K.; Moreau, P. H.; Sullivan, P. M.; Mathis, C. Middle-Aged Human ApoE4 Targeted-Replacement Mice Show Retention Deficits on a Wide Range of Spatial Memory Tasks. *Behav. Brain Res.* **2008**, *193* (2), 174–182.
- (184) Jiang, C. H.; Tsien, J. Z.; Schultz, P. G.; Hu, Y. The Effects of Aging on Gene Expression in the Hypothalamus and Cortex of Mice. *Proc. Natl. Acad. Sci. U. S. A.* **2001**, *98* (4), 1930–1934.
- (185) Jiang, C.; Lin, W. J.; Sadahiro, M.; Labonté, B.; Menard, C.; Pfau, M. L.; Tamminga, C. A.; Turecki, G.; Nestler, E. J.; Russo, S. J.; Salton, S. R. VGF Function in Depression and Antidepressant Efficacy. *Mol. Psychiatry* **2018**, *23* (7), 1632–1642.
- (186) Jiang, C.; Lin, W. J.; Labonté, B.; Tamminga, C. A.; Turecki, G.; Nestler, E. J.; Russo, S. J.; Salton, S. R. VGF and Its C-Terminal Peptide TLQP-62 in Ventromedial Prefrontal Cortex Regulate Depression-Related Behaviors and the Response to Ketamine. *Neuropsychopharmacology* **2019**, *44* (5), 971–981.
- (187) Rosenberg, J. B.; Kaplitt, M. G.; De, B. P.; Chen, A.; Flagiello, T.; Salami, C.; Pey, E.; Zhao, L.; Ricart Arbona, R. J.; Monette, S.; Dyke, J. P.; Ballon, D. J.; Kaminsky, S. M.; Sondhi, D.; Petsko, G. A.; Paul, S. M.; Crystal, R. G. AAVrh.10-Mediated APOE2 Central Nervous System Gene Therapy for APOE4-Associated Alzheimer's Disease. *Hum. Gene Ther. Clin. Dev.* **2018**, *29* (1), 24–47.
- (188) Naldini, L. Gene Therapy Returns to Centre Stage. *Nature* **2015**, *526*, 351–360.
- (189) Palfi, S.; Gurruchaga, J. M.; Scott Ralph, G.; Lepetit, H.; Lavis, S.; Buttery, P. C.; Watts, C.; Miskin, J.; Kelleher, M.; Deeley, S.; Iwamuro, H.; Lefaucheur, J. P.; Thiriez, C.; Fenelon, G.; Lucas, C.; Brugières, P.; Gabriel, I.; Abhay, K.; Drouot, X.; Tani, N.; Kas, A.; Ghaleh, B.; Le Corvoisier, P.; Dolphin, P.; Breen, D. P.; Mason, S.; Guzman, N. V.; Mazarakis, N. D.; Radcliffe, P. A.; Harrop, R.; Kingsman, S. M.; Rascol, O.; Naylor,

- S.; Barker, R. A.; Hantraye, P.; Remy, P.; Cesaro, P.; Mitrophanous, K. A. Long-Term Safety and Tolerability of ProSavin, a Lentiviral Vector-Based Gene Therapy for Parkinson's Disease: A Dose Escalation, Open-Label, Phase 1/2 Trial. *Lancet* **2014**.
- (190) Marks, W. J.; Bartus, R. T.; Siffert, J.; Davis, C. S.; Lozano, A.; Boulis, N.; Vitek, J.; Stacy, M.; Turner, D.; Verhagen, L.; Bakay, R.; Watts, R.; Guthrie, B.; Jankovic, J.; Simpson, R.; Tagliati, M.; Alterman, R.; Stern, M.; Baltuch, G.; Starr, P. A.; Larson, P. S.; Ostrem, J. L.; Nutt, J.; Kieburtz, K.; Kordower, J. H.; Olanow, C. W. Gene Delivery of AAV2-Neurturin for Parkinson's Disease: A Double-Blind, Randomised, Controlled Trial. *Lancet Neurol.* **2010**.
- (191) DePolo, N. J.; Reed, J. D.; Sheridan, P. L.; Townsend, K.; Sauter, S. L.; Jolly, D. J.; Dubensky, T. W. VSV-G Pseudotyped Lentiviral Vector Particles Produced in Human Cells Are Inactivated by Human Serum. *Mol. Ther.* **2000**.
- (192) Thomas, C. E.; Ehrhardt, A.; Kay, M. A. Progress and Problems with the Use of Viral Vectors for Gene Therapy. *Nat. Rev. Genet.* **2003**, *4* (5), 346–358.
- (193) Saffari, M.; Moghimi, H. R.; Dass, C. R. Barriers to Liposomal Gene Delivery: From Application Site to the Target. *Iran. J. Pharm. Res.* **2016**.
- (194) Semple, S. C.; Klimuk, S. K.; Harasym, T. O.; Hope, M. J. Lipid-Base Formulations of Antisense Oligonucleotides for Systemic Delivery Applications. *Methods Enzymol.* **2000**.
- (195) Al Feteisi, H.; Al-Majdoub, Z. M.; Achour, B.; Couto, N.; Rostami-Hodjegan, A.; Barber, J. Identification and Quantification of Blood–Brain Barrier Transporters in Isolated Rat Brain Microvessels. *J. Neurochem.* **2018**.
- (196) Uchida, Y.; Ohtsuki, S.; Katsukura, Y.; Ikeda, C.; Suzuki, T.; Kamiie, J.; Terasaki, T. Quantitative Targeted Absolute Proteomics of Human Blood-Brain Barrier Transporters and Receptors. *J. Neurochem.* **2011**, *117* (2), 333–345.
- (197) Shah, K.; DeSilva, S.; Abbruscato, T. The Role of Glucose Transporters in Brain Disease: Diabetes and Alzheimer's Disease. *International Journal of Molecular Sciences.* 2012, pp 12629–12655.
- (198) Godoy, A.; Ulloa, V.; Rodríguez, F.; Reinicke, K.; Yañez, A. J.; De Los Angeles García, M.; Medina, R. A.; Carrasco, M.; Barberis, S.; Castro, T.; Martínez, F.; Koch, X.; Vera, J. C.; Poblete, M. T.; Figueroa, C. D.; Peruzzo, B.; Pérez, F.; Nualart, F. Differential Subcellular Distribution of Glucose Transporters GLUT1-6 and GLUT9 in Human Cancer: Ultrastructural Localization of GLUT1 and GLUT5 in Breast Tumor Tissues. *J. Cell. Physiol.* **2006**, *207* (3), 614–627.
- (199) Kim, J. Y.; Choi, W. II; Kim, Y. H.; Tae, G. Brain-Targeted Delivery of Protein Using Chitosan- and RVG Peptide-Conjugated, Pluronic-Based Nano-Carrier. *Biomaterials* **2013**, *34* (4), 1170–1178.
- (200) Liu, Y.; Guo, Y.; An, S.; Kuang, Y.; He, X.; Ma, H.; Li, J.; Lv, J.; Zhang, N.; Jiang, C. Targeting Caspase-3 as Dual Therapeutic Benefits by RNAi Facilitating Brain-Targeted Nanoparticles in a Rat Model of Parkinson's Disease. *PLoS One* **2013**, *8* (5), e62905.
- (201) Koren, E.; Torchilin, V. P. Cell-Penetrating Peptides: Breaking through to the Other Side. *Trends Mol. Med.* **2012**, *18* (7), 385–393.
- (202) Jin, G.-Z.; Chakraborty, A.; Lee, J.-H.; Knowles, J. C.; Kim, H.-W. Targeting with Nanoparticles for the Therapeutic Treatment of Brain Diseases. *J. Tissue Eng.* **2020**, *11*, 2041731419897460–2041731419897460.

- (203) Zheng, X.; Pang, X.; Yang, P.; Wan, X.; Wei, Y.; Guo, Q.; Zhang, Q.; Jiang, X. A Hybrid SiRNA Delivery Complex for Enhanced Brain Penetration and Precise Amyloid Plaque Targeting in Alzheimer's Disease Mice. *Acta Biomater.* **2017**, *49*, 388–401.
- (204) Xiang, L.; Zhou, R.; Fu, A.; Xu, X.; Huang, Y.; Hu, C. Targeted Delivery of Large Fusion Protein into Hippocampal Neurons by Systemic Administration. *J. Drug Target.* **2011**, *19* (8), 632–636.
- (205) Fu, A.; Wang, Y.; Zhan, L.; Zhou, R. Targeted Delivery of Proteins into the Central Nervous System Mediated by Rabies Virus Glycoprotein-Derived Peptide. *Pharm. Res.* **2012**, *29* (6), 1562–1569.
- (206) Sun, J.; Xie, W.; Zhu, X.; Xu, M.; Liu, J. Sulfur Nanoparticles with Novel Morphologies Coupled with Brain-Targeting Peptides RVG as a New Type of Inhibitor Against Metal-Induced A β Aggregation. *ACS Chem. Neurosci.* **2018**, *9* (4), 749–761.
- (207) Joo, J.; Kwon, E. J.; Kang, J.; Skalak, M.; Anglin, E. J.; Mann, A. P.; Ruoslahti, E.; Bhatia, S. N.; Sailor, M. J. Porous Silicon-Graphene Oxide Core-Shell Nanoparticles for Targeted Delivery of siRNA to the Injured Brain. *Nanoscale Horizons* **2016**, *1* (5), 407–414.
- (208) Lakkadwala, S.; dos Santos Rodrigues, B.; Sun, C.; Singh, J. Dual Functionalized Liposomes for Efficient Co-Delivery of Anti-Cancer Chemotherapeutics for the Treatment of Glioblastoma. *J. Control. Release* **2019**, *307*, 247–260.
- (209) Škrlić, N.; Drevenšek, G.; Hudoklin, S.; Romih, R.; Čurin Šerbec, V.; Dolinar, M. Recombinant Single-Chain Antibody with the Trojan Peptide Penetratin Positioned in the Linker Region Enables Cargo Transfer across the Blood-Brain Barrier. *Appl. Biochem. Biotechnol.* **2013**, *169* (1), 159–169.
- (210) Xia, H.; Gao, X.; Gu, G.; Liu, Z.; Hu, Q.; Tu, Y.; Song, Q.; Yao, L.; Pang, Z.; Jiang, X.; Chen, J.; Chen, H. Penetratin-Functionalized PEG-PLA Nanoparticles for Brain Drug Delivery. *Int. J. Pharm.* **2012**, *436* (1–2), 840–850.
- (211) Sarko, D.; Beijer, B.; Boy, R. G.; Nothelfer, E. M.; Leotta, K.; Eisenhut, M.; Altmann, A.; Haberkorn, U.; Mier, W. The Pharmacokinetics of Cell-Penetrating Peptides. *Mol. Pharm.* **2010**, *7* (6), 2224–2231.
- (212) Zhang, H. W.; Zhang, L.; Sun, X.; Zhang, Z. R. Successful Transfection of Hepatoma Cells after Encapsulation of Plasmid DNA into Negatively Charged Liposomes. *Biotechnol. Bioeng.* **2007**, *96* (1), 118–124.
- (213) Summers, C.; Fregly, M. J. Modulation of Angiotensin II Binding Sites in Neuronal Cultures by Mineralocorticoids. *Am. J. Physiol. - Cell Physiol.* **1989**, *256* (1), C121–C129.
- (214) dos Santos Rodrigues, B.; Banerjee, A.; Kanekiyo, T.; Singh, J. Functionalized Liposomal Nanoparticles for Efficient Gene Delivery System to Neuronal Cell Transfection. *Int. J. Pharm.* **2019**, *566*, 717–730.
- (215) Layek, B.; Singh, J. Amino Acid Grafted Chitosan for High Performance Gene Delivery: Comparison of Amino Acid Hydrophobicity on Vector and Polyplex Characteristics. *Biomacromolecules* **2013**, *14* (2), 485–494.
- (216) Sharma, D.; Singh, J. Synthesis and Characterization of Fatty Acid Grafted Chitosan Polymer and Their Nanomicelles for Nonviral Gene Delivery Applications. *Bioconjug. Chem.* **2017**, *28* (11), 2772–2783.
- (217) Lipp, L.; Sharma, D.; Banerjee, A.; Singh, J. Controlled Delivery of Salmon Calcitonin Using Thermosensitive Triblock Copolymer Depot for Treatment of Osteoporosis. *ACS Omega* **2019**, *4* (1), 1157–1166.

- (218) Sharma, G.; Lakkadwala, S.; Modgil, A.; Singh, J. The Role of Cell-Penetrating Peptide and Transferrin on Enhanced Delivery of Drug to Brain. *Int. J. Mol. Sci.* **2016**, *17* (6), 806.
- (219) Santos Rodrigues, B. Dos; Lakkadwala, S.; Kanekiyo, T.; Singh, J. Development and Screening of Brain-Targeted Lipid-Based Nanoparticles with Enhanced Cell Penetration and Gene Delivery Properties. *Int. J. Nanomedicine* **2019**, *14*, 6497–6517.
- (220) Nakagawa, S.; Deli, M. A.; Kawaguchi, H.; Shimizudani, T.; Shimono, T.; Kittel, Á.; Tanaka, K.; Niwa, M. A New Blood-Brain Barrier Model Using Primary Rat Brain Endothelial Cells, Pericytes and Astrocytes. *Neurochem. Int.* **2009**, *54* (3–4), 253–263.
- (221) Veszelka, S.; Pásztói, M.; Farkas, A. E.; Krizbai, I.; Dung, N. T. K.; Niwa, M.; Ábrahám, C. S.; Deli, M. A. Pentosan Polysulfate Protects Brain Endothelial Cells against Bacterial Lipopolysaccharide-Induced Damages. *Neurochem. Int.* **2007**, *50* (1), 219–228.
- (222) Sharma, G.; Modgil, A.; Sun, C.; Singh, J. Grafting of Cell-Penetrating Peptide to Receptor-Targeted Liposomes Improves Their Transfection Efficiency and Transport across Blood-Brain Barrier Model. *J. Pharm. Sci.* **2012**, *101* (7), 2468–2478.
- (223) Sharma, G.; Modgil, A.; Layek, B.; Arora, K.; Sun, C.; Law, B.; Singh, J. Cell Penetrating Peptide Tethered Bi-Ligand Liposomes for Delivery to Brain in Vivo: Biodistribution and Transfection. *J. Control. Release* **2013**, *167* (1), 1–10.
- (224) Wöll, S.; Schiller, S.; Bachran, C.; Swee, L. K.; Scherließ, R. Pentaglycine Lipid Derivates – Rp-HPLC Analytics for Bioorthogonal Anchor Molecules in Targeted, Multiple-Composite Liposomal Drug Delivery Systems. *Int. J. Pharm.* **2018**, *547* (1–2), 602–610.
- (225) Sharma, D.; Singh, J. Long-Term Glycemic Control and Prevention of Diabetes Complications in Vivo Using Oleic Acid-Grafted-Chitosan-zinc-Insulin Complexes Incorporated in Thermosensitive Copolymer. *J. Control. Release* **2020**, *323*, 161–178.
- (226) Filali, M.; Lalonde, R. Age-Related Cognitive Decline and Nesting Behavior in an APPswe/PS1 Bigenic Model of Alzheimer’s Disease. *Brain Res.* **2009**.
- (227) Deacon, R. M. J.; Cholerton, L. L.; Talbot, K.; Nair-Roberts, R. G.; Sanderson, D. J.; Romberg, C.; Koros, E.; Bornemann, K. D.; Rawlins, J. N. P. Age-Dependent and -Independent Behavioral Deficits in Tg2576 Mice. *Behav. Brain Res.* **2008**, *189* (1), 126–138.
- (228) Suk, J. S.; Xu, Q.; Kim, N.; Hanes, J.; Ensign, L. M. PEGylation as a Strategy for Improving Nanoparticle-Based Drug and Gene Delivery. *Adv. Drug Deliv. Rev.* **2016**, *99*, 28–51.
- (229) Klibanov, A. L.; Maruyama, K.; Torchilin, V. P.; Huang, L. Amphipathic Polyethyleneglycols Effectively Prolong the Circulation Time of Liposomes. *FEBS Lett.* **1990**, *268* (1), 235–237.
- (230) Kim, J.; Kim, P. H.; Kim, S. W.; Yun, C. O. Enhancing the Therapeutic Efficacy of Adenovirus in Combination with Biomaterials. *Biomaterials* **2012**, *33* (6), 1838–1850.
- (231) Yang, Q.; Lai, S. K. Anti-PEG Immunity: Emergence, Characteristics, and Unaddressed Questions. *Wiley Interdiscip. Rev. Nanomedicine Nanobiotechnology* **2015**, *7* (5), 655–677.
- (232) Vonarbourg, A.; Passirani, C.; Saulnier, P.; Benoit, J. P. Parameters Influencing the Stealthiness of Colloidal Drug Delivery Systems. *Biomaterials* **2006**, *27* (24), 4356–4373.
- (233) Danaei, M.; Dehghankhold, M.; Ataei, S.; Hasanzadeh Davarani, F.; Javanmard, R.; Dokhani, A.; Khorasani, S.; Mozafari, M. R. Impact of Particle Size and Polydispersity

- Index on the Clinical Applications of Lipidic Nanocarrier Systems. *Pharmaceutics* **2018**, *10* (57), 1–17.
- (234) Naahidi, S.; Jafari, M.; Edalat, F.; Raymond, K.; Khademhosseini, A.; Chen, P. Biocompatibility of Engineered Nanoparticles for Drug Delivery. *J. Control. Release* **2013**, *166* (2), 182–194.
- (235) Rosada, R. S.; de la Torre, L. G.; Frantz, F. G.; Trombone, A. P. F.; Zárata-Bladés, C. R.; Fonseca, D. M.; Souza, P. R. M.; Brandão, I. T.; Masson, A. P.; Soares, É. G.; Ramos, S. G.; Faccioli, L. H.; Silva, C. L.; Santana, M. H. A.; Coelho-Castelo, A. A. M. Protection against Tuberculosis by a Single Intranasal Administration of DNA-Hsp65 Vaccine Complexed with Cationic Liposomes. *BMC Immunol.* **2008**, *9* (38), 1–13.
- (236) Lechanteur, A.; Sanna, V.; Duchemin, A.; Evrard, B.; Mottet, D.; Piel, G. Cationic Liposomes Carrying SiRNA: Impact of Lipid Composition on Physicochemical Properties, Cytotoxicity and Endosomal Escape. *Nanomaterials* **2018**, *8* (5), 1–12.
- (237) Fröhlich, E. The Role of Surface Charge in Cellular Uptake and Cytotoxicity of Medical Nanoparticles. *Int. J. Nanomedicine* **2012**, *7*, 5577–5591.
- (238) Mailänder, V.; Landfester, K. Interaction of Nanoparticles with Cells. *Biomacromolecules* **2009**, *10* (9), 2379–2400.
- (239) Pan, Z.; Kang, X.; Zeng, Y.; Zhang, W.; Peng, H.; Wang, J.; Huang, W.; Wang, H.; Shen, Y.; Huang, Y. A Mannosylated PEI-CPP Hybrid for TRAIL Gene Targeting Delivery for Colorectal Cancer Therapy. *Polym. Chem.* **2017**, *8* (35), 5275–5285.
- (240) Pan, C.; Kumar, C.; Bohl, S.; Klingmueller, U.; Mann, M. Comparative Proteomic Phenotyping of Cell Lines and Primary Cells to Assess Preservation of Cell Type-Specific Functions. *Mol. Cell. Proteomics* **2009**, *8* (3), 443–450.
- (241) Alge, C. S.; Hauck, S. M.; Priglinger, S. G.; Kampik, A.; Ueffing, M. Differential Protein Profiling of Primary versus Immortalized Human RPE Cells Identifies Expression Patterns Associated with Cytoskeletal Remodeling and Cell Survival. *J. Proteome Res.* **2006**, *5* (4), 862–878.
- (242) Maurisse, R.; De Semir, D.; Enamekhoo, H.; Bedayat, B.; Abdolmohammadi, A.; Parsi, H.; Gruenert, D. C. Comparative Transfection of DNA into Primary and Transformed Mammalian Cells from Different Lineages. *BMC Biotechnol.* **2010**, *10*, 1–9.
- (243) Janson, J.; Laedtke, T.; Parisi, J. E.; O'Brien, P.; Petersen, R. C.; Butler, P. C. Increased Risk of Type 2 Diabetes in Alzheimer Disease. *Diabetes* **2004**, *53* (2), 474–481.
- (244) Pozueta, J.; Lefort, R.; Shelanski, M. L. Synaptic Changes in Alzheimer's Disease and Its Models. *Neuroscience* **2013**, *251*, 51–65.
- (245) Lepeta, K.; Lourenco, M. V.; Schweitzer, B. C.; Martino Adami, P. V.; Banerjee, P.; Catuara-Solarz, S.; de La Fuente Revenga, M.; Guillem, A. M.; Haidar, M.; Ijomone, O. M.; Nadorp, B.; Qi, L.; Perera, N. D.; Refsgaard, L. K.; Reid, K. M.; Sabbar, M.; Sahoo, A.; Schaefer, N.; Sheean, R. K.; Suska, A.; Verma, R.; Vicidomini, C.; Wright, D.; Zhang, X. D.; Seidenbecher, C. Synaptopathies: Synaptic Dysfunction in Neurological Disorders – A Review from Students to Students. *J. Neurochem.* **2016**, *138* (6), 785–805.
- (246) Wei, L.; Lv, S.; Huang, Q.; Wei, J.; Zhang, S.; Huang, R.; Lu, Z.; Lin, X. Pratensein Attenuates A β -Induced Cognitive Deficits in Rats: Enhancement of Synaptic Plasticity and Cholinergic Function. *Fitoterapia* **2015**, *101*, 208–217.
- (247) McClean, P. L.; Hölscher, C. Liraglutide Can Reverse Memory Impairment, Synaptic Loss and Reduce Plaque Load in Aged APP/PS1 Mice, a Model of Alzheimer's Disease. *Neuropharmacology* **2014**, *76* (PART A), 57–67.

- (248) Vaynman, S. S.; Ying, Z.; Yin, D.; Gomez-Pinilla, F. Exercise Differentially Regulates Synaptic Proteins Associated to the Function of BDNF. *Brain Res.* **2006**, *1070* (1), 124–130.
- (249) Pozzo-Miller, L. D.; Gottschalk, W.; Zhang, L.; McDermott, K.; Du, J.; Gopalakrishnan, R.; Oho, C.; Sheng, Z. H.; Lu, B. Impairments in High-Frequency Transmission, Synaptic Vesicle Docking, and Synaptic Protein Distribution in the Hippocampus of BDNF Knockout Mice. *J. Neurosci.* **1999**, *19* (12), 4972–4983.
- (250) Lima Giacobbo, B.; Doorduyn, J.; Klein, H. C.; Dierckx, R. A. J. O.; Bromberg, E.; de Vries, E. F. J. Brain-Derived Neurotrophic Factor in Brain Disorders: Focus on Neuroinflammation. *Mol. Neurobiol.* **2019**, *56* (5), 3295–3312.
- (251) Helms, H. C.; Abbott, N. J.; Burek, M.; Cecchelli, R.; Couraud, P. O.; Deli, M. A.; Förster, C.; Galla, H. J.; Romero, I. A.; Shusta, E. V.; Stebbins, M. J.; Vandenhoute, E.; Weksler, B.; Brodin, B. In Vitro Models of the Blood-Brain Barrier: An Overview of Commonly Used Brain Endothelial Cell Culture Models and Guidelines for Their Use. *J. Cereb. Blood Flow Metab.* **2015**, *36* (5), 862–890.
- (252) Markoutsas, E.; Pampalakis, G.; Niarakis, A.; Romero, I. A.; Weksler, B.; Couraud, P. O.; Antimisiaris, S. G. Uptake and Permeability Studies of BBB-Targeting Immunoliposomes Using the HCMEC/D3 Cell Line. *Eur. J. Pharm. Biopharm.* **2011**, *77* (2), 265–274.
- (253) Hatherell, K.; Couraud, P. O.; Romero, I. A.; Weksler, B.; Pilkington, G. J. Development of a Three-Dimensional, All-Human in Vitro Model of the Blood-Brain Barrier Using Mono-, Co-, and Tri-Cultivation Transwell Models. *J. Neurosci. Methods* **2011**, *199* (2), 223–229.
- (254) Booth, R.; Kim, H. Characterization of a Microfluidic in Vitro Model of the Blood-Brain Barrier (MBBB). *Lab Chip* **2012**, *12* (10), 1784–1792.
- (255) Daniels, B. P.; Cruz-Orengo, L.; Pasiaka, T. J.; Couraud, P. O.; Romero, I. A.; Weksler, B.; Cooper, J. A.; Doering, T. L.; Klein, R. S. Immortalized Human Cerebral Microvascular Endothelial Cells Maintain the Properties of Primary Cells in an in Vitro Model of Immune Migration across the Blood Brain Barrier. *J. Neurosci. Methods* **2013**, *212* (1), 173–179.
- (256) Sharma, G.; Modgil, A.; Zhong, T.; Sun, C.; Singh, J. Influence of Short-Chain Cell-Penetrating Peptides on Transport of Doxorubicin Encapsulating Receptor-Targeted Liposomes across Brain Endothelial Barrier. *Pharm. Res.* **2014**, *31* (5), 1194–1209.
- (257) Janzer, R. C.; Raff, M. C. Astrocytes Induce Blood-Brain Barrier Properties in Endothelial Cells. *Nature* **1987**, *325* (6101), 253–257.
- (258) Arthur, F. E.; Shivers, R. R.; Bowman, P. D. Astrocyte-Mediated Induction of Tight Junctions in Brain Capillary Endothelium: An Efficient in Vitro Model. *Dev. Brain Res.* **1987**, *36* (1), 155–159.
- (259) Brown, R. C.; Morris, A. P.; O’Neil, R. G. Tight Junction Protein Expression and Barrier Properties of Immortalized Mouse Brain Microvessel Endothelial Cells. *Brain Res.* **2007**, *1130* (1), 17–30.
- (260) Li, S. D.; Huang, L. Nanoparticles Evading the Reticuloendothelial System: Role of the Supported Bilayer. *Biochim. Biophys. Acta - Biomembr.* **2009**, *1788* (10), 2259–2266.
- (261) Haute, D. Van; Berlin, J. M. Challenges in Realizing Selectivity for Nanoparticle Biodistribution and Clearance: Lessons from Gold Nanoparticles. *Ther. Deliv.* **2017**, *8* (9), 763–774.

- (262) Yasutake, C.; Kuroda, K.; Yanagawa, T.; Okamura, T.; Yoneda, H. Serum BDNF, TNF- α and IL-1 β Levels in Dementia Patients: Comparison between Alzheimer's Disease and Vascular Dementia. *Eur. Arch. Psychiatry Clin. Neurosci.* **2006**, *256* (7), 402–406.
- (263) Qin, X. Y.; Cao, C.; Cawley, N. X.; Liu, T. T.; Yuan, J.; Loh, Y. P.; Cheng, Y. Decreased Peripheral Brain-Derived Neurotrophic Factor Levels in Alzheimer's Disease: A Meta-Analysis Study (N=7277). *Mol. Psychiatry* **2017**, *22* (2), 312–320.
- (264) Weinstein, G.; Beiser, A. S.; Choi, S. H.; Preis, S. R.; Chen, T. C.; Vargha, D.; Au, R.; Pikula, A.; Wolf, P. A.; DeStefano, A. L.; Vasan, R. S.; Seshadri, S. Serum Brain-Derived Neurotrophic Factor and the Risk for Dementia: The Framingham Heart Study. *JAMA Neurol.* **2014**, *71* (1), 55–61.
- (265) Álvarez, A.; Aleixandre, M.; Linares, C.; Masliah, E.; Moessler, H. Apathy and APOE4 Are Associated with Reduced BDNF Levels in Alzheimer's Disease. *J. Alzheimer's Dis.* **2014**, *42* (4), 1347–1355.
- (266) Qiu, T.; Liu, Q.; Chen, Y. X.; Zhao, Y. F.; Li, Y. M. A β 42 and A β 40: Similarities and Differences. *J. Pept. Sci.* **2015**, *21* (7), 522–529.
- (267) Sadigh-Eteghad, S.; Sabermarouf, B.; Majidi, A.; Talebi, M.; Farhoudi, M.; Mahmoudi, J. Amyloid-Beta: A Crucial Factor in Alzheimer's Disease. *Med. Princ. Pract.* **2015**, *24* (1), 1–10.
- (268) Shin, M. K.; Kim, H. G.; Baek, S. H.; Jung, W. R.; Park, D. I.; Park, J. S.; Jo, D. G.; Kim, K. L. Neuropep-1 Ameliorates Learning and Memory Deficits in an Alzheimer's Disease Mouse Model, Increases Brain-Derived Neurotrophic Factor Expression in the Brain, and Causes Reduction of Amyloid Beta Plaques. *Neurobiol. Aging* **2014**, *35* (5), 990–1001.
- (269) Nigam, S. M.; Xu, S.; Kritikou, J. S.; Marosi, K.; Brodin, L.; Mattson, M. P. Exercise and BDNF Reduce A β Production by Enhancing α -Secretase Processing of APP. *J. Neurochem.* **2017**, *142* (2), 286–296.
- (270) De Pins, B.; Cifuentes-Díaz, C.; Thamila Farah, A.; López-Molina, L.; Montalban, E.; Sancho-Balsells, A.; López, A.; Ginés, S.; Delgado-García, J. M.; Alberch, J.; Gruart, A.; Girault, J. A.; Giralt, A. Conditional BDNF Delivery from Astrocytes Rescues Memory Deficits, Spine Density, and Synaptic Properties in the 5xFAD Mouse Model of Alzheimer Disease. *J. Neurosci.* **2019**, *39* (13), 2441–2458.
- (271) Ginsberg, S. D.; Malek-Ahmadi, M. H.; Alldred, M. J.; Chen, Y.; Chen, K.; Chao, M. V.; Counts, S. E.; Mufson, E. J. Brain-Derived Neurotrophic Factor (BDNF) and TrkB Hippocampal Gene Expression Are Putative Predictors of Neuritic Plaque and Neurofibrillary Tangle Pathology. *Neurobiol. Dis.* **2019**, *132*, 104540.
- (272) Arancibia, S.; Silhol, M.; Moulière, F.; Meffre, J.; Höllinger, I.; Maurice, T.; Tapia-Arancibia, L. Protective Effect of BDNF against Beta-Amyloid Induced Neurotoxicity in Vitro and in Vivo in Rats. *Neurobiol. Dis.* **2008**, *31* (3), 316–326.
- (273) Mattson, M. P.; Maudsley, S.; Martin, B. BDNF and 5-HT: A Dynamic Duo in Age-Related Neuronal Plasticity and Neurodegenerative Disorders. *Trends Neurosci.* **2004**, *27* (10), 589–594.
- (274) McAllister, A. K. Spatially Restricted Actions of BDNF. *Neuron* **2002**, *36* (4), 549–550.
- (275) Tanaka, J. I.; Horiike, Y.; Matsuzaki, M.; Miyazaki, T.; Ellis-Davies, G. C. R.; Kasai, H. Protein Synthesis and Neurotrophin-Dependent Structural Plasticity of Single Dendritic Spines. *Science* (80-.). **2008**, *319* (5870), 1683–1687.
- (276) Yoshii, A.; Constantine-Paton, M. Postsynaptic BDNF-TrkB Signaling in Synapse Maturation, Plasticity, and Disease. *Dev. Neurobiol.* **2010**, *70* (5), 304–322.

- (277) Kowiański, P.; Lietzau, G.; Czuba, E.; Waśkow, M.; Steliga, A.; Moryś, J. BDNF: A Key Factor with Multipotent Impact on Brain Signaling and Synaptic Plasticity. *Cell. Mol. Neurobiol.* **2018**, *38* (3), 579–593.
- (278) Ben Abdallah, N. M. B.; Slomianka, L.; Vyssotski, A. L.; Lipp, H. P. Early Age-Related Changes in Adult Hippocampal Neurogenesis in C57 Mice. *Neurobiol. Aging* **2010**, *31* (1), 151–161.
- (279) Daynac, M.; Morizur, L.; Chicheportiche, A.; Mouthon, M. A.; Boussin, F. D. Age-Related Neurogenesis Decline in the Subventricular Zone Is Associated with Specific Cell Cycle Regulation Changes in Activated Neural Stem Cells. *Sci. Rep.* **2016**, *6*.
- (280) Yang, T. T.; Lo, C. P.; Tsai, P. S.; Wu, S. Y.; Wang, T. F.; Chen, Y. W.; Jiang-Shieh, Y. F.; Kuo, Y. M. Aging and Exercise Affect Hippocampal Neurogenesis via Different Mechanisms. *PLoS One* **2015**, *10* (7).
- (281) Kitiyanant, N.; Kitiyanant, Y.; Svendsen, C. N.; Thangnipon, W. BDNF-, IGF-1- and GDNF-Secreting Human Neural Progenitor Cells Rescue Amyloid β -Induced Toxicity in Cultured Rat Septal Neurons. *Neurochem. Res.* **2012**, *37* (1), 143–152.
- (282) Zhang, Y.; Qiu, B.; Wang, J.; Yao, Y.; Wang, C.; Liu, J. Effects of BDNF-Transfected BMSCs on Neural Functional Recovery and Synaptophysin Expression in Rats with Cerebral Infarction. *Mol. Neurobiol.* **2017**, *54* (5), 3813–3824.
- (283) Yoshii, A.; Constantine-Paton, M. Postsynaptic Localization of PSD-95 Is Regulated by All Three Pathways Downstream of TrkB Signaling. *Front. Synaptic Neurosci.* **2014**, *6* (MAR).
- (284) Tampellini, D.; Capetillo-Zarate, E.; Dumont, M.; Huang, Z.; Yu, F.; Lin, M. T.; Gouras, G. K. Effects of Synaptic Modulation on β -Amyloid, Synaptophysin, and Memory Performance in Alzheimer's Disease Transgenic Mice. *J. Neurosci.* **2010**, *30* (43), 14299–14304.
- (285) Masliah, E.; Mallory, M.; Alford, M.; DeTeresa, R.; Hansen, L. A.; McKeel, D. W.; Morris, J. C. Altered Expression of Synaptic Proteins Occurs Early during Progression of Alzheimer's Disease. *Neurology* **2001**, *56* (1), 127–129.
- (286) Samaey, C.; Schreurs, A.; Stroobants, S.; Balschun, D. Early Cognitive and Behavioral Deficits in Mouse Models for Tauopathy and Alzheimer's Disease. *Front. Aging Neurosci.* **2019**, *11*.
- (287) Filali, M.; Lalonde, R.; Rivest, S. Cognitive and Non-Cognitive Behaviors in an APPswe/PS1 Bigenic Model of Alzheimer's Disease. *Genes, Brain Behav.* **2009**, *8* (2), 143–148.